UNIVERSITÀ DEGLI STUDI DI NAPOLI FEDERICO II

Geochemical mapping and environmental risk of areas polluted by mining, industrial and agricultural activities: the Huelva Province, Spain, and Zambales Province, the Philippines, case studies

Doctoral Thesis Research in Internal Dynamics of Active Volcanoes and Hydrogeological-Environmental Risks - XXVIII

Maria Clara Zuluaga Vélez

Tutor: Professor Benedetto De Vivo

Co-Tutor: Professor José Miguel Nieto

NAPLES-ITALY

2017

Index

To my parents for they support
And to Gianluca for make this way imaginable.

Acknowledgments

I would like to thank Professor De Vivo for the opportunity to perform this PhD project and his valued advices, to Professor Lima for her valuable professional and life advices, to Claudia Canatelli and Stefano Albanese for their support and to all the members of the University of Napoli Federico II Prof. De Vivo research Team: Angela Doherty, Giulia Minolfi, Carmela Rezza, Rosario Esposito, Matar Thiombane, Denis Zamboni, Chengkai Qu for the good advices, companionship and the infinite coffees in the bar.

I also want to thank José Miguel Nieto and his geology group at the University of Huelva for their support during field work in Spain. The owners of the beauty salon in Huelv, Aroche and El Campillo for their collaboration. The University of the Philippines for their help during the fieldwork in Zambales. Also to Dr. Sadeghi for his geostastistic advices.

To Robert Ayuso, Rani Indela, Sayon Robinson and to U.S. Geological Survey for the possibility to perform the isotopic analyses in the laboratory in Reston, USA. To Professor Renguang Zuo for the opportunity to work in the laboratory of the China University of Geosciences Wuhan and their team for the hospitality, also Daniela Zuzolo for the advices and her friendship during the China experience.

También quiero agradecer a las personas con quien compartí en estos cuatro años de trabajo, aventuras y aprendizaje, no solo de geoquímica ambiental sino sobre la vida, conociendo culturas, comidas, aromas, paisajes e idiomas diferentes. Este espacio no sería suficiente para agradecer todas las personas que pasaron por mi vida quedándose en mi corazón en estos cuatro años. Gracias a Rosetta Colombo por su amor y sus recetas, a Carmine Minichello por su calamarata, 'mpepata di cozze y los otros suculentos platos, a Michele Lapolla por la pizzica y sus paseos en motorino por su amada Nápoles, a Luigi Lavanga por sus cuentos increíbles, a Ilaria Cibelli por los spriz en nuestra banquita, a Nicoleta Zanaleti por las charlas interminables en la cocina, A Fulvio por sus correcciones ortográficas, a Federico Weber por sus cenas y hospitalidad, a Eduardo, Ciro y Vittorio por su buen humor y capuchinos con corazones, a Lola y Carmen por las tardes de tapas en Huelva, a los señores de la ferrocarril del puerto de Huelva por parar el tren para rescatarme en medio de un campo, a los mineros artesanales de arenas negras por el aventón en el "volcó" de su camión hasta el Monte Pinatubo, a Mattew Merrill por su simpatia y llevarme en bicicleta por los senderos de Reston, a Annia, Celeste Lohr y Sally the cat por hacerme sentir como en casa, a Ed por su comida china, a Guxion por mostrarme su cultura, a Marco Cavaliere por i cocci, China, los cuentos chinos, los paseos en la vespa naranja y todo su cariño en los momentos difíciles lejos de casa, A Nacho Piedrahita y Paula Castillo por ser mis raíces en esta tierra lejana, a mis hermanos Andrés y Ana por su apoyo, a mis padres Lucia y Gustavo por su paciencia y soporte. Muy especialmente quiero agradecer Gianluca Norini por su amor, paciencia, dedicación y compañía, sin él, este proyecto no habría sido completado. Por ultimo quiero inmortalizar en esta tesis mi amor profundo por Nápoles, ciudad que me hace suspirar, queda claro el dicho popular: "vedi Napoli e poi muori".

Abstract

In the last decades, many efforts have been made to predict and monitor the effects of natural and anthropogenic phenomena that can affect the quality of life of the human beings. Among these potentially dangerous phenomena, the geochemical contamination of the water, soils and sediments requires an accurate knowledge of the distribution and origin of the potential harmful elements in the environment for the assessment and management of the consequent risks. The wide availability of new and advanced tools, like Geographic Information Systems (GISs), sophisticated analytical techniques (ICP-MS and Pb isotopic ratios) and geostatistics (multivariate statistics), provides a efficient methodology for geochemical mapping and environmental analysis, depicting the distribution and interactions among hazardous phenomena, geogenic and anthropogenic sources and objects exposed to the risk.

This thesis investigates advanced techniques to develop geochemical exploration studies for the environmental quality assessment in the Huelva Province (Spain) and Zambales Province (the Philippines), which has been analyzed through the calculation of accurate geochemical maps and the analysis of the relationships between geochemical anomalies and contamination sources. One of these techniques is the use of Pb isotopic ratios, measured in soil and human hair, as signature to identify the anthropogenic and geogenic sources of harmful elements in the environment.

The Huelva Province, where three sub-areas have been selected, is located in Andalusia, in the southwest of the Iberian Peninsula. Soil and human hair samples were collected prepared and analyzed using ICP-MS. These analytical results have been used in a GIS to obtain accurate geochemical maps and an environmental hazard assessment based on the calculation of contamination factors and pollution index. To individuate the source of contamination, lead isotopic analysis where performed for selected soil and human hair samples. The spatial analysis of the geochemical concentrations and isotopic signatures allowed to recognize the main relationships among geology, land use and the occurrence of harmful elements in the environment and human beings. The environmental assessment shows sectors in the three study areas where multi-element concentration of metals may represent a risk for the human health. Lead isotopic analysis for soil and human hair evidenced two signatures of the contamination sources, one related to the mineralization and the other to pesticides and gasoline.

The Zambales Province is located in the western part of the Luzon Island in the Philippines. Stream sediment samples have been collected, prepared and analyzed with ICP-MS. Geochemical elements have been grouped in three associations by means of a factor analysis. Finally, the spatial distribution of the element concentrations in the environment has been identified with a new GIS algorithm

developed to produce geochemical maps at the watershed level. The calculation of background values for harmful elements has been accomplished for the first time in the area. Anomalous sectors with concentration of geochemical elements well above the background values were identified, representing a potential environmental risk. The study also identified the occurrence of metals and other elements of economic interest.

Additional researches, not strictly related to the main topic of the thesis, have been carried out during the PhD. In these studies, GIS tools have been used to analyze different factors having an influence on the environment, like marine and coastal pollution, and hydrogeological, seismic and volcanic events, to provide a comprehensive view of a territory and its relationships with the human activities. These studies have been focused on:

1) marine and coastal pollution in the area of the decommissioned industrial site of Bagnoli, in the city of Naples (Italy). Sediment samples have been analyzed for inorganic elements, Polychlorobiphenyls (PCB) and Polycyclic Aromatic Hydrocarbons (PAHs). Geochemical maps and identification of areas under geochemical risk in the marine area have then been produced by means of a GIS;

2) hydrogeological events, with the definition of a new GIS algorithm for semi-automated and accurate alluvial fans mapping over wide regions;

3) volcano-basement interplay, with the analysis and GIS modeling of the relationships between the evolution of the Colima Volcanic Complex (Mexico) and the occurrence of active volcano-tectonic and regional faults;

4) seismic risk, with the GIS analysis of the spatial relationships among geological, geotechnical and geophysical data, for the seismic characterization of the sector of the Lombardia Region (Italy) affected by the May-June 2012 seismic crisis.

The different studies that have been carried out during the PhD program represent a contribution toward the definition of efficient tools and technical procedures, useful for accurate natural and anthropogenic hazards assessment, risks mitigation and better land use plans.

Chapter 1 – Introduction

The main objective of geochemistry is to quantify the composition of the Earth and understand the processes that control the distribution of the chemical elements, for both theoretical and applied purposes (Goldschmidt 1937, 1954). In the past, applied geochemistry has been mainly focused on the identification of mineral deposits of economic interest, allowing the development and improvement of sophisticated techniques, like elemental analysis, geochemical mapping and isotopic analysis.

In the last decades, the increasing concern about the negative effects of human activities on the environment prompted an extensive use of the same geochemical techniques, to determine the degree and extension of the environmental contamination and its implications on the quality of the soil, sediments, air and water. Geochemical analysis in environmental studies allow the visualization, understanding and classification of the complex relationships among the geogenic and anthropogenic sources of chemical elements, their concentration in the environment and the influence on the living being. One of the consequences of these complex relationships is the variable distribution of the chemical elements over the Earth surface, which can be studied with the production of geochemical maps.

The objective of geochemical mapping is to predict the concentration of single elements in an unknown area, based on the analytical results from scattered sampling points. The type, number and location of the samples, with respect to the characteristics of the territory under analysis and the objective of the study, have a great influence on the final geochemical maps. For example, at least two different approaches can be used depending on the nature of the samples. The first uses interpolators based on the autocorrelation principles, applying the concept of Euclidian points distance regardless of the topography and complexity of the drainage in a determinate area. These interpolation techniques, like kriging and Inverse Distance Weighted (IDW), consider each sample in relationship with the nearest neighbors and works properly for continues sampling grids of soil, marine sediments and air (e.g., Matheron, 1965; Wakernagel, 1995; Webster and Oliver, 2001; Lima et al., 2003; Zumlot et al., 2009). Geochemical maps from scattered samples can also be calculated considering the geomorphological features, drainage characteristics and hydrodynamic processes of the area under study. These methods are suited where the proximity of the sampling points on a map does not often imply that they share correlated variables, like in the case of stream sediment and stream water samples (e.g., Spadoni et al., 2005; Spadoni, 2006; Zuluaga et al., 2017). The geochemical maps produced with different sampling and interpolation methodologies are required to analyze the spatial relationships between the

concentration of chemical elements in the environment and the characteristics of the territory, necessary to identify the sources of geochemical anomalies and to evaluate the environmental risk factors.

In recent times, the availability of new and advanced techniques provides tools for accurate geochemical mapping, environmental hazard assessment and identification of contamination sources. The methods used in the present study constitute a complete suit to obtain reliable results in areas affected by environmental contamination. These techniques include geochemical analyses to determine the composition of soil, sediment and human hair samples, univariate and multivariate statistics, geochemical mapping, Pb isotopic analysis to identify the origin of pollutants, and assessment of environmental risk.

The objective of the thesis is to develop geochemical exploration studies for the analysis of the environmental quality and the evaluation of the risk in areas with diverse characteristics. The study areas have been selected in the Huelva Province (Spain), the Zambales Province (the Philippines), and, subordinately, the Bagnoli site (Italy). These areas have different geology, climate, land use and knowledge of the geochemical concentrations in the environment, but all of them have been submitted to an intense industrial use and/or mining activity.

1.1. Huelva Province (Chapter 2)

The Huelva Province, where three sub-areas have been selected for this study, is located in Andalusia, in the southwest of the Iberian Peninsula. The Province has heterogeneous geology, from metamorphic and igneous rocks with volcanic massive sulfide ore deposits, to sedimentary rocks and recent alluvial and coastal deposits. The province is characterized by a Mediterranean climate with low precipitation, poor soil development and low vegetation cover. It is surrounded by two important industrial complexes and a huge mining district. Also, the agricultural activity is spread in the whole province. The area has a long history of geochemical studies, mainly devoted to the identification of ore deposits.

The three case studies were selected to compare the role of the geology and land use in the distribution and the potential risk of elements harmful to health. To analyze the concentration of the selected potentially toxic metals in the environment and their presence in the human beings, soil and human hair samples were collected, prepared and analyzed using ICP-MS.

These analytical results have been used in a GIS to obtain accurate geochemical maps of the study areas and an environmental hazard assessment, based on the calculation of contamination factors and pollution index compared to the Andalucía Region environmental regulations (CMAJA, 1999). Also, selected soil and hair samples were prepared for ICP-MS Pb isotopic analysis to determine the geogenic or/and anthropogenic origin of contamination in the three areas. The spatial analysis of the geochemical concentrations and isotopic

signatures allowed to recognize the main relationships among geology, land use and the occurrence of harmful elements in the environment and human beings.

The results obtained in the Huelva Province are reported in the article: Zuluaga M.C., Norini, G., Ayuso, R., Lima, A., Nieto, J.M., Albanese, S., De Vivo, B. *Geochemical mapping, environmental assessment and Pb isotopic signatures of geogenic and anthropogenic sources in El Campillo, Aroche and Huelva town (Spain)*, submitted for publication in the Journal of Geochemical Exploration.

1.2. Zambales Province (Chapter 3)

The Zambales Province is located in the western part of the Luzon Island in the Philippines. The area is characterized by the presence of the active Mount Pinatubo volcano and the abandoned Dizon porphyry Cu mine. The area is dominated by forests, intense rainfalls and a dense drainage network. In the area there are not published works related to environmental geochemistry. The study was performed in order to analyze the contribution of the active volcano and the abandoned mine to the dispersion of the chemical elements in the environment through the dense drainage network.

Stream sediment samples have been collected, prepared and analyzed with ICP-MS. By means of a factor analysis (FA) geochemical elements have been grouped in three associations. Finally, the spatial distribution of the element concentrations in the environment has been identified with a new GIS algorithm developed to produce geochemical maps at the watershed level. The study allow a first assessment of the background values, an environmental risk analysis based on available reference concentration values (VROM, 2000) and the evaluation of spatial relationships among geochemical anomalies, geology and the occurrence of potential mineral resources.

The results obtained in Zambales Province have been published in the paper: Zuluaga, M.C., Norini, G., Lima, A., Albanese S., David, C.P., De Vivo, B. 2017. *Stream sediment geochemical mapping of the Mount Pinatubo-Dizon Mine area, the Philippines: Implications for mineral exploration and environmental risk*. Journal of Geochemical Exploration. 175, 18–35.

1.3. Other studies about geologic hazard, environmental geochemistry and GIS (Chapter 4)

As mentioned above, GISs have wide applications for the analysis of different factors controlling the geological evolution and environmental risks of an area. During the PhD course, the same GIS tools used for the environmental geochemistry analysis of the Huelva Province, Zambales Province and Bagnoli area (*Chapters 2 and 3*) have been applied for the analysis of marine and coastal pollution, and volcanic, tectonic,

hydrogeological and seismic processes and related risks. The main outcomes of these studies are listed below and have been published or are under consideration for publication as scientific papers and technical reports.

A. Environmental hazard assessment in the Bagnoli site (Italy), with the analysis of chemical elements, Polychlorobiphenyls (PCB) and Polycyclic Aromatic Hydrocarbons (PAHs) and the geochemical mapping and environmental assessment of the marine area, with the application of the intervention limits established by the Italian law of 2009 (*Chapter 4.1*). This work is in progress, and will be published in the: *Geochemical Atlas of sea sediments in Napoli and Salerno Gulfs*, Aracne Editrice, Roma;

B. Delineation of alluvial fans from Digital Elevation Models with a GIS algorithm for the geomorphological mapping of the Earth and Mars (*Chapter 4.2*). This work is already published in Norini, G., Zuluaga, M.C., Ortiz, I.J., Aquino, D.T., Lagmay, A.M.F., 2016*., Delineation of alluvial fans from Digital Elevation Models with a GIS algorithm for the geomorphological mapping of the Earth and Mars.* Geomorphology, 273, 134–149.

C. Basement-volcano interplay in the Colima Volcanic Complex: origin and behavior of active faults systems in the edifice interior (*Chapter 4.3*). This work is accepted for publication in Norini, G., Agliardi, F, Crosta, G., Groppelli1, G., Zuluaga, M.C., 2017., *Basement-volcano interplay in the Colima Volcanic Complex: origin and behavior of active faults systems in the edifice interior. Volcán de Colima-Managing the Threat*, Varley N., Komorowski J.C. (Eds.), Springer-Verlag, Berlin, Heidelberg.

D. Acquisition and processing of geological, geotechnical and geophysical data for the seismic characterization of a sector of the Lombardia Region (Italy) affected by the 2012 seismic crisis (*Chapter 4.4*). The work is already published as a technical report in the official Lombardia Region web site. Norini, G., et al., 2015., Acqisizione ed elaborazione di dati geologici, geotecnici e geofisici per la caratterizzazione sismica di parte del territorio lombardo ricadente nell' Area Pilota del Progetto GeoMol-Programma Europeo "Spazio Alpino". Rapporto Tecnico. Regione Lombardia.

Chapter 2 – Huelva Province case study

This article was submitted for publication to the Journal of Geochemical Exploration.

Geochemical mapping, environmental assessment and Pb isotopic signatures of geogenic and anthropogenic sources in three localities in SW Spain with different land use and geology

Maria Clara Zuluaga[1], Gianluca Norini[2], Robert Ayuso[3], Annamaria Lima[1], Jose Miguel Nieto[3], Stefano Albanese[1], Benedetto De Vivo[1]

[1]Dipartimento di Scienze della Terra, dell'Ambiente e delle Risorse, Università di Napoli Federico II, Napoli, Italy

[2]Istituto per la Dinamica dei Processi Ambientali - Sezione di Milano, Consiglio Nazionale delle Ricerche, Milano, Italy

[3] U.S. Geological Survey (USGS), Reston, Virginia, USA

[4] Departamento de Geología, Universidad de Huelva, Huelva, Spain.

Abstract

The Huelva Province located in the southwest of Spain has a long history of mining, industry and agriculture. These anthropogenic activities have a potential environmental impact, with the dispersion of chemical elements in soils and water, and a potential negative effect on the food production and human health. In this study, the concentration of harmful chemical elements in the soil of three case study areas in the Huelva Province are analyzed and related with the land use and local geology. These study areas correspond to the agricultural Aroche village, mining El Campillo site and urban and industrial in the town of Huelva. Topsoil samples have been collected and analyzed by ICP-MS. The analytical results have been used to calculate geochemical maps for As, Cd, Co, Cr, Cu, Hg, Ni, Pb and Zn. Also, the background ranges for these elements and the environmental limits suggested by the Andalusia Government have been used to calculate the contamination factor and pollution index, useful to identify the areas that represent a risk for the population. Finally, lead isotopic analysis of topsoil samples have been carried out, to identify the geogenic and anthropogenic origin of the geochemical anomalies detected in the three study areas. Similarly, human hair samples of donators living in these areas have been analyzed for lead isotopes, to trace the diffusion of selected harmful chemical elements through the tropic chain. The study shows that anomalies of harmful elements are present in the topsoil of the three areas, even in the rural Aroche site, where neither industrial nor mining activities occur. The spatial distribution of those geochemical anomalies is associated to the local geology and land use. Lead isotopic analysis evidenced two well defined signatures of the contamination sources in topsoil and human hair, one related to ore deposits and mining and the other to pesticides and gasoline lead sources.

Keywords: Lead isotopic signature, ICP-MS, environmental risk assessment, Iberian Pyrite Belt, geochemical mapping.

2. 1. Introduction

In the last decades, much effort has been made in the understanding of relationships between environmental quality and human health, which are strongly dependent on economic activities, geological setting, regional and local soil characteristics, and patterns of land use. In order to better understand these complex relationships, significant attempts have been made to acquire realistic geochemical background values of metals and other materials thought to pose threats to human health, and identify possible contamination sources (e.g. Salminen et al., 2005; De Vivo et al., 2016). With the use of new and widely available analytical techniques (e.g., ICP-MS), it has become possible to determine metal concentrations in water, air, stream sediments and soils.(e.g. Guillen et al., 2011; Li et al., 2014; Rezza et al, 2017). Also, it is possible to measure isotopic signatures to infer the geogenic or anthropogenic provenance of the elements in the environment. For example, lead isotopes are commonly used as isotopic tracers of pollution sources (e.g. Hansmann and Köppel 2000; Komárek et al. 2008; Adánez-Sanjuán et al., 2016).

Such geochemical studies are required in order to establish realistic metal concentration baselines so that environmental regulations can be implemented and result in effective management of natural resources (e.g. CCME. 1995; Vrom, 2000). One of the most important concerns in terms of human health is soil quality and its role in the production of food due to the potential content of harmful elements, its close relationship with regional geology, effects of atmospheric processes leading to metal deposition. Soil contamination due to heavy metals and metalloids represents the source of a severe potential hazard for ecosystem equilibrium and health of humans and other biological systems (Nagajyoti et al., 2010). Analysis of soil pollution and related environmental hazard requires in-depth knowledge of the spatial distribution of contaminants. This can be achieved through the production of maps depicting the geochemical concentrations in soil, the contamination factors, and the pollution index (e.g., Hakanson, 1980; Qingjie et al., 2008; Banu et al., 2013; Zuluaga et al., 2017).

In this paper we focus on three case studies in southwester Spain. All are in Huelva Province, share a type of Mediterranean climate with low precipitation and are separated by only a few kilometers. Each area, however, has different geologic settings and different land use (Fig. 2.1). From north to south the areas are designated as Aroche, El Campillo and the town of Huelva. The study areas have low vegetation cover and the soils are poorly developed. The regional economy is based on mining, industrial complexes linked to the mining industry, oil refinery, animal husbandry, agriculture, and tourism. The three case studies were selected to compare the role of the geology and land use in the distribution and the potential risk of elements harmful to health. We analyzed using ICP-MS a selection of heavy metals in soils and human hair samples collected in Aroche, El Campillo and the town of Huelva. These analytical results have been processed in a Geographic Information System (GIS) to obtain geochemical maps. The data were used to provide an environmental hazard assessment based on the calculation of contamination factors and pollution indices. We also selected soil and human hair samples for ICP-MS lead isotopic analysis to identify the geogenic and/or anthropogenic origin of contamination.

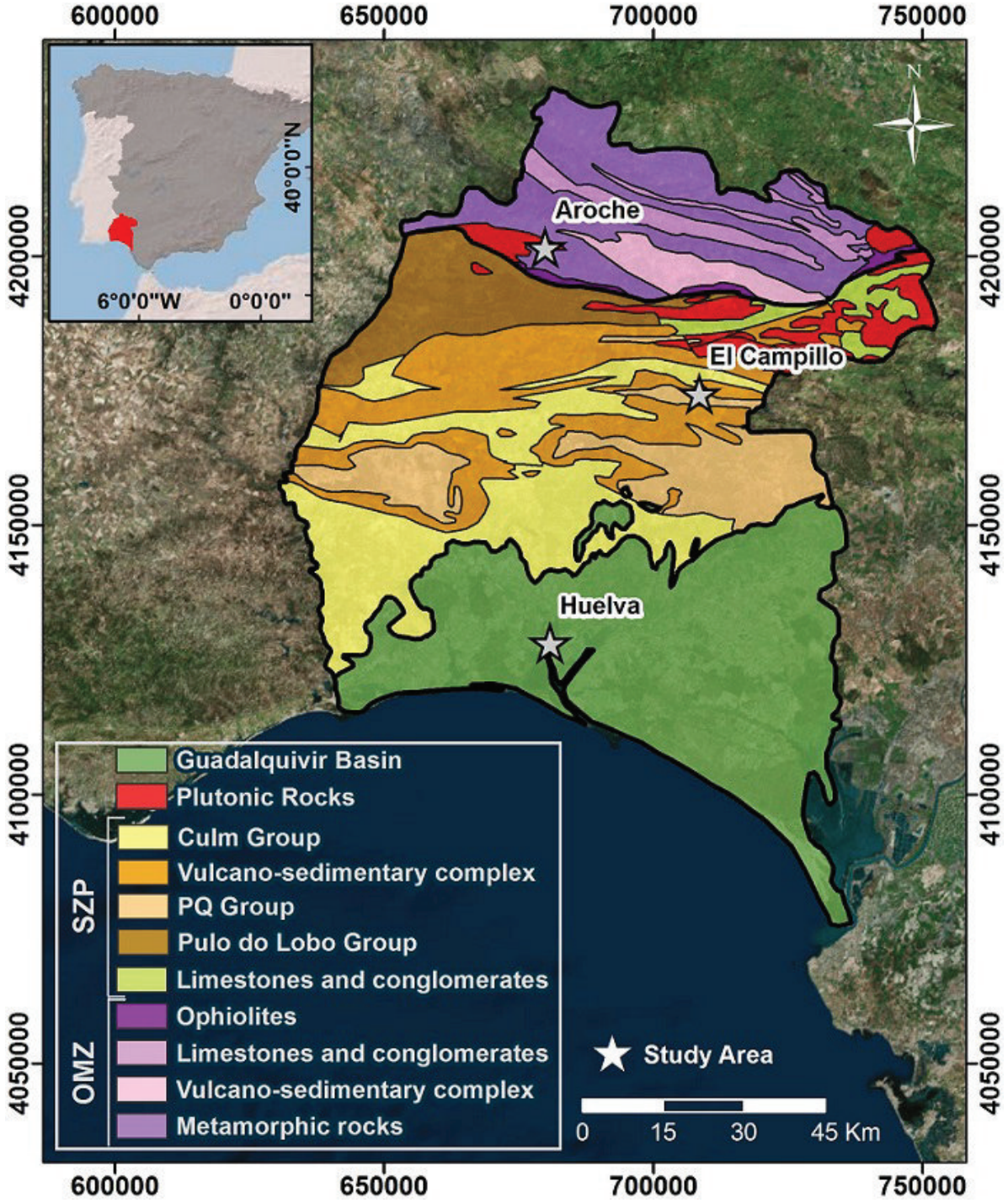

Figure 2.1. Map with the localization of the study area and the schematic geology (modified from Apalategui-Isasa et al., 1979; Junta de Andalucía, 1998; 1999)

2.2. Background: geology, soil, mineralization, climate and land use of the study areas

2.2.1. Geology

Huelva Province is divided in three main geological blocks (Lotze, 1945; Julivert et al., 1972; Vera, 2004) (Fig. 2.1). In the northern part, the Ossa Morena Zone (OMZ) crops out in the Sierra de Huelva area, characterized by Precambrian and Paleozoic units (Julivert et al., 1972; Azor, 2004; Vera, 2004) (Fig. 2.1). Southward, the Upper Paleozoic South Portuguese Zone (SPZ) crops out (Crespo-Blanc and Orozco, 1991; Simancas, 2004) (Fig. 2.1). More to the south, the Guadalquivir Basin, composed of sedimentary Cenozoic rocks, overlies the SPZ and is partly covered by recent sediments from the Holocene to the present (Civis et al., 2004) (Fig. 2.1).

The OMZ is a continental block mainly composed of metamorphic rocks with ages ranging from the end of Proterozoic to the end of the Carboniferous. This block was sutured with the SPZ during the Variscan orogeny along a narrow ophiolitic belt composed of metabasitic rocks (Quesada et al., 1994; Gómez-Pugnaire et al., 2003). The OMZ is made of a deformed succession of schist, black quartzites, slates, sandstones, conglomerates, mafic granulites, gneisses and amphibolites, interbedded with volcano-sedimentary rocks and limestone, and intruded by plutonic rocks (Azor, 2004) (Fig. 2.1).

The SPZ is a thin-skinned fold and thrust belt (Lotze, 1945; Julivert el al., 1972; Mantero et al., 2007). The SPZ is in contact to the OMZ block through the Variscan ophiolitic suture zone, where rocks having oceanic affinity crop out (Bard and Moine, 1979; Crespo-Blanc and Orozco, 1988; Crespo-Blanc and Orozco, 1991; Castro et al., 1996a, b). The SPZ is composed of igneous and sedimentary rocks from Devonian to Carboniferous (Fig. 2.1) (Oliveira el al., 1983). The Pulo do Lobo domain is mainly constituted by phyllitic and quartzitic rocks, characterized by an intense deformation and interpreted as an accretionary prism (Moreno, 1987) (Fig. 2.1).

To the south is the Iberian Pyrite Belt (IPB), which is composed of (1) slates with intercalations of quartzite levels of the Middle Devonian to Upper Devonian PQ group; (2) a volcano-sedimentary complex of Upper Devonian age; (3) the Culm Group flysch succession (Moreno, 1987) (Fig. 2.1). The IPB probably is the largest volcanogenic massive sulfide (VMS) ore province in the world (Tornos, 2008; Fernandez-Caliani, 2008). The IPB contains over 85 VMS deposits. The VMS deposits occur as stratabound lenses at several stratigraphic horizons within black shales and felsic volcanic rocks of the volcano-sedimentary complex (Saez et al., 1999). Some of these deposits have been mined since the

pre-Roman times for precious metals and copper from gossan and underlying supergene enrichment zones of the exposed VMS deposits (Salkield, 1987). The SPZ borders to the south with the Tertiary Guadalquivir Basin, composed by deltaic and shallow marine sediments and covered by Quaternary lagoon and estuarine sediments (Civis et al., 1987; López-Gónzalez et al., 2006) (Fig. 2.1). The three study areas are located in the three different blocks described above. Aroche town is in the OMZ block, El Campillo, within the Rio Tinto mines area, is located in the IPB of the SPZ block, and the town of Huelva is in the Guadalquivir Basin (Fig. 2.1).

2.2.2. Climate and land use

The regional climate is Mediterranean but it is influenced by the Atlantic Ocean, which produces long dry summers and short mild winters. Precipitation is around 500 mm/year near to coast (town of Huelva), increasing northward up to 1000 mm/year in the mountainous Aroche area (Galván et al., 2016).

Land use is directly related to geology and topography. The area of Aroche has 3233 inhabitants and is one of the main settlements in the Sierra de Huelva region. It is characterized by forests with oak, cork oaks and other species favoring breeding pigs, important for the Spanish industry of Iberic ham (INE, 2014) (Figs. 2.1, 2.2). Also, olive plantations for the production of olive oil are located in this region (Fig. 2.2). Pyrenean oak and chestnut forests are present in the steep slopes (Fig. 2.2). The dominant soil is the lithic leptosol (CSIC-IARA, 1989).

The mining area where the second area is located, el Campillo, is characterized by abundant polymetallic sulfides that have been exploited for over 5000 years (Fig. 2.3A). The town of El Campillo has 2169 inhabitants (INE, 2014). The decline of mining in the 80s, due to falling prices, emergence of other mining sites and the use of other metals, prompted the area to look for new economic activities, which included developing citrus crops around Minas de Riotinto, Salamea La Real, Nerva and Campofrio (Fig. 2.2). El Campillo is traversed by the Rio Tinto river that is characterized by acidic waters (pH 1.5 and 2.5) and high contents of heavy metals (mainly iron, copper, cadmium, and manganese) (Fig. 3B). In general, the soil is made of poorly developed regosols, leptosols and cambisols (Mudarra et al., 1989).

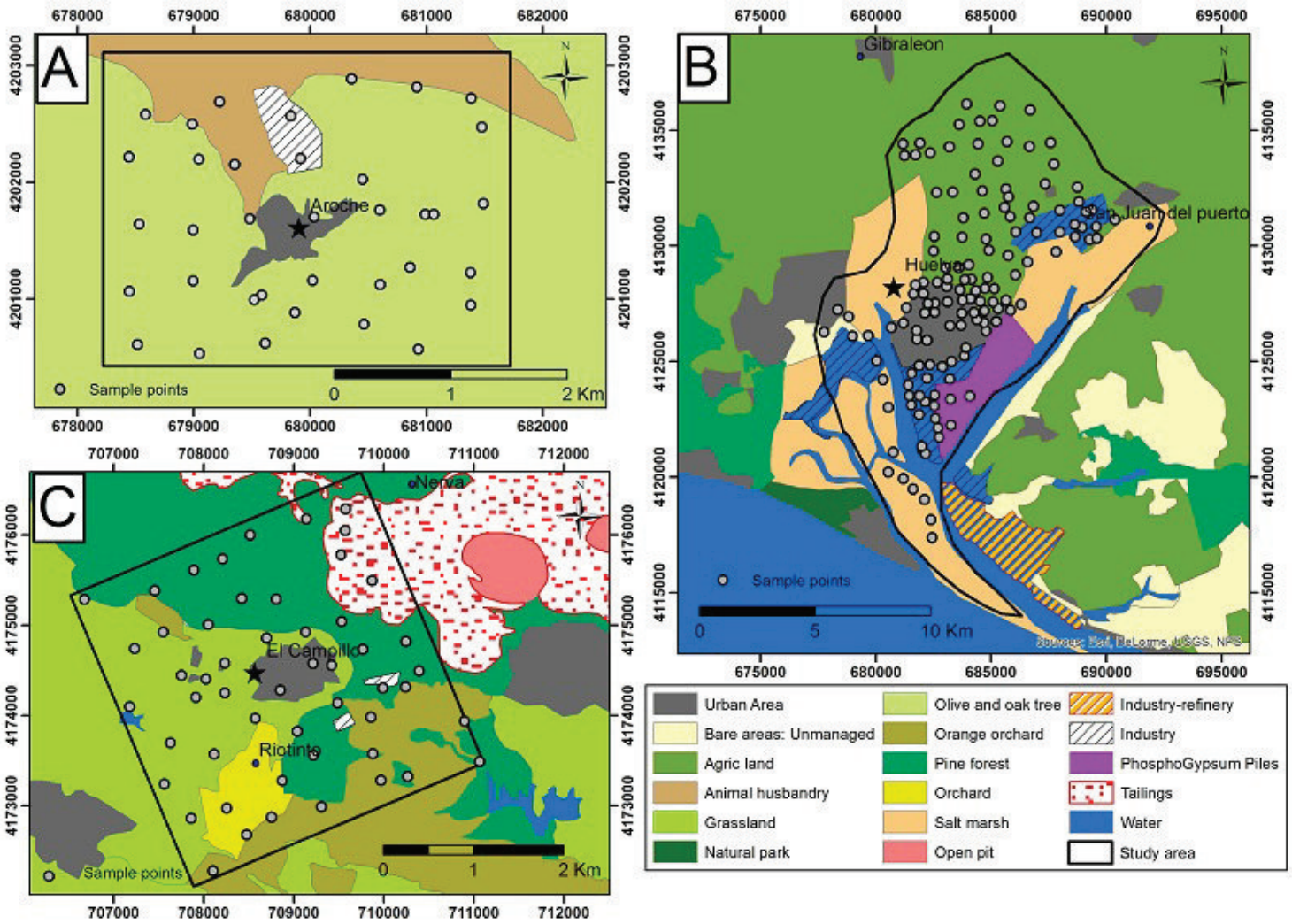

Figure 2.2. Land use map and the sampling points of the three study areas. (A) Aroche, (B) Huelva, (C) El Campillo

The town of Huelva has 519,229 inhabitants and is located at the confluence of Rio Tinto and Odiel rivers. The area is characterized by smooth relief, low hills and coastal plains (Fig. 2.2) (INE, 2014). This area is the site of intensive agricultural activities (mainly strawberry and citrus crops) (Fig. 2.2). Also, the town became an important industrial center since the 60s, and sites such as an oil refinery, electrical power site, and other industrial activities (production of fertilizer, cellulose, etc.). All of these human endeavors release contaminants into the environment (Guillen et al., 2011). The soil in the area is poorly developed. Marsh areas are dominated by saline soils, almost exclusively solonchacks. Arenosols mainly occurs along the coast line. In sectors with the extensive presence of organic matter and/or where the freatic level is close to the surface, the soil is mainly of the cambisols and gleysols types (Mudarra et al., 1989).

2.3. Sampling, analytical methods and geochemical mapping

2.3.1. Soil sampling, sample preparation and ICP-MS analysis

Sampling was done in two different periods, in the autumn of 2007 (Guillen et al., 2011) and in the spring of 2013. 229 topsoil samples have been sampled following the protocols for geochemical studies suggested by Salminen et al. (1998). Topsoil has been sampled combining five individual specimens collected between 0 and 25 cm depth at the center and vertices of a 2 m wide cross. In the first sampling campaign 145 top soils were collected in the town of Huelva over an area of 163 km^2 using a 0.5 x 0.5 km grid in urban and industrial areas and 1.0 x 1.0 km in rural areas (Guillen et al., 2011) (Fig. 2.2). In the second sampling campaign the following samples were collected: 4 topsoil in the town of Huelva, 52 topsoil using a sampling grid of 0.5 x 0.5 km over an area of 16 km^2 in El Campillo, and 36 topsoil samples using a sampling grid of 0.5 x 0.5 km over an area of 10 km^2 in Aroche (Fig. 2.2).

Each sampling point was documented with photographs, notes, and spatial information, in order to form a complete GIS database. Samples were left to dry thoroughly at room temperature and sieved at <100 mesh fraction (150 µm). The pulps were stored in plastic containers of approximately 30 g and then sent to ACME Analytical Laboratories Ltd (Vancouver, Canada) for chemical analysis by aqua regia digestion followed by ultratrace ICP-MS for the determination of 53 elements: Ag, Al, As, Au, B,

Ba, Be, Bi, Ca, Cd, Ce, Co, Cr, Cs, Cu, Fe, Ga, Ge, Hf, Hg, In, K, La, Li, Mg, Mn, Mo, Na, Nb, Ni, P, Pb, Pd, Pt, Re, Rb S, Sb, Sc, Se, Sn, Sr, Ta, Te, Th, Ti, Tl, U, V, Y, W, Zn and Zr. Accuracy and precision were within acceptable limits. Precision of the analysis was calculated using five in-house replicate and six blind duplicates submitted by the authors. Accuracy was determined using in-house (ACME) reference materials (STD DS10, STD OXC109) (Table 2.1). Analytes were not present at detectable levels using method blanks with six samples provided by the laboratory. Detection limits for Al, Ca, Fe, K, Mg, Na, P, S and Ti range from 0.001 wt. % (Na, P, Ti) to 0.02 wt. % (S), and from 0.01 mg/kg to 5 mg/kg for all the other elements (Table 2.1).

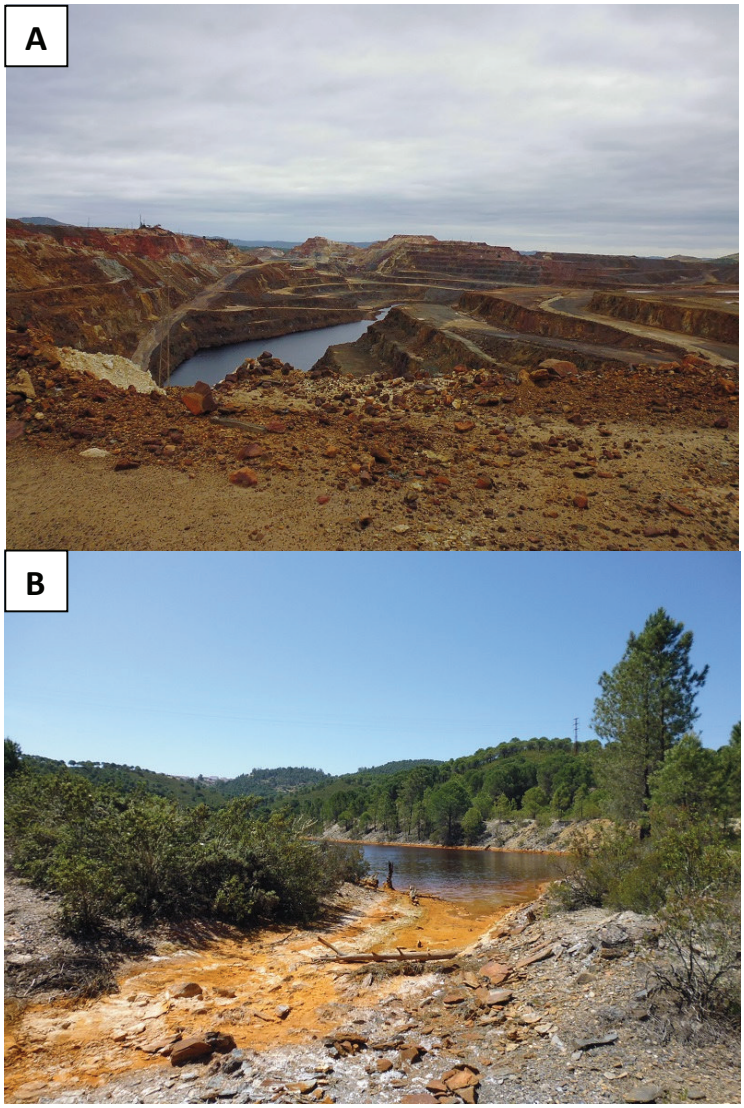

Figure 2.3. (A) Abandoned open pit (Cerro Colorado) near to El Campillo Town. (B) Rio Tinto river near to El Campillo.

Analyte	Method	Unit	Detection limit (DL)	Accuracy (%)	Precision (%relative percent difference.)
Fe	AQ252	%	0.01	3.97	0.37
Ca	AQ252	%	0.01	4.00	1.88
P	AQ252	%	0.001	4.34	4.11
Mg	AQ252	%	0.01	1.94	0
Ti	AQ252	%	0.001	7.10	3.67
Al	AQ252	%	0.01	5.27	0.97
Na	AQ252	%	0.001	7.96	1.49
K	AQ252	%	0.01	1.58	2.96
S	AQ252	%	0.02	0.57	0.00
Mo	AQ252	mg/kg	0.01	5.67	4.77
Cu	AQ252	mg/kg	0.01	5.11	2.11
Pb	AQ252	mg/kg	0.01	3.92	3.95
Zn	AQ252	mg/kg	0.1	5.48	0.35
Ni	AQ252	mg/kg	0.1	4.29	0.27
Co	AQ252	mg/kg	0.1	3.62	4.65
Mn	AQ252	mg/kg	1	2.46	2.74
As	AQ252	mg/kg	0.1	5.72	1.60
U	AQ252	mg/kg	0.05	4.63	2.32
Th	AQ252	mg/kg	0.1	7.56	6.67
Sr	AQ252	mg/kg	0.5	4.52	5.66
Cd	AQ252	mg/kg	0.01	5.15	0.80
Sb	AQ252	mg/kg	0.02	7.70	1.70
Bi	AQ252	mg/kg	0.02	7.58	3.95
V	AQ252	mg/kg	2	5.04	2.33
La	AQ252	mg/kg	0.5	7.24	3.43
Cr	AQ252	mg/kg	0.5	6.56	4.58
Ba	AQ252	mg/kg	0.5	0.67	5.65
W	AQ252	mg/kg	0.05	0.55	8.43
Sc	AQ252	mg/kg	0.1	8.33	7.14
Tl	AQ252	mg/kg	0.02	1.50	2.16
Se	AQ252	mg/kg	0.1	0.72	0
Te	AQ252	mg/kg	0.02	3.59	0.20
Ga	AQ252	mg/kg	0.1	5.43	2.33
Cs	AQ252	mg/kg	0.02	1.52	2.28
Ge	AQ252	mg/kg	0.1	35.42	0
Hf	AQ252	mg/kg	0.02	33.33	16.67
Nb	AQ252	mg/kg	0.02	0.82	3.09
Rb	AQ252	mg/kg	0.1	5.05	0.72
Sn	AQ252	mg/kg	0.1	5.21	6.25
Zr	AQ252	mg/kg	0.1	2.38	0
Y	AQ252	mg/kg	0.01	7.59	1.54
Ce	AQ252	mg/kg	0.1	2.57	4.32
In	AQ252	mg/kg	0.02	1.45	8.70
Be	AQ252	mg/kg	0.1	4.76	31.75
Li	AQ252	mg/kg	0.1	5.33	2.58

Ag	AQ252	µg/kg	2	3.98	3.22
Au	AQ252	µg/kg	0.2	9.61	13.06
Hg	AQ252	µg/kg	5	0.44	17.67
Re	AQ252	µg/kg	1	0.67	4.00
Pd	AQ252	µg/kg	10	5.15	8.18
Pt	AQ252	µg/kg	2	3.05	11.52

Table 2.1: Detection limits, accuracy and precision for top soil samples in the three study areas. *RPD=relative percent difference.

2.3.2. Hair sampling and analysis

A total of 26 human hair samples were collected at local barber and hairdresser shops in Aroche, Huelva and El Campillo in the spring of 2014. Each hair sample, weighing 10 g, corresponds to one adult donator. An interview with the donators was conducted using a form prepared in advance, including the place of residence, profession, diet and habits. The hair samples were rinsed in purified water, dried at room temperature, stored in plastic containers of approximately 0.1 g, and shipped to Act Labs laboratories (Toronto, Canada) for the determination of 17 elements by ICP-MS (Al, As, Cd, Co, Cr, Cu, Fe, Hg, Mn, Mo, Ni, Pb, Se, Th, U, V, Zn). Accuracy and precision were within acceptable limits. Precision of the analysis was calculated using seven in-house replicate. Accuracy was determined using in-house (ACME) reference materials (NCS ZC 81002b, NCS DC73347a) (Table 2.1). Analytes were not present at detectable levels using method blanks with three samples provided by the laboratory. Detection limits are indicated in table 2.2.

2.3.3. Pb isotopic analysis

To determine whether the content of metals in soils is of anthropic or geogenic origin, 27 topsoil and 18 hair human samples were selected for lead isotopic analysis. The soil samples were selected to account for the different geology and land use within each case study areas (Figs. 2.2 and 2.3). The selection of the hair samples was based on the lead content in order to have a complete range from high to low lead contents represented in the Pb isotopic determinations (Table 2.3).

The soil samples were sieved at <60 mesh fraction (250µm). A leaching procedure has been applied with a 1.5M HCl + 3N HNO_3 solution, which preferentially dissolves amorphous Fe- and Mn-oxyhydroxides, whose coating are considered to catch most of the anthropogenic Pb (Ayuso et al.,

2016). About 200 mg of each sample have been leached with 3 ml of the acid solution, placed in an ultrasonic bath and centrifuged for 5 min. Two fractions of the same sample were produced: one liquid (leached) and one in a solid state (residue). The leached portion of the sample has been first digested in an Ethos Plus Microwave Lab station for 15 min and then placed on warm hot plates to dry at < 50° C. Once dried, the samples have been processed and evaporated using a multistep chemistry procedure with different amount of concentrated HNO_3, concentrated HF, 4N HCL and 0.5N HBr. In order to separate Pb, samples were finally passed thought Pb exchange columns by using an anion-exchange resin, 0.5N HNO3 and 0.5N HBr (Ayuso et al., 2004, 2013, 2016). About 5 g of human hair sample was weighed, cut in pieces of 1 cm, washed with acetone, rinsed with purified water in the sonicator for 10 min, dried at room temperature and dissolved in HNO_3. Then, the same analytical procedure used for the soil samples, including leaching, microwave digestion, multistep chemistry and Pb elution columns, has been applied. Lead isotopic analysis of the processed soil and human hair samples have been run with an ICP-MS in the USGS Radiogenic Isotope Laboratory in Reston (VA, USA).

2.3.4. Statistical analysis and geochemical mapping

Univariate analysis of the elements concentration in the soil and human hair samples collected in the three study areas has been performed (Tables 2.2, 2.3 and Figs. 2.4, 2.5). For statistical computation, data below the instrumental detection limit (DL) have been assigned to ½ of the DL.

The statistical distributions of the geochemical data were converted in lognormal to normalize their values (Reimann and Filzmoser, 2000; Reimann et al., 2005). The cumulative frequency curves (CFCs) of the elements analyzed in the topsoil show inflections and break-points, reflecting the presence of multiple populations, originated by the geogenic and/or anthropogenic contribution to the concentration values (e.g. Fig. 2.5) (Reimann et al., 2005). Seven intervals have been identified on these CFCs using flexion points of the curve near the 10, 25, 50, 75, 90 and 98 percentiles (e.g. De Vivo et al., 2016; Zuluaga et al., 2017). These intervals were used to plot the topsoil geochemical maps (De Vivo et al., 2004; Albanese et al., 2007).

For the study areas of El Campillo and Aroche, the topsoil background ranges have been defined by the analysis of the CFCs, at the first and snappish flex of the curve (Table 2.3 and Fig. 2.5) (e.g.

Reimann et al., 2005; De Vivo et al., 2006; Zuluaga et al., 2017). In town of Huelva, the topsoil background ranges calculated by Guillen et al. (2011) have been used (Table 3). The final topsoil geochemical maps for the selected elements were calculated using the Inverse Distance Weighted (IDW) interpolation method in a GIS (Figs. 2.6, 2.7, 2.8, 2.9).

		As (µg/g)	Cd (µg/g)	Co (µg/g)	Cr (µg/g)	Cu (µg/g)	Hg (µg/g)	Ni (µg/g)	Pb (µg/g)	Zn (µg/g)	Pb208/Pb207	Pb206/Pb207
	Detection Limit	**0.001**	**0.0001**	**0.2**	**0.015**	**0.035**	**0.0004**	**0.15**	**0.04**	**0.3**		
Human Hair Aroche	N° samples	**7**	**7**	**7**	**7**	**7**	**7**	**7**	**7**	**7**	3	3
	Media	0.02	0.04	0.04	0.12	68.6	1.19	0.31	1.38	354.16	2.447	1.159
	Median	0.01	0.03	0.03	0.09	94.50	1.45	0.31	0.77	173.00	-	-
	Range	0.07	0.12	0.10	0.38	137.98	1.79	0.47	4.28	1189.85	-	-
	DesvStas	0.02	0.04	0.03	0.13	52.97	0.59	0.19	1.55	399.12	0.010	0.008
	Max	0.07	0.12	0.11	0.39	138.00	1.85	0.54	4.30	1190.00	2.459	1.168
	Min	0.001	0.0001	0.01	0.01	0.02	0.06	0.08	0.02	0.15	2.441	1.153
	Assimetria	2.38	0.89	1.28	1.80	-0.16	-1.22	-0.14	1.41	1.90	-	-
	95th percentile	0.05	0.11	0.09	0.32	127.80	1.76	0.53	3.82	973.10	-	-
	Kurtosis	6.01	-0.11	1.43	3.45	-1.95	1.61	-1.82	1.12	3.96	-	-
	MAD	0.01	0.03	0.02	0.08	42.63	0.41	0.16	1.03	245.12	-	-
Human Hair El Campillo	N° samples	11	11	11	11	11	11	11	11	11	10	10
	Media	0.04	0.03	0.08	0.06	55.9	1.60	0.71	2.31	321.18	2.450	1.166
	Median	0.02	0.03	0.05	0.06	39.60	1.55	0.54	1.00	203.00	-	-
	Range	0.28	0.05	0.41	0.05	122.80	3.36	1.22	15.98	1018.00	-	-
	DesvStas	0.08	0.02	0.12	0.02	36.85	0.94	0.43	4.64	342.73	0.009	0.003
	Max	0.29	0.06	0.42	0.08	140.00	3.62	1.38	16.20	1120.00	2.460	1.171
	Min	0.01	0.01	0.01	0.03	17.20	0.26	0.16	0.22	102.00	2.436	1.159
	Assimetria	3.22	0.33	2.91	-0.49	1.23	0.61	0.23	3.23	1.97	-	-
	95th percentile	0.17	0.06	0.26	0.08	114.10	3.02	1.27	9.30	1001.00	-	-
	Kurtosis	10.51	-1.56	9.04	-0.43	1.44	1.22	-1.54	10.54	2.65	-	-
	MAD	0.03	0.02	0.06	0.01	27.07	0.65	0.36	1.76	178.91	-	-
Human Hair Huelva Town	N° samples	8	8	8	8	8	8	8	8	8	5	5
	Media	0.03	0.03	0.18	0.12	40.9	2.47	0.75	1.68	564.50	2.446	1.161
	Median	0.02	0.03	0.02	0.08	26.90	2.38	0.46	1.57	320.00	-	-
	Range	0.09	0.04	1.19	0.34	118.10	2.34	2.16	3.96	1975.00	-	-
	DesvStas	0.03	0.02	0.41	0.11	39.50	0.71	0.78	1.37	661.42	0.003	0.004
	Max	0.10	0.05	1.20	0.37	129.00	3.58	2.23	4.19	2180.00	2.451	1.166
	Min	0.01	0.01	0.01	0.03	10.90	1.24	0.08	0.23	205.00	2.442	1.156
	Assimetria	2.61	-0.29	2.77	2.23	1.89	-0.05	1.30	0.79	2.69	-	-
	95th percentile	0.07	0.05	0.83	0.30	103.77	3.46	2.02	3.71	1609.50	-	-
	Kurtosis	7.18	-1.87	7.74	5.35	3.89	0.56	0.58	0.09	7.38	-	-
	MAD	0.01	0.01	0.17	0.06	26.64	0.51	0.55	1.08	307.00	-	-
Italy	Rezza et al., 2017 (average)	36.00	36.90	278.80	388.90	50.27	662.00	1.10	1.23	25.08	-	-
Certified values of human hair	Yoshinaga et al., 1997	0.10	0.23±0.03	0.07	-	15.3 ±1.3	4.42±0.2	-	4.6±0.4	172±11	-	-

Table 2.2: Statistics of human hair samples for the three study areas.

Case Study		As (mg/Kg)	Cd (mg/Kg)	Co (mg/Kg)	Cr (mg/Kg)	Cu (mg/Kg)	Hg (µg/Kg)	Ni (mg/Kg)	Pb (mg/Kg)	Zn (mg/Kg)	$^{208}Pb/^{207}Pb$	$^{206}Pb/^{207}Pb$
Topsoil Aroche	Min	1.20	0.01	9.50	18.50	8.54	13.00	10.20	3.19	18.30	2.446	1.176
	Max	987.10	2.31	40.40	153.10	141.04	246.00	201.90	472.61	675.20	2.452	1.194
	Media	32.72	0.16	18.88	53.97	42.04	71.50	37.64	33.41	88.14	-	-
	Median	4.45	0.06	16.50	43.45	29.33	52.00	23.40	17.63	54.70	-	-
	Range	985.90	2.31	30.90	134.60	132.50	233.00	191.70	469.42	656.90	-	-
	DesvStas	163.67	0.40	7.21	29.70	30.80	58.63	40.19	76.89	123.29	-	-
	Assimetria	5.99	4.94	1.23	1.36	1.90	1.51	2.85	5.63	3.90	-	-
	95th percentile	16.83	0.58	31.06	94.23	94.94	194.10	89.34	59.12	285.09	-	-
	Kurtosis	35.94	26.34	1.41	2.18	3.22	2.18	8.55	32.83	16.25	-	-
	MAD	29.76	0.13	5.27	21.83	19.29	42.50	20.24	23.09	51.06	-	-
	Background	3.71	0.05	16.98	43.65	26.90	43.65	25.12	18.32	53.70	-	-
Topsoil El Campillo	Min	7.00	0.02	0.40	0.60	12.79	34.00	1.40	19.10	17.90	2.439	1.158
	Max	2233.70	3.33	95.50	268.00	1119.34	20922.00	94.60	3494.04	722.90	2.456	1.172
	Media	110.47	0.31	15.55	37.44	125.20	648.79	24.82	220.58	121.42	-	-
	Median	35.05	0.16	15.05	26.55	89.01	146.50	27.70	80.58	92.20	-	-
	Range	2226.70	3.31	95.10	267.40	1106.55	20888.00	93.20	3474.94	705.00	-	-
	DesvStas	319.18	0.55	14.26	45.21	167.05	2885.80	17.71	546.06	130.16	-	-
	Assimetria	6.09	4.31	3.51	3.17	4.82	7.07	1.02	4.91	3.38	-	-
	95th percentile	386.35	0.88	29.05	113.83	251.05	943.00	46.25	1124.31	366.03	-	-
	Kurtosis	40.16	20.24	19.03	12.99	26.29	50.54	3.03	26.93	12.13	-	-
	MAD	89.45	0.22	8.40	24.66	67.65	541.98	14.08	169.00	60.79	-	-
	Background	45.71	0.16	13.49	21.38	83.18	147.91	19.50	89.12	93.32	-	-
Topsoil Town of Huelva	Min	1.70	0.01	0.80	3.00	5.27	9.00	0.90	7.22	13.70	2.435	1.157
	Max	2121.40	25.67	123.70	169.90	10000.00	20117.00	52.10	5270.67	4706.70	2.463	1.189
	Media	72.92	0.86	11.14	35.12	429.91	650.66	16.62	149.06	310.63	-	-
	Median	10.40	0.17	7.70	30.40	50.97	98.00	14.80	35.37	60.10	-	-
	Range	2119.70	25.67	122.90	166.90	9994.73	20108.00	51.20	5263.45	4693.00	-	-
	DesvStas	208.78	2.99	16.00	23.50	1318.13	2498.79	9.57	479.04	697.56	-	-
	Assimetria	7.18	6.66	4.97	2.43	5.95	6.59	0.83	8.92	4.45	-	-
	95th percentile	351.72	2.30	28.98	72.86	1703.53	2338.80	31.82	548.13	1264.66	-	-
	Kurtosis	65.34	46.89	28.41	9.51	39.10	45.62	1.02	92.36	22.01	-	-
	MAD	65.11	0.75	6.88	15.34	404.89	606.03	7.59	128.21	267.70	-	-
	Background (Guillen et al 2011)	8.45	0.13	9.72	45.20	17.60	500.00	24.20	26.80	47.20	-	-
	Maximum values allowed in agric soils (CMJA, 1999)	20.00	2.00	20.00	100.00	50.00	1000.00	40.00	100.00	200.00		

Table 2.3: Statistics, backgrounds, intervention limits of topsoil for the three study areas.

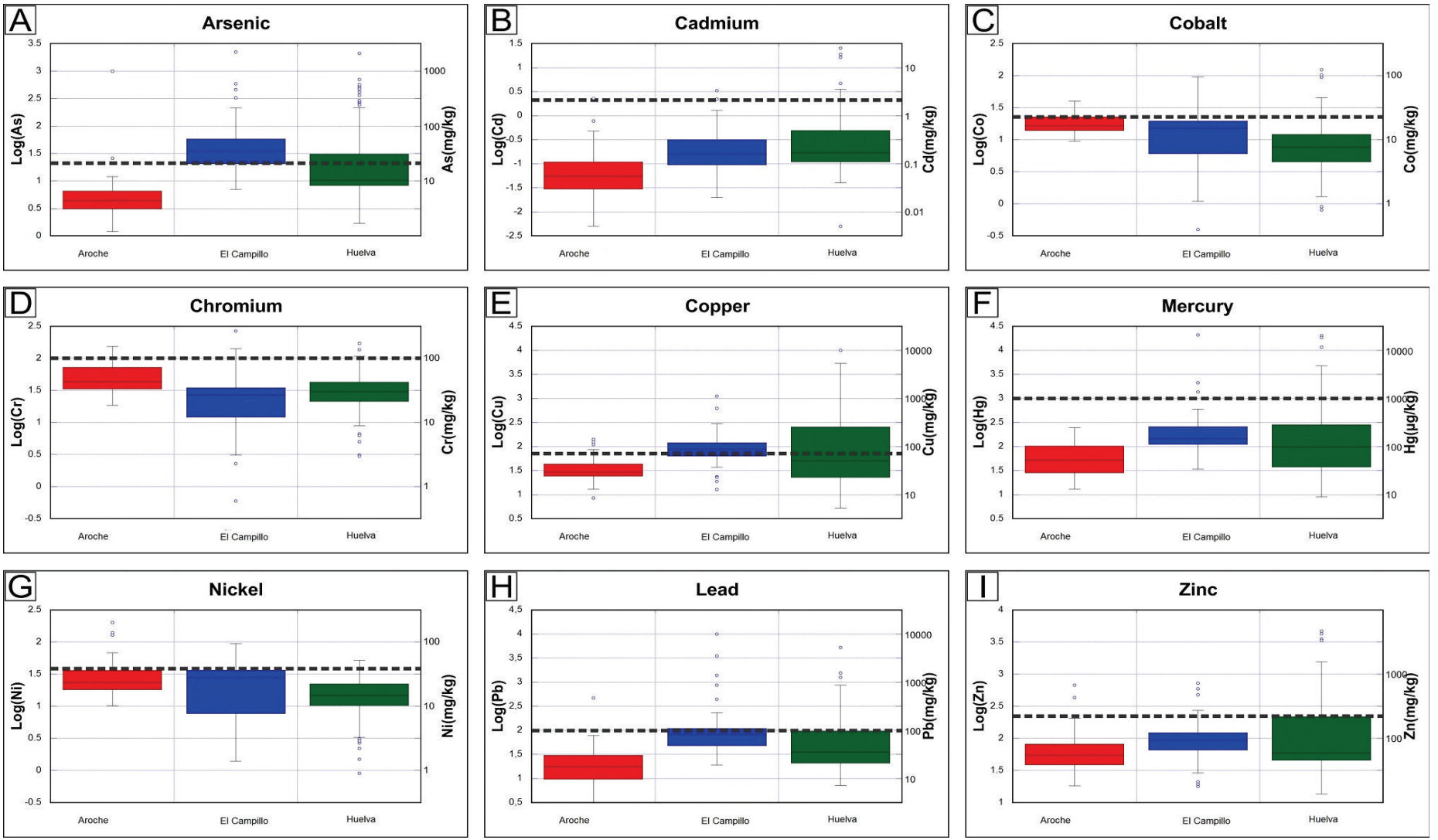

Figure 2.4. Comparison box plot for elemental concentration of top soil in the three study case. (A) As, (B) Cd, (C) Co, (D) Cr, (E) Cu, (F) Hg, (G) Ni, (H) Pb and (I) Zn. The dot line represents the limits allowed for agric land by the Andalusia Government (Junta de Andalucía, 1999).

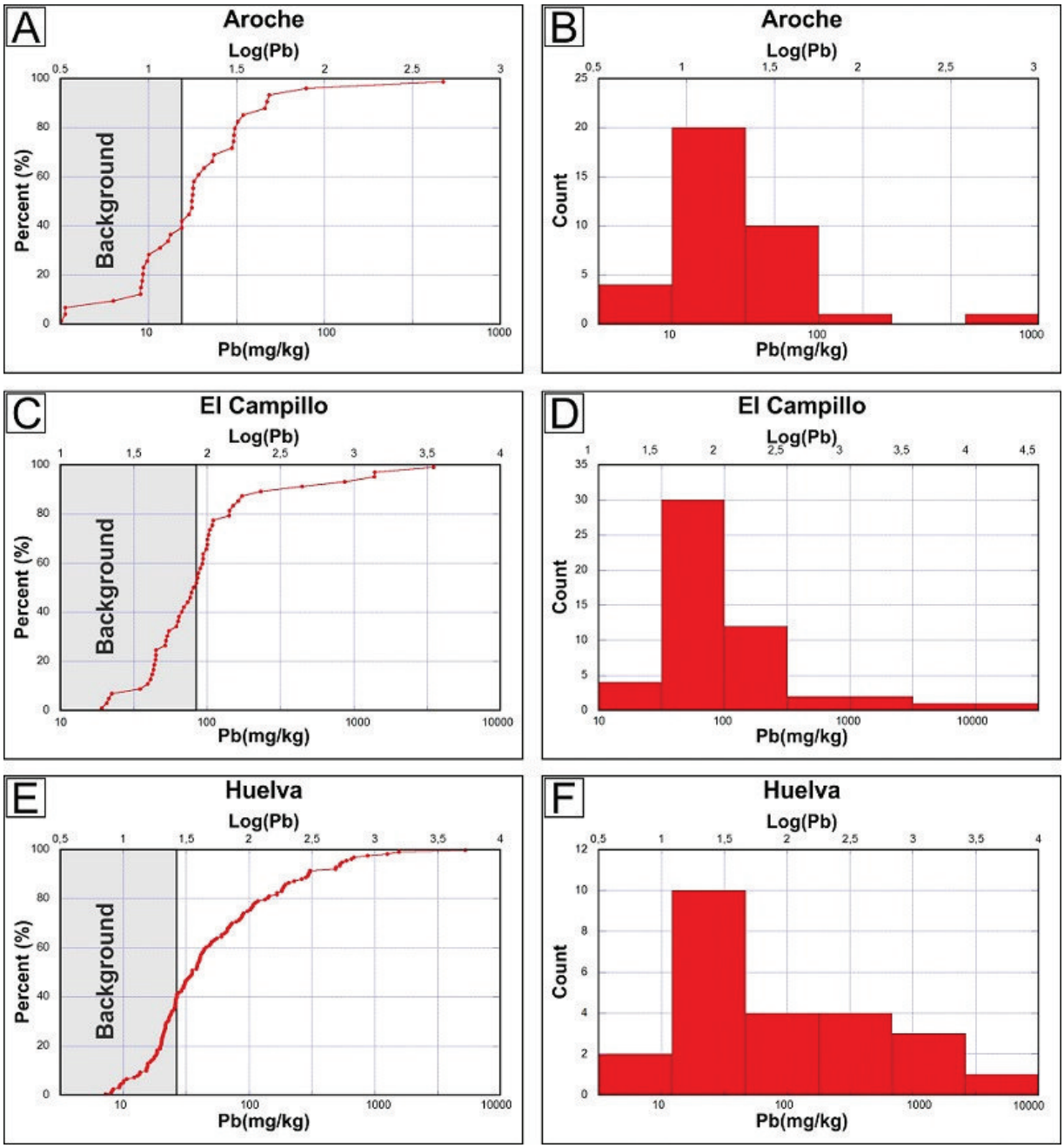

Figure 2.5 Accumulative frequency curves with the background and histograms of lead for the three study case. (A and B) Aroche; (C and D) El Campillo and (E and F) Huelva.

2.4. Results

This section presents the results of the geochemical and isotopic analysis and geochemical mapping of selected elements (As, Cd, Co, Cr, Cu, Hg, Ni, Pb and Zn) in the soils and human hair of the three study areas.

2.4.1. El Campillo mining area

The topsoil of the mining and rural area of El Campillo has the highest concentrations of As (up to 2234 mg/kg), Cd (up to 3.3 mg/kg), Co (up to 95.6 mg/kg), Cu (up to 1119 mg/kg), Hg (up to 20922 μg/kg), Pb (up to 3494 mg/kg) and Zn (up to 723 mg/kg) near the abandoned open pit and mine tailings to the northeast of the village (Figs. 2.2, 2.4, 2.6C, 2.7A,B,C,E,F,H and Table 2.3). The concentration of Cr (up to 268 mg/kg) and Ni (up to 95 mg/kg) are higher in the center and toward the southwest of the study area (Fig. 2.4, 2.7D,G and Table 2.2). The concentration in the human hair samples for selected elements range between 0.01 and 0.29 μg/g for As, 0.01 and 0.06 μg/g for Cd, 0.01 and 0.42 μg/g for Co, 0.03 and 0.08 μg/g for Cr, 17.2 and 140 μg/g for Cu, 0.26 and 3.62 μg/g for Hg, 0.16 and 1.38 μg/g for Ni, 0.22 and 16.2 μg/g for Pb, 102 and 1120 μg/g for Zn (Table 2.3). The values of the Pb isotope ratios in topsoil are 1.158-1.172 $^{206}Pb/^{207}Pb$ and 2.439-2.456 $^{208}Pb/^{207}Pb$ and in human hair are 1.159-1.171 $^{206}Pb/^{207}Pb$ and 2.436-2.460 $^{208}Pb/^{207}Pb$ (Tables 2.2 and 2.3).

2.4.2. Huelva industrial and urban area

In the town of Huelva and its industrial district the topsoil shows high concentration values of As (up to 2121.4 mg/kg), Cd (up to 25.7 mg/kg), Co (up to 123.7 mg/kg), Cu (up to 10000.0 mg/kg), Hg (up to 20117.0 μg/kg), Pb (up to 5270.7 mg/kg) and Zn (up to 4706.7 mg/kg) in the southern sector of the study area (Fig. 2.2, 2.4, 2.6B, 2.8A,B,C,E,F,H, 2.10F). Ni (up to 52 mg/kg) and Cr (up to 170 mg/kg) have a more uniform distribution, with small high concentration spots in the central sector (Fig. 2.4, 2.8D,G, 2.10E). The concentrations of the selected elements in the human hair samples range between 0.01 and 0.10 μg/g for As, 0.01 and 0.05 μg/g for Cd, 0.01 and 1.2 μg/g for Co, 0.03 and 0.37 μg/g for Cr, 10.9 and 129 μg/g for Cu, 1.24 and 3.58 μg/g for Hg, 0.08 and 2.23 μg/g for Ni, 0.23 and 4.19 μg/g for Pb, 205 and 2180 μg/g for Zn (Table 2.3). The values of the Pb isotope ratios in topsoil

are 1.157-1.189 $^{206}Pb/^{207}Pb$ and 2.435-2.463 $^{208}Pb/^{207}Pb$ and in human hair are 1.156-1.166 $^{206}Pb/^{207}Pb$ and 2.442-2.451 $^{208}Pb/^{207}Pb$ (Tables 2.2 and 2.3).

2.4.3. Aroche agricultural area

The topsoil of the rural Aroche case study has the highest concentrations of Co (up to 40.4 mg/kg), Cr (up to 153.1 mg/kg), Cu (up to 141.0 mg/kg) and Ni (up to 201.9 mg/kg) in the center of the mapped area, near the urbanized village (Fig. 2.2, 2.4, 2.9C,D,E,G and Table 2.3). Cd (up to 2.3 mg/kg), Zn (up to 675.2 mg/kg) and Pb (up to 472.6 mg/kg) show the highest contents in the southwestern sector of the study area, with high values of Cd and Zn also to the southwest of the Aroche village (Fig. 2.2, 2.4, 2.6A,2.9B,H, Table 2.3). The concentration of As (up to 987.1 mg/kg) is higher in the southwestern half of the area (Fig. 2.4, 2.9A, Table 2.3). The spatial distribution of Hg content (up to 246.0 µm/kg) shows higher concentration in three limited spots to northeast, center and west of the study area (Table 2.3). The concentration of the selected elements in the human hair samples ranges between 0.001 and 0.07 µg/g for As, 0.0001 and 0.12 µg/g for Cd, 0.01 and 0.11 µg/g for Co, 0.01 and 0.39 µg/g for Cr, 0.02 and 138 µg/g for Cu, 0.06 and 1.85 µg/g for Hg, 0.08 and 0.54 µg/g for Ni, 0.02 and 4.3 µg/g for Pb, 0.15 and 1190 µg/g for Zn (Table 2.3). The values of the Pb isotope ratios in topsoil are 1.176-1.194 $^{206}Pb/^{207}Pb$ and 2.446-2.452 $^{208}Pb/^{207}Pb$ and in human hair are 1.153-1.168 $^{206}Pb/^{207}Pb$ and 2.441-2.559 $^{208}Pb/^{207}Pb$ (Tables 2.2 and 2.3).

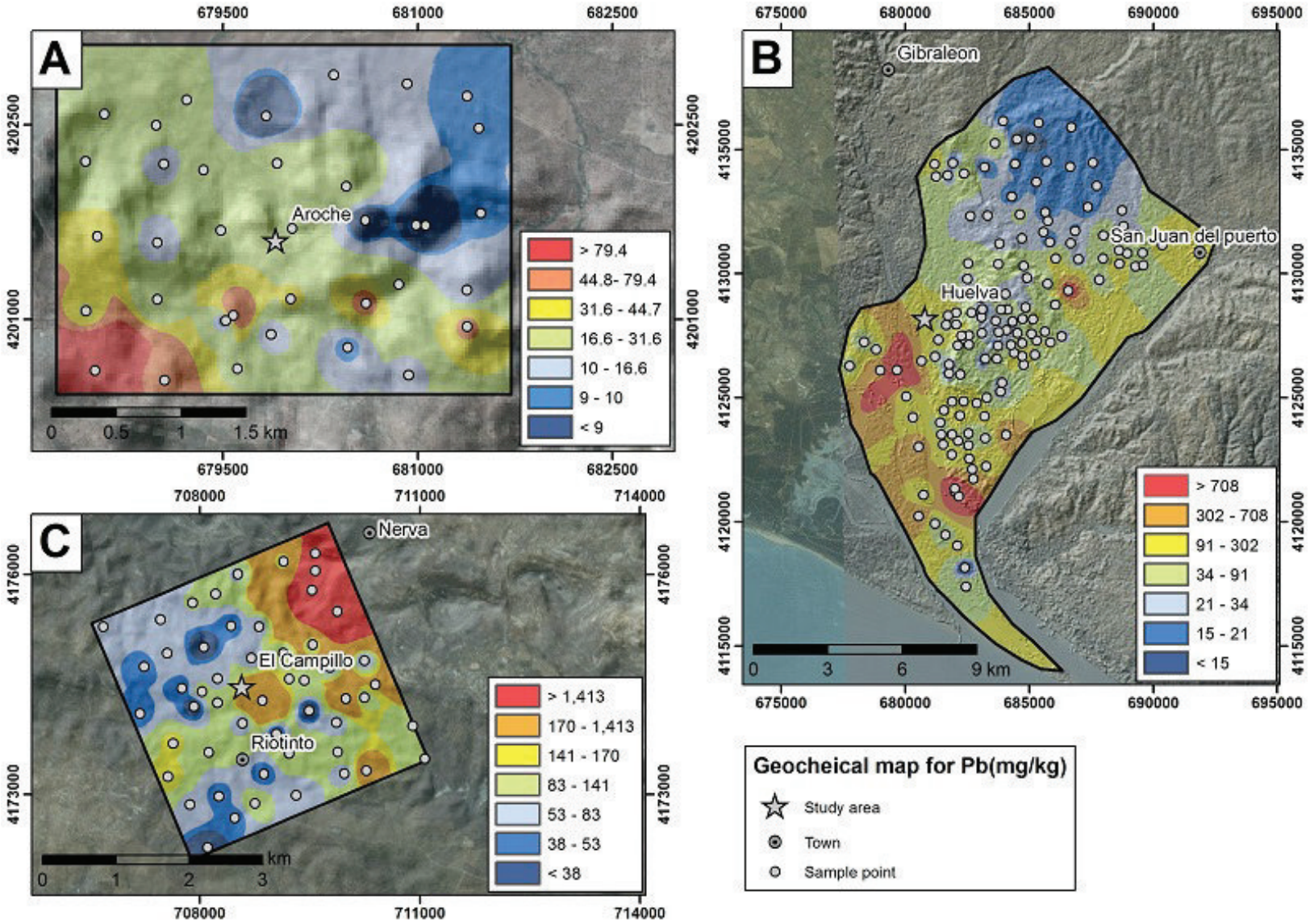

Figure 2.6: Geochemical map of Pb for the three study case using IDW. (A) Aroche, (B) Huelva and (C) El Campillo

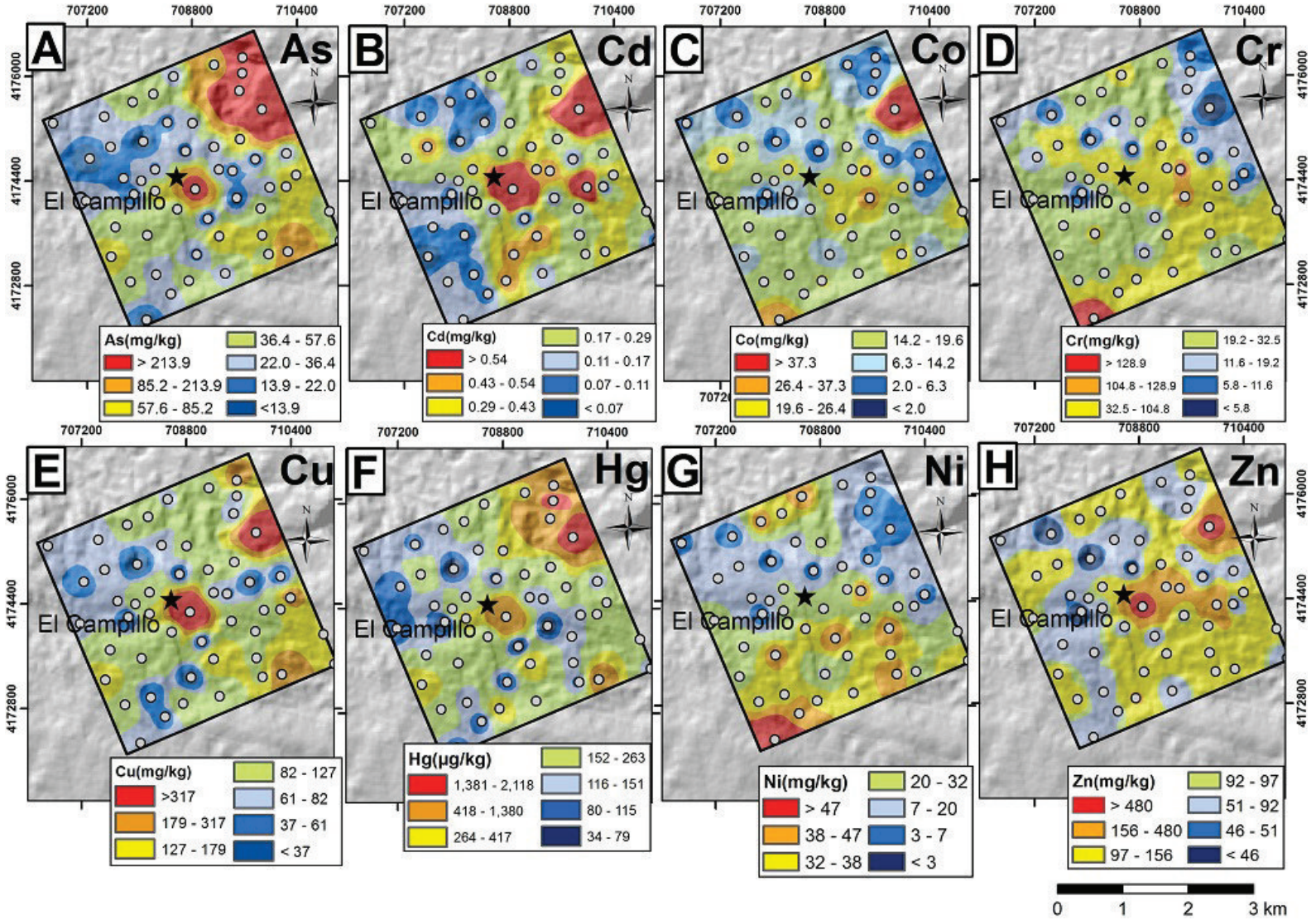

Figure 2.7 Geochemical map of El Campillo (A) As, (B) Cd, (C) Co, (D) Cr, (E) Cu, (F) Hg, (G) Ni and (H) Zn.

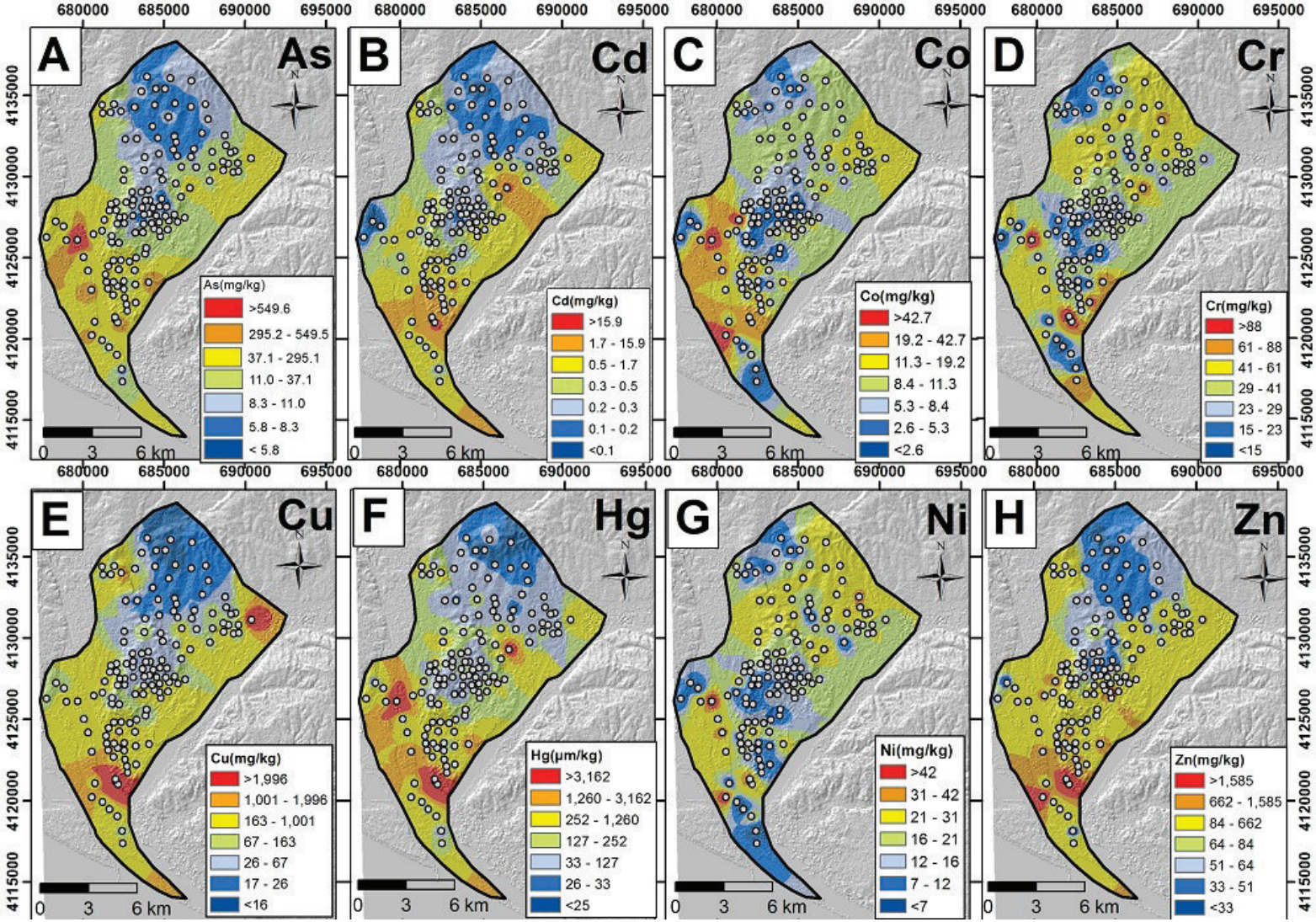

Figure 2.8 Geochemical map of Huelva (A) As, (B) Cd, (C) Co, (D) Cr, (E) Cu, (F) Hg, (G) Ni and (H) Zn.

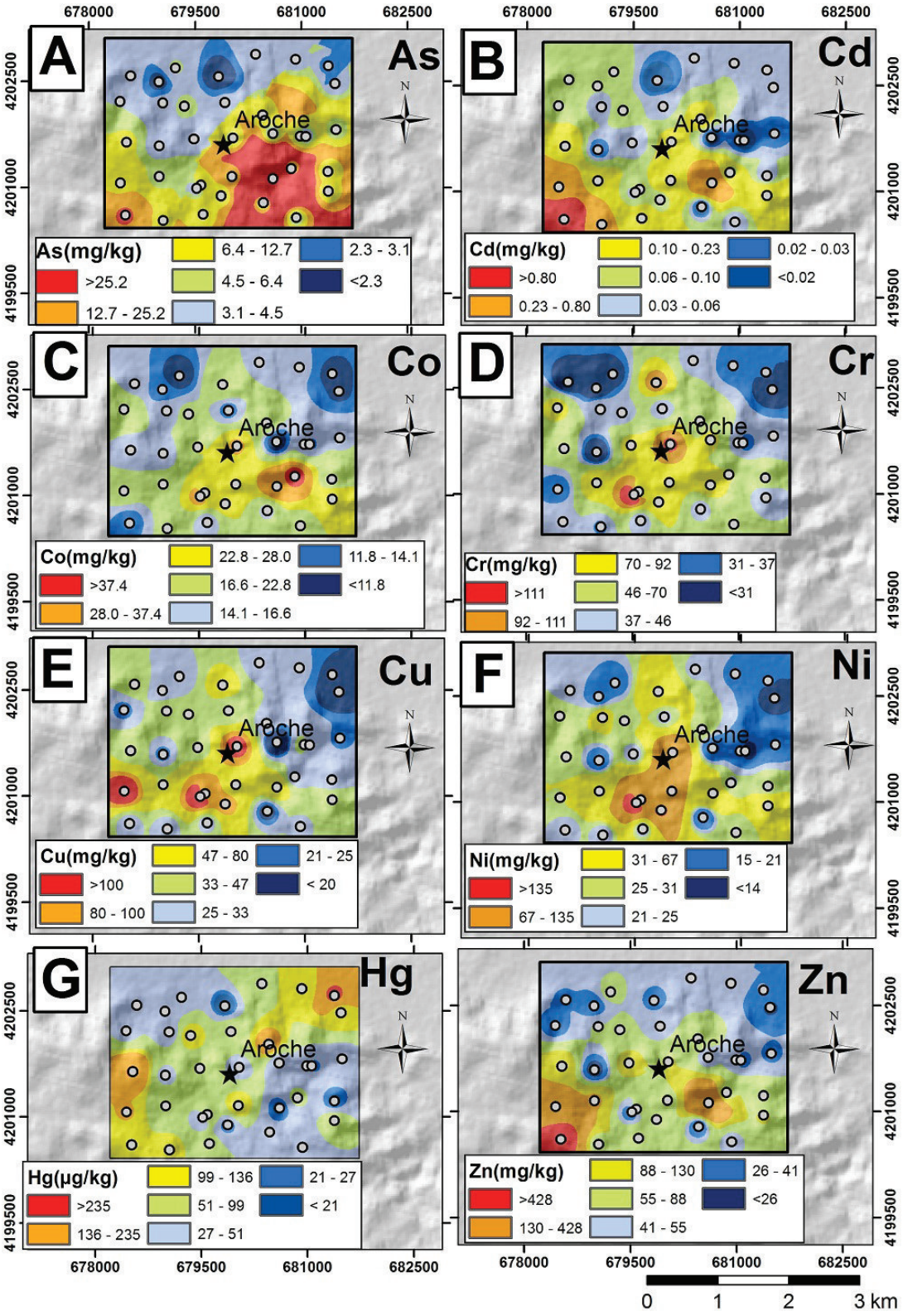

Figure 2.9 Geochemical map of Aroche (A) As, (B) Cd, (C) Co, (D) Cr, (E) Cu, (F) Hg, (G) Ni and (H) Zn.

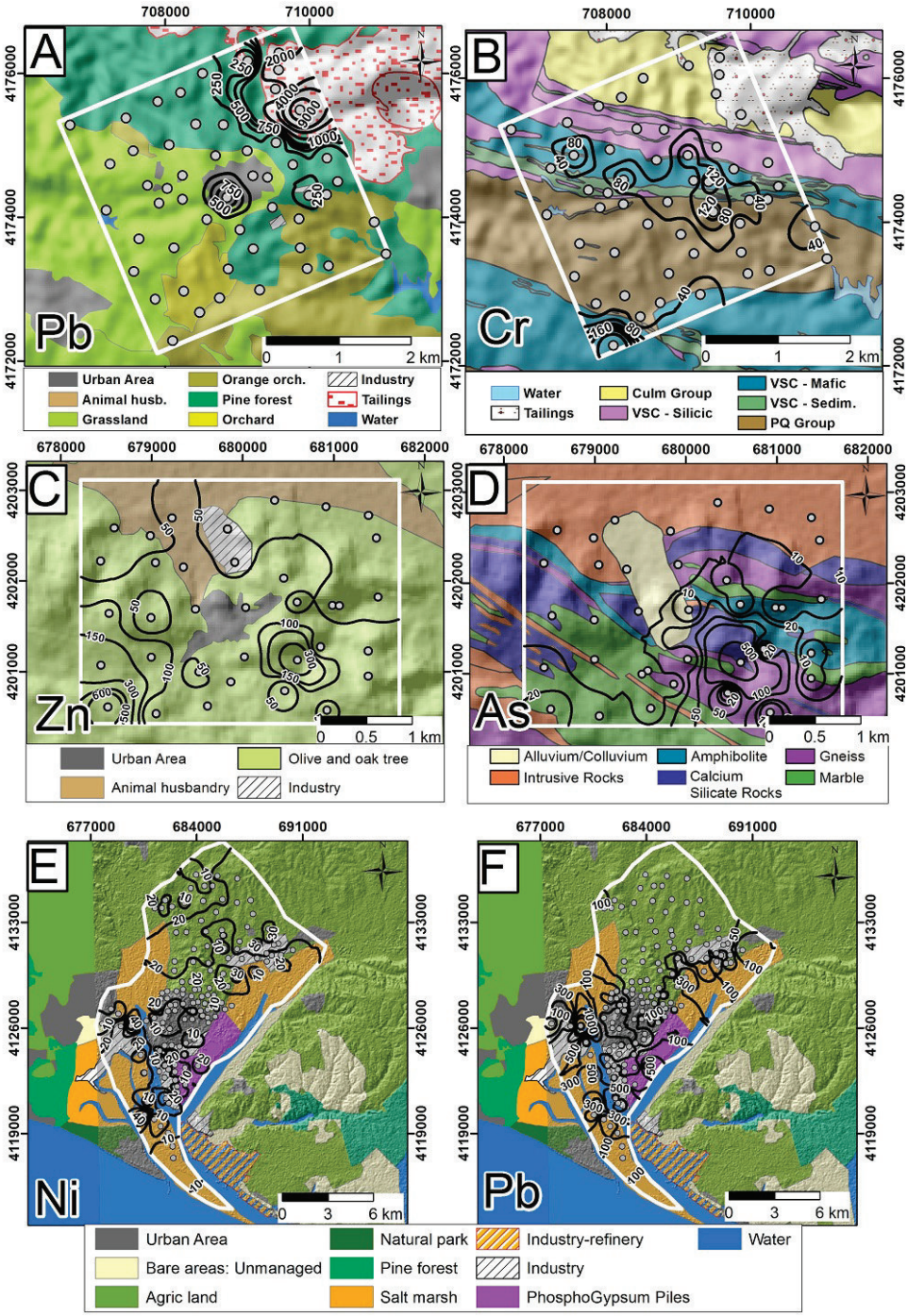

Figure 2.10 Concentration of selected elements in the topsoil represented by contour lines compared to the geology and land use maps. (A) Pb concentration vs. land use in El Campillo. (B) Cr concentration vs. geology in. El Campillo. (C) Zn concentration vs. land use in Aroche. (D) As concentration vs. geology in Aroche. (E) Ni concentration vs. land use in Huelva town. (F) Pb concentration vs. land use in Huelva town.

2.5. Discussion

2.5.1 Relationships among geochemical elements distribution, geology and land use

The spatial distribution of the chemical elements in the three case study areas allows the identification of geochemical anomalies and the spatial analysis of their relationships with the geology and land use. In this section, geochemical maps of the selected elements (As, Cd, Co, Cr, Cu, Hg, Ni, Pb, Zn) are presented and compared to geologic and land use maps.

In El Campillo there is a strong spatial correlation between the concentration values of many elements (As, Cd, Co, Cu, Hg, Pb and Zn) and the geology and land use maps (Figs. 2.1, 2.2, 2.6B, 2.7). The occurrence of high concentration values of Pb is spatially coincident with the open pit and tailings of the Rio Tinto mine, the urbanized zone of El Campillo village and an industrial site to the east (Fig. 2.10A). Also, the highest values of Cr in the topsoil are spatially coincident with the area where the VMS deposits occur as stratabound lenses within the felsic volcanic rocks of the SPZ crop out (Figs. 2.1, 2.10B) (Adamides, 2013). High Cr concentrations are also spatially coincident with mafic volcanic and subvolcanic rocks of the SPZ volcano-sedimentary complex (Fig. 2.10B).

The geology in the town of Huelva is homogeneous, with recent alluvial sediments and shale and marlstone outcrops (Fig. 2.1). The geochemical anomalies detected in this area seem to be mainly associated to the location of industrial activities and the Odiel and Rio Tinto rivers, carrying stream sediments from the mining activities upstream (i.e. Rio Tinto mines in El Campillo). High concentrations of many metallic elements (e.g. Pb) spatially correspond to an abandoned mineral harbor and the El Rincon phosphogypsum stack (Guillen et al., 2012) (Fig 2.10F).

Most of the elements analyzed in Aroche (i.e. Pb, Hg) show no clear spatial relationships with the geology and land use maps (Fig. 2.1, 2.2, 2.9). Other elements, like As and Zn, have highest values in the central-southern part of the study area, which corresponds to metamorphic rocks and olive/oak tree orchards (Fig. 2.10C,D). To the north, both As and Zn have lower concentrations, corresponding to intrusive rocks and animal husbandry (Fig. 2.10C,D). The tenuous spatial coincidence of geology, land use and the As and Zn concentrations suggests a possible link among these factors, whose origin may deserves more in-depth studies.

2.5.1.1. Concentration of harmful elements in human hair samples

One of the main concerns in environmental studies is the influence of the soil geochemical composition on the potential accumulation of harmful elements in human beings (e.g. Dziubanek et al., 2015). The geochemical analysis that has been conducted in Aroche, Huelva and El Campillo indicates that a direct correlation between the concentration of metals in human hair samples and in the topsoil of the three case study areas cannot be established. For example, human hair samples collected in the rural Aroche site have the highest average concentration of Cd and Cu, compared to the average concentrations measured in the human hair samples collected in the El Campillo and Huelva sites. This distribution is opposite to the concentration values measured in the topsoil, where the Cd and Cu abundances are higher in the Huelva and El Campillo areas, compared to the Aroche site (Table 2.2, Fig. 2.11).

The lack of a direct correlation between the geochemical composition of the soil and the accumulation of some contaminants in human hair suggests that the processes bringing chemical elements from soils, through the food chain and water, into human beings are complex. Thus, lead isotopic analysis has been performed to get better insights into the sources of the harmful elements that reach the inhabitants of Aroche, El Campillo and Huelva (Section 2.5.3).

2.5.2. Environmental assessment

Environmental contamination is not only associated to the presence of just one element, but frequently results from multi-element concentration representing a risk for the human health. Anomalies of the selected potential harmful elements were recognized in all the three case study areas, even in the rural Aroche site, where neither industrial nor mining activities occur. For these reasons, contamination factors (CFs), contamination degree (CD) and pollution index (PI) maps have been calculated. The CD and PI maps are especially useful to identify the multi-element concentration in the soil (e.g. Hakanson, 1980; Jung, 2001).

2.5.2.1. Contamination Factors and Contamination Degree

Although the CFs and CD calculations has been originally used as diagnostic tools for the purpose of controlling water pollution, they can also be applied for assessing the quality of sediments and soils

(Hakanson, 1980; Jung, 2001; Qingjie et al., 2008). The CFs and CD calculations have been based on the uppermost values of the local background concentration interval of the 9 selected elements (Section 2.3.4, Table 2.2). A CF map has been produced for each element using the following formula (Hakanson, 1980):

$$CF = \frac{CO}{Bk}$$

where CO is the concentration of the element in the soil (As Cd, Cu Co, Cr, Hg, Ni, Pb, Zn), and Bk is the uppermost value of the local background concentration interval of the element (Table 2.3).
The resulting CF map shows the abundance of a single element in comparison with its local background range. The soil is considered contaminated or enriched in the element where CF > 1 (Fig. 2.12).

In addition, a CD map has been calculated with the following formula (Hakanson, 1980):

$$CD = \sum_{1}^{n} CF$$

The CD map shows the areas where a high multi-element concentration occurs (Fig. 13). Following Hakanson's (1980) classification of CD, the areas in Aroche with very high multi-element contamination (CD > 27), and taken to represent anthropogenic pollution, represent about 10.2% of the total study area. This contaminated sector is in the south, which is characterized by olive and oak plantation and some small industrial sites, where high CF values for As, Cd, Ni, Pb, Zn occur (Figs. 2.2, 2.12A,B,C, 2.13A). At the Huelva site, the high multi-element contamination covers about 53% of the total study area (CD > 27) is located mainly in the south, and the contamination is probably associated with the industrial port, and the refinery and phospho-gypsum activities (Figs.2.2, 2.13B). In this sector, CF is high for As, Cd, Cu, Pb, Zn (Fig. 2.12 G,H,I). At the El Campillo site, about 12.3% of the total study area is classified as high multi-element-contaminated (CD > 27). This contaminated sector

includes the mine tailings and the urbanized area of El Campillo, where CF values are high for As, Cd, Cu, Hg, Pb (Figs. 2.1, 2.2, 2.12D,E,F, 2.13C).

2.5.2.2. Pollution Index

PI maps are used by many authors to identify multi-element contamination. PI values are calculated using the following formula (e.g. Jung et al., 2001; Nimik and Moor, 1991):

$$PI = \sum_{1}^{n} \frac{CO/IV}{n}$$

where CO is the concentration of the element in the soil (As Cd, Cu Co, Cr, Hg, Ni, Pb, Zn), IV is a contamination threshold and n is the number of elements. Environmental Laws defining contamination thresholds for trace elements in soil are not available in Spain, thus the PI has been obtained using the intervention values established by the environmental regulations of the Andalucía Region (CMJA, 1999). Agricultural activities occur in all the three study areas and the IVs have been set equal to the intervention values indicated for agriculture land (CMJA, 1999) (Fig. 2.4, Table 2.3).

The PI maps show the distribution of the areas with significant multi-element contamination (where PI > 1, Jung et al., 2001). In Aroche, areas where PI > 1 represent about 8.2% of the total area; these areas partly corresponding to urban land (Figs. 2.2, 2.14A). In Huelva, the areas with multi-element contamination represent the 51.0% of the total, mainly corresponding to the industrialized and urban land (Figs. 2.2, 2.14B). In El Campillo, a wide sector of the total area (41.3%) is affected by multi-element contamination. These contaminated soils are mainly in the east, linked to the site of mine tailings, urban area, and where some industrial activities take place. Notably, cultivation of oranges is also conducted in areas where the PI indicates multi-element contamination of the agricultural soil (Figs. 2.2, 2.14C).

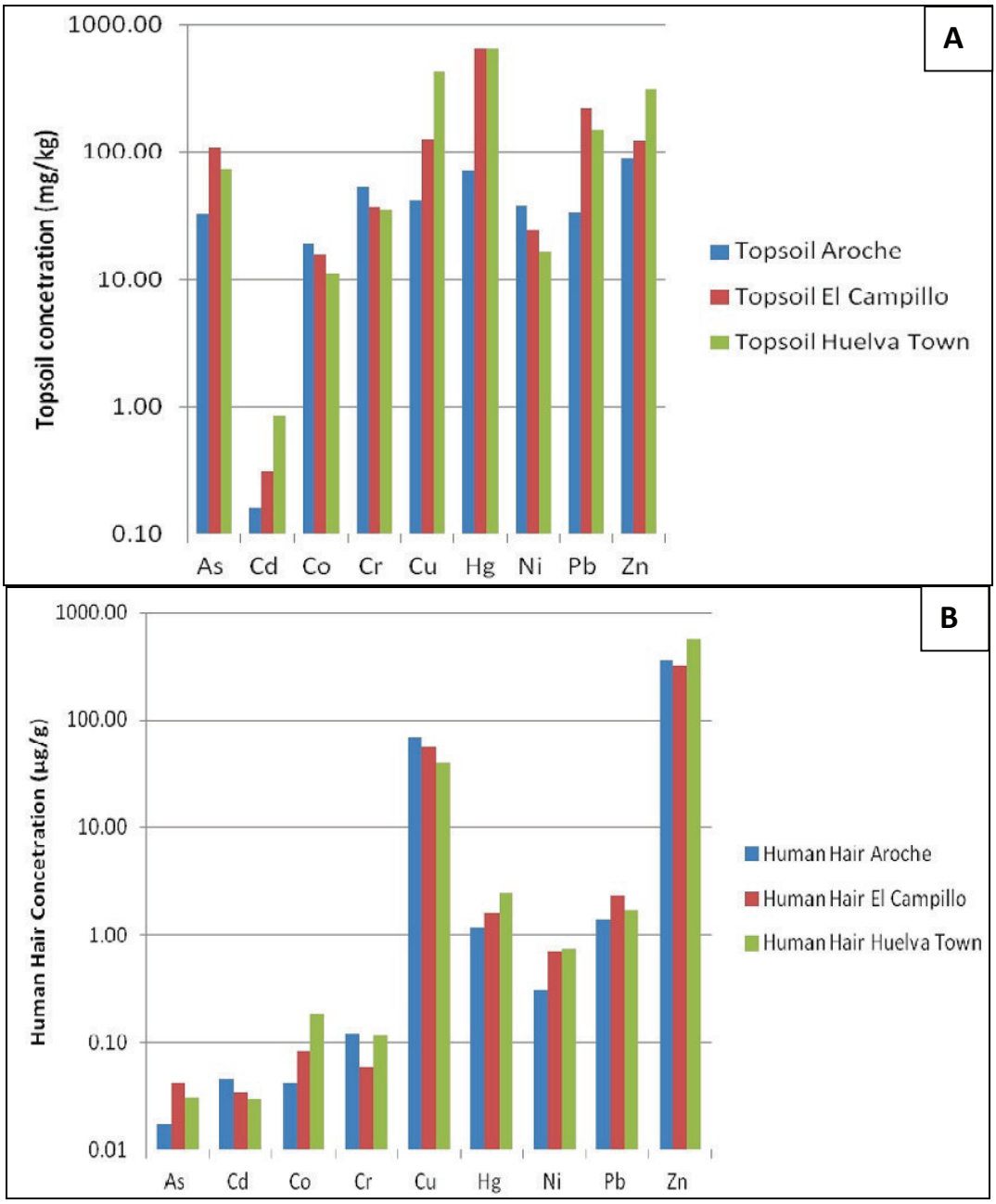

Figure 2.11. (A) Concentration of selected Topsoil. (B) Concentration of selected elements Human hair.

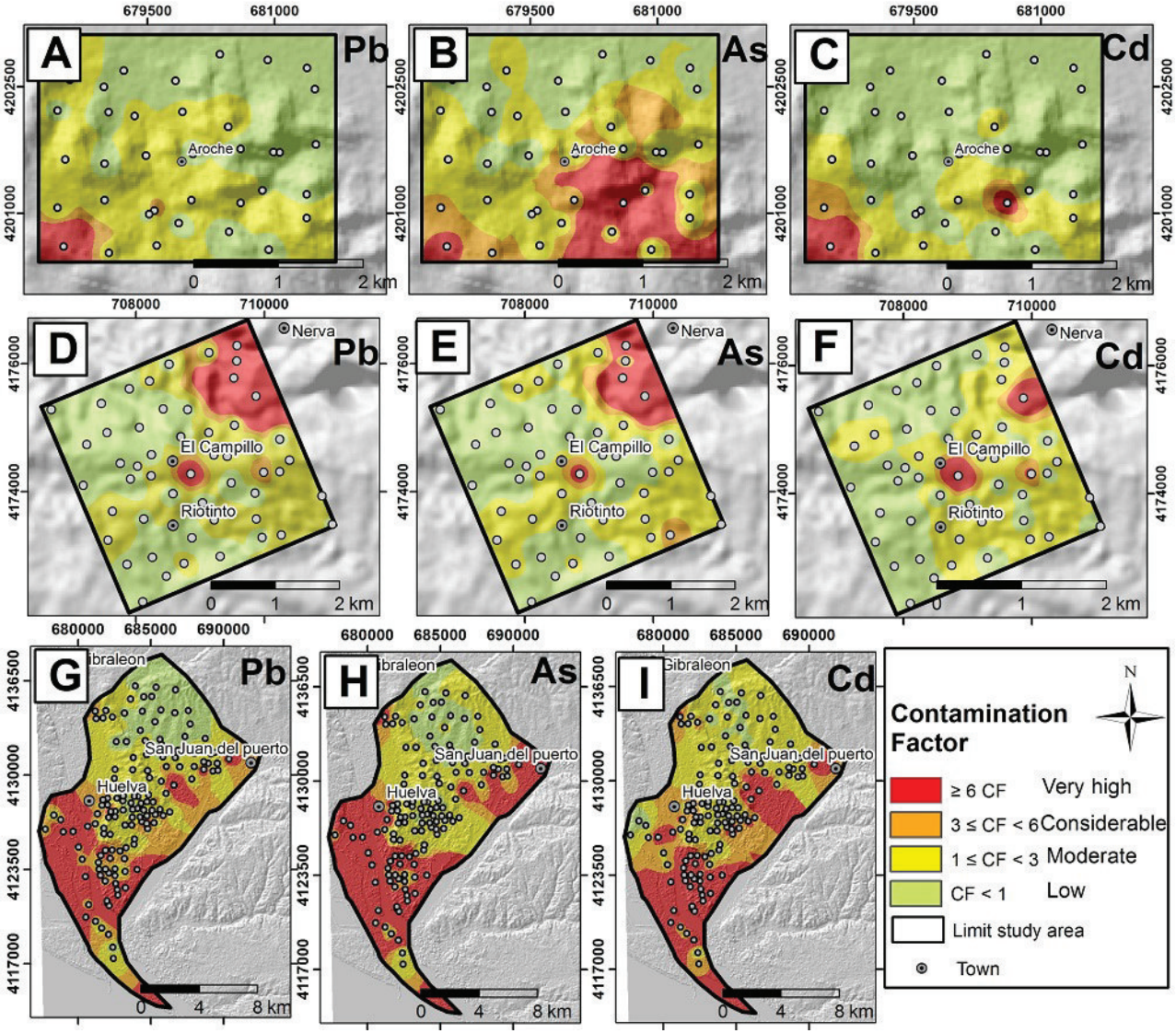

Figure 2.12 Contamination Factor of the three study areas, (A) Aroche Pb, (B) Aroche As, (C) Aroche Cd, (D) El Campillo Pb, (E) El Campillo e As, (F) El Campillo Cd, (G) Huelva Pb, (H) Huelva As, (I) Huelva Cd

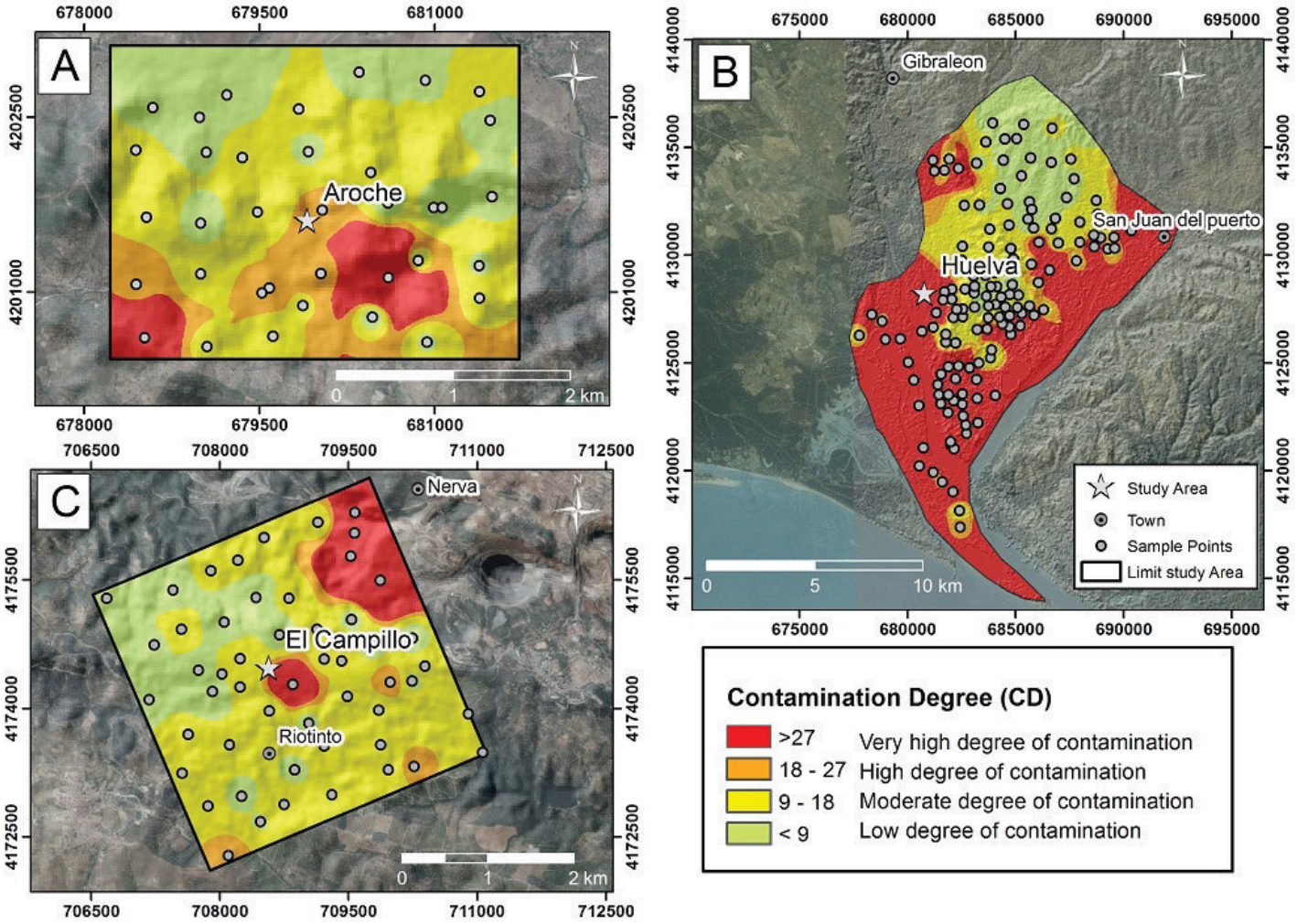

Figure 2.13 Contamination Degree of the three study areas (A) Aroche, (B) Huelva and (C) El Campillo

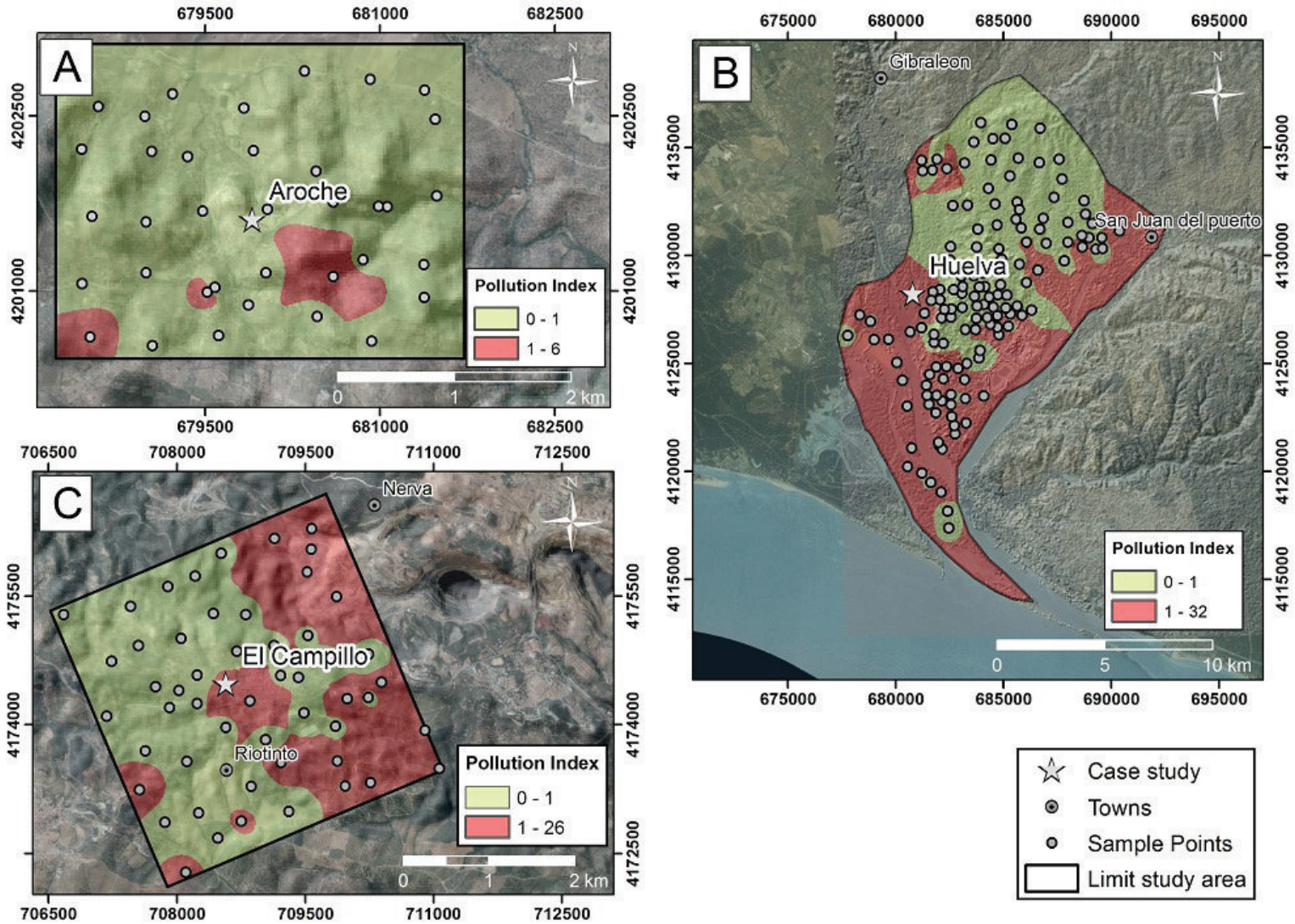

Figure 2.14 Pollution Index of the three study areas (A) Aroche, (B) Huelva and (C) El Campillo

2.5.3. Sources of Pb occurring in soil and human hair

Because most natural materials have characteristic Pb isotopic ratios they can be distinguished from anthropogenic pollution sources (e.g. Graney et al., 1995; Erel et al., 1997; Kramers and Tolstikhin, 1997; Ayuso et al., 2008, 2016).

Topsoil samples (leached) collected in the study areas and analyzed for $^{206}Pb/^{207}Pb$ and $^{208}Pb/^{207}Pb$ isotopic ratios show two isotopic trends. The trends correspond to two different main isotopic signatures (Fig. 2.15). The topsoil samples with medium-high Pb contents show small variations of the $^{206}Pb/^{207}Pb$ ratio, resulting in a horizontal trend in the $^{206}Pb/^{207}Pb$ vs. $^{208}Pb/^{207}Pb$ plot (Fig. 2.15). These samples mainly belong to the mineralized area of El Campillo, and to a sector of the town of Huelva near the Rio Tinto and Odiel rivers banks (Figs. 2.2, 2.3 and 2.15). The topsoil samples with medium-low Pb concentrations have been mostly collected in the agricultural sectors of Aroche, Huelva and El Campillo, and show a diagonal trend in the isotopic ratios plot, with a direct linear relationship between $^{206}Pb/^{207}Pb$ and $^{208}Pb/^{207}Pb$ (Figs. 2.2 and 2.15).

Similarly, the isotopic signatures measured in human hair samples exhibit two trends in the $^{206}Pb/^{207}Pb$ vs. $^{208}Pb/^{207}Pb$ plot (Fig. 2.16). The first trend, defined by the samples collected in El Campillo, is horizontal and is characterized by a small variation of $^{206}Pb/^{207}Pb$ compared to $^{208}Pb/^{207}Pb$ (Fig. 2.16). The second trend is defined by the samples collected at Huelva and Aroche and follows a diagonal trend band in the $^{206}Pb/^{207}Pb$ vs. $^{208}Pb/^{207}Pb$ plot (Fig. 2.16).

The Province of Huelva is characterized by (1) the natural occurrence of VMS ore deposits in the IPB, where mining activities occurred in the past, and, secondarily, by (2) agricultural and (3) industrial activities (*Section 2*). Thus, lead isotopic ratios measured in topsoil and human hair samples collected in the Aroche, El Campillo and the town of Huelva sites have been compared to the isotopic signatures of all these potential contamination sources. For the purpose of this comparison, the following Pb isotopic signatures have been used: (1) Pb isotopic measurements of the VMS deposits, mine tailings and sediments originated from the mining works and transported by the Odiel and Rio Tinto rivers (Marcoux, 1998; Adánez-Sanjuán et al., 2016); (2) Pb isotopic data of pesticides used as tracer for the agricultural activities (Ayuso et al., 2004; Grezzi et al 2010); (3) Pb isotopic analyses of gasoline used as tracer for urban areas and industrial activities (Monna et al., 1997, 1999).

Isotopic compositions for the VMS mineralization and the sediments of the Odiel and Rio Tinto rivers plot along a horizontal trend in the $^{206}Pb/^{207}Pb$ vs. $^{208}Pb/^{207}Pb$ plot (Fig. 17) (Marcoux, 1998; Adánez-Sanjuán et al., 2016). This trend, characterized by a limited variation of the $^{206}Pb/^{207}Pb$ ratio, is similar to the trend shown by most of the topsoil and human hair samples collected in El Campillo (Figs. 2.15, 2.16 and 2.17). The coincidence between the isotopic signature of the VMS mineralization and the El Campillo samples suggests that the lead found in the soil and lead found in human hair is likely related to the occurrence of the IPB ore deposits and mining endeavors related to the exploitation of the ore. Also, some soil samples collected in the town of Huelva show the same trend of lead isotopic ratios (Figs. 2.15, 2.16 and 2.17). These samples belong to the Rio Tinto and Odiel rivers banks, and these are mainly composed of sediments from the VMS mineralized area and from open pit mine (Figs. 2.15 and 2.17).

A second trend in the plot of Fig. 2.17 is defined by the lead isotopic ratios of gasoline (Monna et al., 1997, 1999) and pesticides (Ayuso et al., 2004; Grezzi et al., 2010). This diagonal trend of town is also evident by: (1) the topsoil and human hair samples collected in Aroche; (2) the topsoil samples from the rural sector of Huelva and the human hair samples collected in town; and (3) some of the topsoil samples collected far from the mining activities in El Campillo (Figs. 2.15, 2.16 and 2.17). The similarity of lead isotopic trends of these samples, compared to pesticides and gasoline, suggests that the most important contamination sources in the town of Huelva and in Aroche are of anthropogenic origin. We suggest that they are related to urbanization, industrial activities, and agriculture.

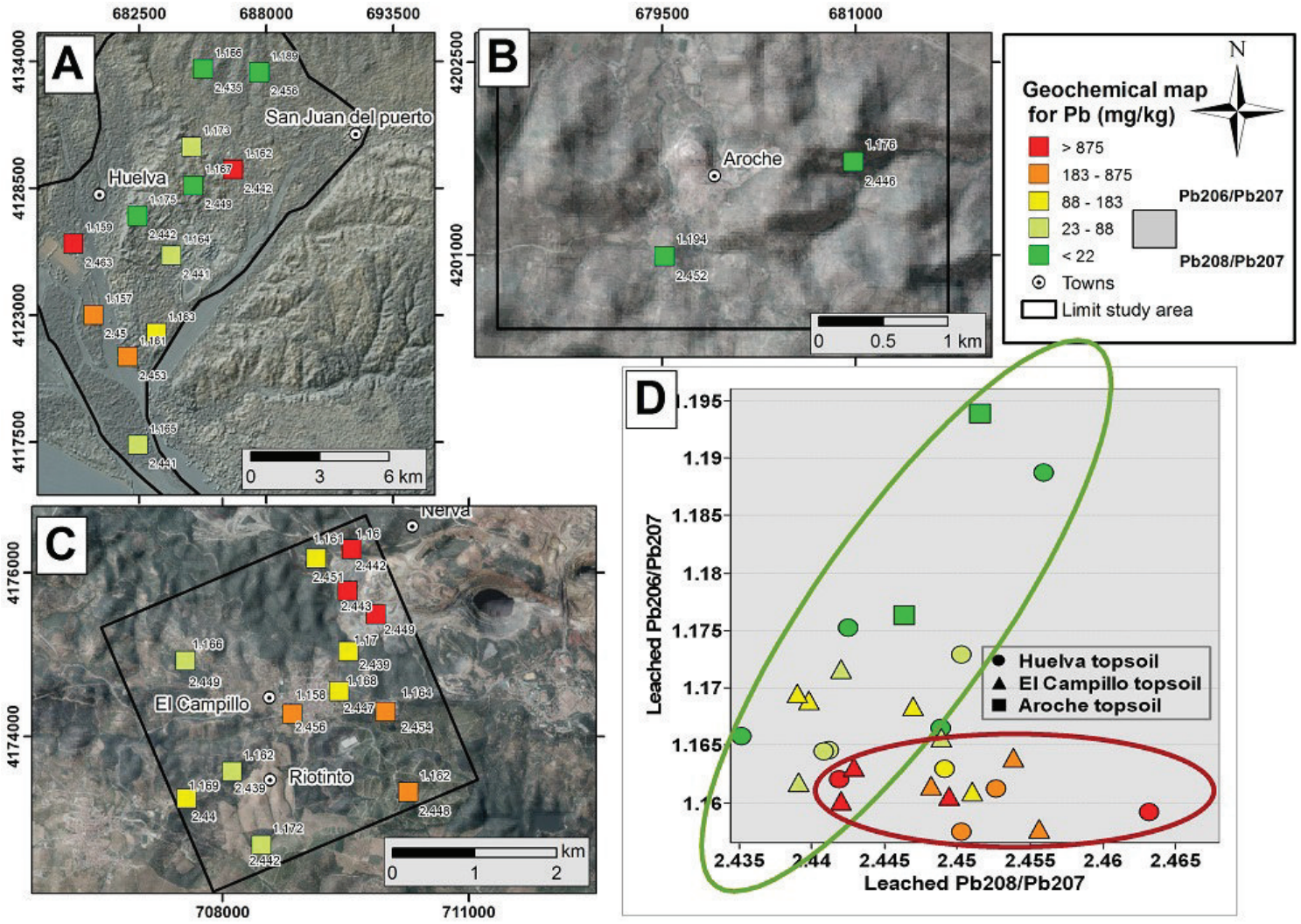

Figure 2.15 Map of the samples analyzed for isotopic lead in (A) Aroche, (B) Huelva, (C) El Campillo. (D) Graphic of Pb isotopes measured in topsoil samples, the green and red ellipses show the two isotopic trends discussed in the text (Section 2.5.3).

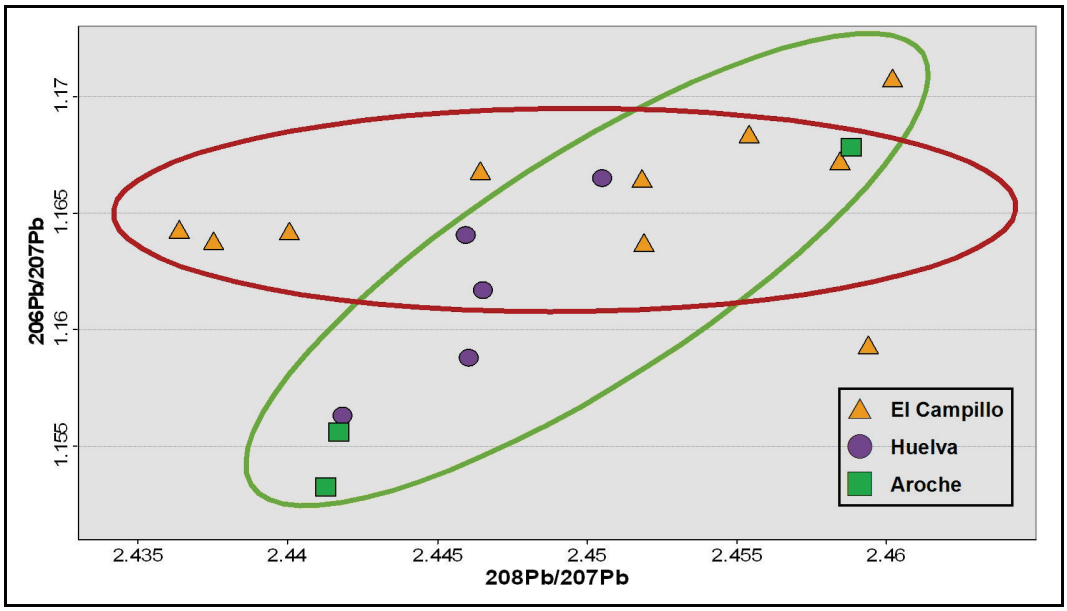

Figure 2.16. Graphic of Pb isotopes of measured in human hair samples. Green and red ellipses show the two isotopic trends discussed in the text (Section 2.5.3).

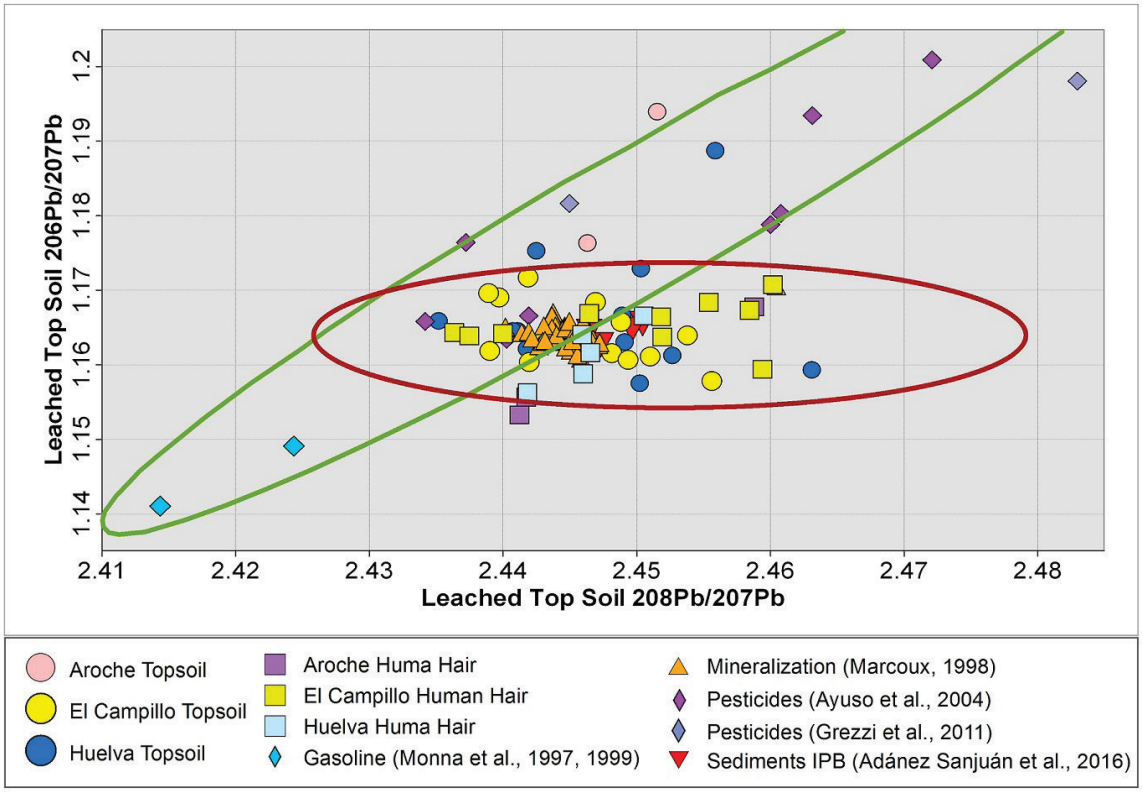

Figure 2.17 Comparison of isotopic ratios from the literature and from the data of the present work. Green and red ellipses show the two isotopic trends discussed in the text (Section 2.5.3).

2.6. Concluding remarks

The principal suggestions of our study can be summarized as follows.

1) The geochemical analysis and maps obtained in El Campillo, the town of Huelva, and Aroche indicate that the spatial distribution of metals in soil is frequently closely linked to the local geology and to historical patterns of land use. In El Campillo, the geochemical maps show a spatial coincidence between areas with high concentration of As, Cd, Co, Cu, Hg, Pb and Zn, the regional widespread IPB mineralization, and mine tailings generated by the long-lived exploitation of the deposits. At Huelva, high levels of As, Cd, Co, Cu, Hg, Pb and Zn in the soil are clearly spatially related to industrial sites and to alluvial deposits, ultimately related to the IPB mineralized areas, and to sediments transported by the Rio Tinto and Odiel rivers. Finally, in the Aroche study area the relatively homogeneous geology and history of land use does not provide clear evidence linking the concentration of metals in soil, the occurrence of different geological units and anthropogenic activities.

2) The environmental assessment that has been carried out in this study allows us to identify sectors in the three study areas where multi-element concentration of metals may represent a risk for human health. The CD and PI maps show a significant environmental risk in the urbanized sectors of the three study areas. Also, the industrialized sectors in Huelva and the mine tailings and surrounding area in El Campillo also have high values of CD and PI, associated to a considerable environmental risk.

3) Lead isotopic analysis demonstrates two well defined signatures related to the sources of contamination. One signature, characterized by a limited variation of the $^{206}Pb/^{207}Pb$ ratio, is related to the VMS ore deposits and mine tailings, which has been mainly found in the soil and human hair samples of the El Campillo study area. The other isotopic signature, with a direct linear trend between the $^{206}Pb/^{207}Pb$ and the $^{208}Pb/^{207}Pb$ ratios, indicates pesticides and gasoline lead sources and has been mainly found in the soil and human hair samples collected in Aroche and Huelva.

Acknowledgments

The authors are grateful to R. Indela and S. Kuns for their support at the USGS Radiogenic Isotope Laboratory in Reston (VA, USA), and to F. Macías, R. Pérez-López and A.M. Sarmiento (Univ. Huelva) for their collaboration in the hair sampling. The UHU also provided logistic support for the soil sampling campaigns in the Huelva Province.

References

Adamides,N.G., 2013. Rio Tinto (Iberian Pyrite Belt): a world-class mineral field reopens. Applied Earth Science (Trans. Inst. Min. Metall. B), 122, 2-15.

Adánez Sanjuán, P., Flem, B., Llamas Borrajo, J.F., Locutura Rupérez, J., Garcia Cortés, A., 2016. Application of lead isotopic methods to the study of the anthropogenic lead provenance in Spanish overbank floodplain deposits. Environ Geochem Health. 38: 449–468.

Albanese, S., De Vivo, B., Lima, A., Cicchella, D., 2007. Geochemical background and baseline values of toxic elements in stream sediments of Campania region (Italy). Journal of Geochemical Exploration 93, 21–34.

Andalucia Region-CMAJA (Consejería de Medio Ambiente de la Junta de Andalucía), 1999. Los criterios y estándares para declarar un suelo contaminado en Andalucía y la metodología y técnicas de toma de muestra y análisis para su investigación. http://www.juntadeandalucia.es

Apalategui-Isasa, O., Barranco Serrano,e., Contreras Vazquez, F., Roldàn Garcia, F.J., 1979. Mapa geologico de Espana, hoja Aroche 916 09-37 escala 1:50.000. Instituto geologico y minero de España.

Ayuso, R.A., Foley, N., Robinson, G., Wandless, G., Dillingham, J., 2004. Lead Isotopic compositions of common arsenial pesticides used in New England: USGS Open File Report 2004-1342, 14.

Ayuso, R.A., Foley, N.K., 2008. Anthropogenic and natural lead isotopes in Fe-hydroxides and Fe-sulphates in a watershed associated with arsenic-enriched groundwater, Maine, USA. Geochemistry: Exploration, Environment, Analysis 8: 77-89.

Ayuso, R.A., Foley, N.K., Seal, R., Bove, M., Civitillo, D., Cosenza, A., and Grezzi, G., 2013. Lead isotope evidence for metal dispersal at the Callahan Cu-Zn-Pb mine: Goose Pond tidal estuary, Maine, USA: Journal of Geochemical Exploration, v. 126, p. 1-22.

Ayuso, R.A., and Foley, N.K., 2016, Pb-Sr isotopic and geochemical constraints on sources and processes of lead contamination in well waters and soil from former fruit orchards, Pennsylvania, USA: A legacy of anthropogenic activities. Journal of Geochemical Exploration, v. 170, p. 125–147.

Azor, A., 2004. Zona de Ossa-Morena. In: Geología de España (J.A. Vera, Ed.), SGE-IGME, Madrid, 165-199.

Banu, Z., Chowdhury, S.A., Hossain, D., Nakagami, K., 2013. Contamination and ecological risk assessment of heavy metals in the sediment of Turag River, Bangladesh: an index analysis approach. Journal of Water Resource and Protection, 5: 239–248.

Bard, J. P., Moine, B., 1979. Acebuches amphibolites in the Aracena hercynian metamorphic belt (southwest Spain): Geochemical variations and basaltic affinities. Lithos, 12: 271-282.

Castro, A., Fernández, C., El-Hmidi, H., El-Biad, M., Díaz, M., De La Rosa, J. D., Stuart, F., 1999a. Age constraints to the relationships between magmatism, metamorphism and tectonism in the Aracena metamorphic belt, southern Spain. International Journal of Earth Sciences, 88: 26-37.

Castro A., Patiño Douce A. E., Corretgé L. G., De La Rosa J. D., El-Biad M., El-Hmidi H., 1999b. Origin of peraluminous granites and granodiorites, Iberian Massif, Spain: an experimental test of granite petrogenesis. Contributions to Mineralogy and Petrology, 135: 255-276.

CCME (Canadian council of ministers of the Environment), 1995. Protocol for the Derivation of Canadian Sediment Quality Guidelines for the Protection of Aquatic Life. Report CCME EPC-98E. Prepared by the Technical Secretariat of the Water Quality Task Group. Winnipeg, Manitoba. 38 pp.

Civis, J., Dabrio, C.J., Gonzalez-Delgado, J.A., Goy,J.L., Ledesma,S., Pais,J., Sierro, F.J. and Zazo, C. 2004. Cuenca del Guadalquivir. In: Geología de España (J.A. Vera, Ed.), SGE-IGME., Madrid, 543-550.

Crespo-Blanc, A., Orozco, M., 1988. The Southern Iberian Shear Zone: A major boundary in the Hercynian folded belt. Tectonophysics, 148: 221-227.

Crespo-Blanc, A. ,1991. Evolución geotectónica del contacto entre la Zona de Ossa-Morena y la Zona Surportuguesa en las Sierras de Aracena y Aroche (Macizo Ibérico Meridional): Un contacto mayor en la Cadena Hercínica Europea. Universidad de Sevilla, 327 p.

CSIC-IARA., 1989. Memoria del Mapa de Suelos de Andalucía a escala 1:400000. C.S.I.C. y Junta deAndalucía, Madrid. 95 pp.

De Vivo, B., Lima, A., Siegel., F. 2004. Geochimica Ambientale, Metalli Potenzialmente Tossici. Liguori ed. Napoli, Italia. 448 p.

De Vivo, B., Lima, A., Albanese S., Cicchella, D., 2006. Atlante geochimico-ambientale della Regione Campania. Aracne Editrice, Roma. ISBN 88-548-0819-9, 216 p.

De Vivo, B., Lima, A., Albanese S., Cicchella, D., Rezza, C., Civitillo D., Minolfi, G., Zuzolo, D., 2016. Atlante geochimico–ambientale dei suoli della Campania. Aracne Editrice, Roma. 330 pp.

Dziubanek, G., Piekut, A., Rusin, M., , Baranowska, R., Hajok, I., 2015. Contamination of food crops grown on soils with elevated heavy metals content. Ecotoxicology and Environmental Safety. 118 p.

Erel, Y., Veron, A., Halicz, L., 1997. Tracing the transport of anthropogenic lead in the atmosphere and in soils using isotopic ratios. Geochim Cosmochim Acta. 61: 3193–3204.

Fernandez-Caliani, J.C., 2008. Una aproximación al conocimiento del impacto ambiental de la minería de la Faja Pirítica Ibérica. Macla, 10: 24-29.

Galván, L., Olías, M., Cánovas, C.R., Sarmiento, A.M., Nieto, J.M. (2016). Hydrological modeling of a watershed affected by acid mine drainage (Odiel River, SW Spain).

Gómez-Pugnaire, M. T., Azor, A., Fernández Soler, J. M., Sánchez Vizcaıno, V. L., 2003. The amphibolites from the Ossa–Morena/Central Iberian Variscan suture (Southwestern Iberian Massif): geochemistry and tectonic interpretation. Lithos, 68(1), 23-42.

Graney, J. R., Halliday, A. N., Keeler, G. J., Nriagu, J. O., Robbins J. A., Norton S. A.., 1995. Isotopic record of lead pollution in lake sediments from the northeastern United States, Geochim. Cosmochim. Acta, 59, 1715–1728.

Grezzi, G., Ayuso, R.A., De Vivo, B., Lima, A., Albanese, S., 2011. Lead isotopes in soils and groundwaters as tracers of the impact of human activities on the surface environment:the Domizio-Flegreo Littoral (Italy) case study. J. Geochem. Explor. 109 (1–3), 51–58.

Guillén, M. T., Delgado, J., Albanese, S., Nieto, J.M., Lima, A.,De Vivo, B., 2011. Environmental geochemical mapping of Huelva municipality soils (SW Spain) as a tool to determine background and baseline values. Journal of Geochemical exploration. 109: 56-69.

Guillén, M. T., Delgado, J., Albanese, S., Nieto, J. M., Lima, A., and De Vivo, B., 2012. Heavy metals fractionation and multivariate statistical techniques to evaluate the environmental risk in soils of Huelva Township (SW Iberian Peninsula). Journal of Geochemical Exploration, 119-120: 32-43.

Hakanson, L, 1980. An Ecological Risk Index for Aquatic Pollution Control: A Sedimentological Approach, Water Research, 14, 975–1001.

Hansmann, W., Köppel, V., 2000. Lead-isotopes as tracers of pollutants in soils. Chemical Geology. 171: (1-2), 123-144.

Instituto Nacional de Estadística, 2014. Spain

Julivert, M., Fontboté, J.M., Ribeiro, A., Conde, L., 1972. Mapa tectónico de la Península Ibérica y Baleares, E: 1:1,000,000. Instituto Geológico y Minero de España, Madrid.

Jung, M.C., 2001. Heavy metal contamination of soils and waters in and around the Imcheon Au–Ag mine, Korea. Applied Geochemestry. 16: 1369-1375.

Junta de Andalucía, 1998. Mapa Geológico y Minero de Andalucía a escala 1:400.000

Junta de Andalucía, 1999. Mapa Geológico Escala 1:25.000 hoja Nerva 938 IV. Investigación geológica y cartografía básica en la faja pirítica y áreas aledañas. Madrid.

Komárek, M., Ettler, V., Chrastny, V. and Mihaljevic, M., 2008. Lead isotopes in environmental sciences: A review. Environment International, 34, 562-577.

Kramers J.D. & Tolstikhin I. N. ,1997. Two terrestrial lead isotope paradoxes , forward transport modelling , core formation and the history of the continental crust. Chemical Geology 139: 75-110.

Li, X., Chen, Z., Chen, Z., 2014. Distribution and fractionation of rare earth elements in soil–water system and human blood and hair from a mining area in southwest Fujian Province, China. Environ Earth Science. 72: 3599-3608.

López-Gónzalez, N., Borrego, J., Ruiz, F., Carro, B., Lozano-Soria, O., Abad, M., 2006. Geochemical variations in estuarine sediments: provenance and environmental changes (Southern Spain). Estuarine, Coastal and Shelf Science 67 (1–2), 313–320.

Lotze, F., 1945. Zur Gliederung des Varisciden der Iberischen Meseta. Geotektonische Forschungen, 6:78-92.

Mantero, E., García-Navarro, E., Alonso-Chaves, F.M., Martín Parra, L.M., Matas, J., Azor, A. 2007. La Zona Sudportuguesa: propuesta para la división de un bloque continental en dominios. Geogaceta, 43: 27-30.

Marcoux, E., 1998. Lead isotope systematics of the giant massive sulphide deposits in the Iberian Pyrite Belt. Miner. Depos., 33: 45–58.

Monna, F., Lancelot, J., Croudace,I.W., Cundy, A.B.,Lewis, J.T., 1997. Pb isotopic composition of airborne particulate material from France and the southern United Kingdom: implications or Pb pollution sources in urban areas. Environ. Sci. Technol., 31 , pp. 2277–2286.

Monna, F., Aiuppa, A., Barrica, D., Dongarrà, G., 1999. Pb isotope composition in lichens and aerosol from eastern Sicily: insights into the regional impact of volcanoes on the environment. Environmental Science & Technology 33, 2517–2523.

Moreno, C., 1987. Las facies Culm del Anticlinorio de Puebla de Guzmán, Huelva, España. Universidad de Granada, 375 p.

Mudarra, J.L.; Barahona, E.; Baños, C.; Iriarte, A.; Santos, F., 1989. Mapa de suelos de Andalucía 1:400.000. Junta de Andalucía-CSIC, Sevilla, 95 p + 1 Map.

Nagajyoti, P.C., Lee, K.D., Sreekanth., T. V. M., 2010. Heavy metals, occurrence and toxicity for plants: a review. Environ. Chem. Lett. 8:199–216.

Nimick, D.A., Moor, J.M., 1991. Prediction of water-soluble metal concentrations in fluvially deposited tailings sediments, Upper Clark Fork Valley, Montana, USA. Applied Geochem.6, 635–646.

Oliveira, J. T. 1983. The marine Carboniferous of south Portugal: A stratigraphic and sedimentological approach, in The Carboniferous of Portugal, edited by M. J. L. Sousa and J. T. Oliveira, Comm. Serv. Geol. Portugal, 29, 3 – 37.

Quingjie G., Deng J., Xiang Y., Liqiang Y.,2008, Calculating Pollution Indices by Heavy Metals in Ecological Geochemistry Assessment and a Case Study in Parks of Beijing, Journal of China University of Geosciences 19(3):230-241.

Quesada, C, Fonseca, P., Munhà, J., Oliveira, J. T., Ribeiro, A., 1994. The Beja-Acebuches Ophiolite (Southern Iberia Variscan fold belt): geological characterization and geodynamic significance. Bol Geol Min 105: 3-49.

Reimann, C., Filzmoser, P., 2000. Normal and lognormal data distribution in geochemistry: death of a myth. Consequences for the statistical treatment of geochemical and environmental data. Environmental Geology. 9: 1001-1014.

Reimann, C., Filzmoser, P., Garrett, R.G., 2005. Background and threshold: critical comparison of methods of determination. Science of the Total Environment, 346, 1-16.

Rezza, C., Albanese, S., Ayuso, R., Lima, A., Sorvari, J., De Vivo., B., 2017. Geochemical and Pb isotopic characterization of soil, groundwater, human hair, and corn samples from the Domizio Flegreo and Agro Aversano area (Campania region, Italy). Journal of Geochemical Exploration. In press.

Sáez, R., Pascual, E., Toscano, M., & Almodóvar, G.R., 1999. The Iberian type of volcano-sedimentary massive sulphide deposits. Mineralium Deposita, 34, 549-570.

Salkield, L.U., 1987. A technical history of the Río Tinto mines: some notes on exploitation from pre-phoenician times to the 1950s. Institution of Mining and Metallurgy. London.

Salminen, R., Tarvainen, T., Demetriades, A., Duris M., Fordyce F.M., Gregorauskiene V., Kahelin H., Kivisilla J., Klaver G., Klein H., Larson J. O., Lis J., Locutura J., Marsina K., Mjartanova H., Mouvet C., O'Connor P., Odor L., Ottonello G., Paukola T., Plant J.A., Reimann C., Schermann O., Siewers U., Steenfelt A., Van der Sluys J., De Vivo B. and Williams L. 1998. FOREGS Geochemical Mapping Field Manual, Geological Survey of Finland, Espoo, 42 pp.

Salminen R. (Chief Editor), Batista M.J., Bidovec M., Demetriades A., De Vivo B., De Vos W., XLIII, No 5 – 2359 Ψηφιακή Βιβλιοθήκη Θεόφραστος - Τμήμα Γεωλογίας. Α.Π.Θ. Duris M., Gilucis A., Gregorauskiene V., Halamic J., Heitzmann P., Lima A., Jordan G., Klaver G., Klein P., Lis J., Locutura J., Marsina K., Mazreku A., O'Connor P.J., Olsson S.Å., Ottesen R.T., Petersell V., Plant J.A., Reeder S., Salpeteur I., Sandström H., Siewers U., Steenfelt A. and Tarvainen T. 2005. FOREGS Geochemical Atlas of Europe, Part 1: Background Information, Methodology and Maps. Geological Survey of Finland, Espoo, 526 pp. Available online at: http://www.gtk.fi/publ/foregsatlas/ (last accessed on 11/01/2017).

Simancas, J.F., 2004. Zona Sudportuguesa. In: Geología de España (J.A. Vera, Ed.), SGE-IGME, Madrid, 199-221.

Tornos, F., 2008. La geología y metalogenía de la Faja Piritica Ibérica. Macla, 10: 12-24.

Vera, J.A., 2004. Geología de España. SGE-IGME, Madrid, 890 p.

VROM (Ministry of Housing, Spatial Planning and the Environment, the Netherlands), 2000. Circular on target and intervention values for soil remediation. Netherlands Government Gazette of the 24th February 2000, no. 39.

Zuluaga, M.C., Norini, G., Lima, A., Albanese S., David, C.P., De Vivo, B. 2017.Stream sediment geochemical mapping of the Mount Pinatubo-Dizon Mine area, the Philippines: Implications for mineral exploration and environmental risk Journal of Geochemical Exploration. 175: 18–35.

Chapter 3 – Zambales Province case study

This article was published in the Journal of Geochemical Exploration 175 (2017), 18-35.

Stream sediment geochemical mapping of the Mount Pinatubo-Dizon Mine area, the Philippines: Implications for mineral exploration and environmental risk

Maria Clara Zuluaga[1], Gianluca Norini[2], Annamaria Lima[1], Stefano Albanese[1], Carlos Primo David[3], Benedetto De Vivo[1]

[1]Dipartimento di Scienze della Terra, dell'Ambiente e delle Risorse, Università di Napoli Federico II, Napoli, Italy

[2]Istituto per la Dinamica dei Processi Ambientali - Sezione di Milano, Consiglio Nazionale delle Ricerche, Milano, Italy

[3]University of the Philippines Diliman, National Institute of Geological Sciences, Quezon City, Philippines

Abstract

Stream sediments transport elements that are mobilized from adjacent slopes, representing the composition of the upstream watersheds. Thus, the analysis of the stream sediments allows to depict the spatial distribution of geochemical anomalies at the watershed level. In this study, 39 samples of stream sediments were collected in the Zambales Province, in the Philippines, characterized by the presence of the Mount Pinatubo volcano, the abandoned Cu Dizon Mine, small-mining of black sand, agriculture of rice, animal breeding, and fishing. Each sample was digested in aqua regia and was analyzed by ICP-MS to detect the content of 53 elements. This study is focused on elements with an environmental impact or associated to mineralization/ore occurring in the area. Background values for these elements have been evaluated by cumulative frequency curve to identify the occurrence of geochemical anomalies of geogenic or anthropogenic origin, mainly associated to the mining activity. Factor analysis, performed on normalized data with Additive Log Ratio transformation (ALR), *allowed to identify three geochemical data associations, and a Geographic Information System (GIS) has been used to define the spatial distribution of the anomalies at the watersheds level. The GIS procedure assigns the value of the element concentration in the sampling location to the upstream watershed by hydrologic analysis of a Digital Elevation Model (DEM) of the study area. The main result of this study is a new type of geochemical mapping of the of the Mount Pinatubo-Dizon Mine area, representing a first approach to the definition of the environmental risk and the assessment of potential mineral resources.*

Keywords: Stream sediments; ICP-MS; Factor Analysis; GIS; Environmental risk assessment; Mineral resources.

3.1. Introduction

During the last few decades much effort has been made in understanding the link between the natural or anthropogenic chemical composition of the Earth's surface and the health of organisms in contact with it (e.g. Gupta et al., 1996; Kampa et al., 2008). For this purpose, geochemical mapping and advanced analytical techniques are achieving a prominent role in the assessment and monitoring of spatial and temporal distribution of contaminants that interact with the food chain (Cicchella et al., 2005; Chen et al., 2012). One of the most effective techniques to map the geochemical distribution is the analysis of stream sediment samples, that has proven to be a very strong exploration method, because they are a composite product of erosion and weathering, reflecting the bedrock geology of the catchment area, overburden cover and metalliferous mineralization (Fletcher, 1997; Salminen, et al., 1998; Sadeghi et al., 2015).

This work presents the results of a detailed analysis and geochemical mapping of geogenic and anthropogenic elements dispersed downstream by the river sediment transport in a sector of the Zambales Province in the Philippines. The study area of 800 km^2 is characterized by a gentle slope, interrupted by a low range in its northern part. To the east is the Bataan Volcanic Complex which includes the active Mount Pinatubo volcano. The abandoned Dizon Copper Mine is located within its slopes. Towards the west are the coastal municipalities of Castillejos, San Felipe, San Antonio, San Marcelino and San Narciso (Fig. 3.1). Mount Pinatubo is an andesitic-dacitic stratovolcano, whose last eruption occurring on June 1991 deposited a large amount of pyroclastic materials on the western slopes of the Bataan Volcanic Complex and the Zambales Mountain Range (Rodolfo et al., 1996) (Fig. 3.2). The Plinian eruption, ejecting 5 km^3 of material, was the second largest volcanic explosive event of the XX century and by far the one that most affected a densely populated area, also with significant global environmental effects (e.g. Newhall and Punongbayan, 1997). The Dizon Mine porphyry Cu-Au deposit has been genetically related to a Pliocene-Pleistocene quartz diorite stock that intruded the volcanic sequence of Late Miocene age (Malihan, 1982; Imai, 2005). Both volcanic land and ore deposit resources render this area an important target of economic interest, with a growing population of about 200,000 inhabitants, mainly dedicated to agriculture, fishing and mining activities (Philippines Statistics Authority, 2010) (Fig. 3.3).

In this study, 39 sediment samples have been collected along the most representative stream channels (Figs. 3.4 and 3.5), then prepared and analyzed with ICP-MS (Section 3.3). The geochemical data have been processed with univariate and multivariate statistical analysis to identify the main populations, background values and anomalies for selected elements. By means of a factor analysis (FA) geochemical elements have been grouped in three associations (Section 3.4). Finally, the spatial distribution of the element concentrations

in the environment has been performed by the Geographic Information System (GIS), to produce geochemical maps of the area at the watershed level (Section 3.4.1).

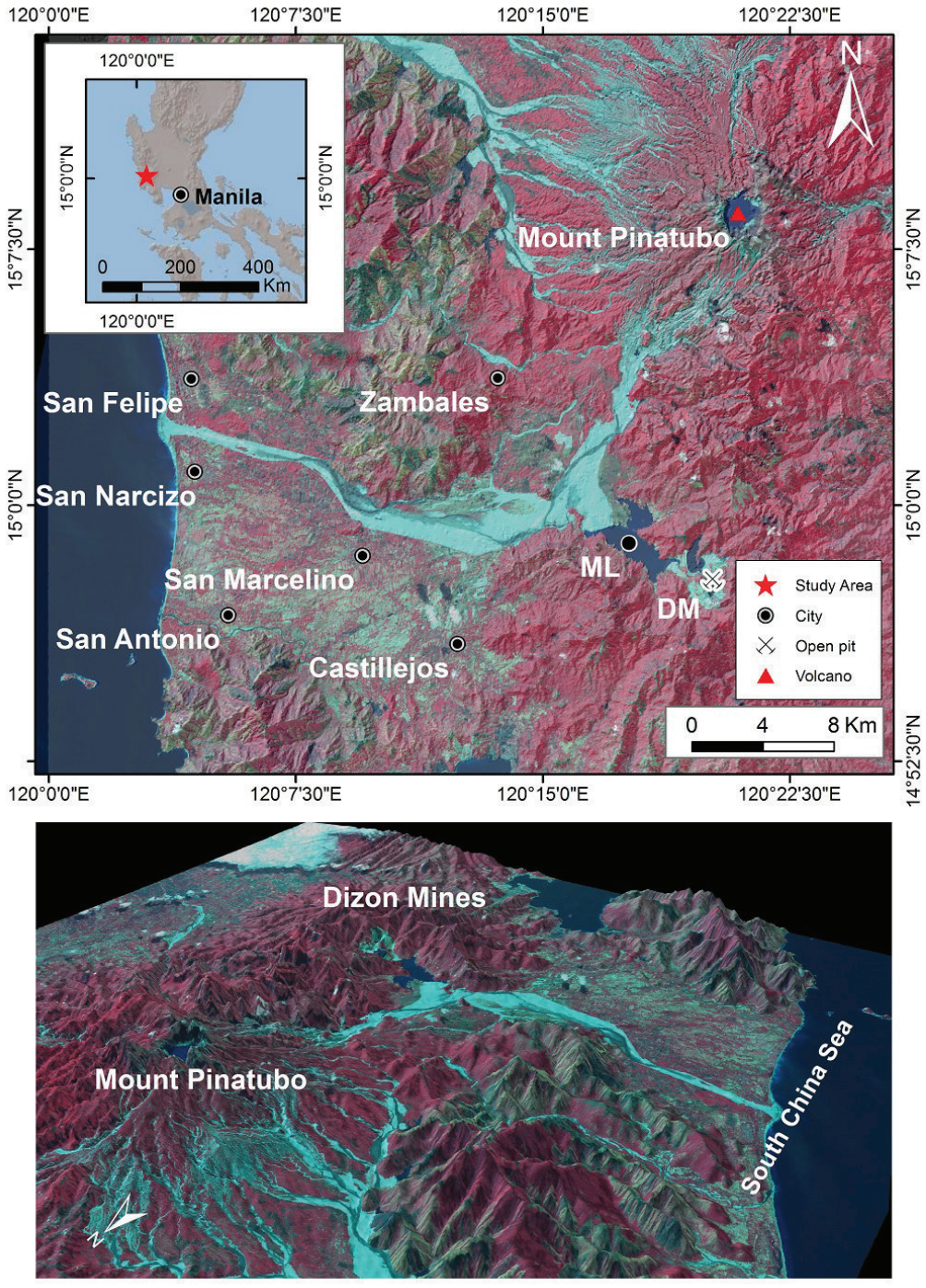

Figure 3.1: Map with the localization of the study area, and perspective view from the NW to appreciate the topography and the two main sources of stream sediments, Mount Pinatubo and Dizon Mine.

The research attempts to relate the geochemical composition of the river sediments with the geology, ore mineralization and anthropogenic activities in the area. The presented data and geochemical maps allow a first assessment of the background values, an environmental risk analysis based on available reference concentration values (VROM, 2000) and the evaluation of spatial relationships among geochemical anomalies, geology and the occurrence of potential mineral resources in the area. The final aim of the present work is to contribute to the knowledge of the environmental risk and natural resources in the Zambales Province, useful for better land use management and environmental regulations.

3.2. Background: geology, mineralization, climate and land use of the study area

3.2.1. Geology and mineralization

The Philippines islands are located in the western Pacific Ocean, along two converging plate margins, with active subduction at the Manila trench in the west and the East Luzon trough in the east (Aurelio, 2000; Imai, 2005). The study area is in the Zambales Province in the Luzon Island, 100 km northwest of Metro Manila, the capital of the country. The area is located on the western flank of the Miocene-Holocene Bataan Volcanic Complex, which includes the Mount Pinatubo, an andesitic-dacitic stratovolcano associated with the subduction of the South China sea Plate at the Manila Trench (De Boer et al., 1980; Karig, 1983; Wolfe and Self, 1983; Defant et al., 1991).

In the study area, the local basement is composed of peridotite and gabbro of the Eocene Zambales Ophiolite Complex (ZOC), an easterly-dipping slab of oceanic crust uplifted during the late Oligocene (Corby et al., 1951; Villones, 1980; Evans et al., 1991; Yumul et al., 1997). The ZOC is partially covered by the late Miocene to Pliocene marine, non-marine, and volcaniclastic sediments of the Tarlac Formation, locally composed by the dominantly volcanic rocks of the magmatic arc (Corby et al., 1951; Roque et al., 1972). One of the intrusive bodies of the Tarlac Formation is exposed in the southeast part of the study area (Fig. 3.2). This small, 2.5±0.2 Ma, steeply dipping quartz diorite porphyry stock, intruded in late Miocene volcanic rocks, is genetically linked to the mineralization of the Dizon Mine (Malihan, 1982; Imai, 2002, 2005). The mineralization is hosted mainly by the potassic and phyllic zones of the hydrothermal alteration in the quartz diorite porphyry and in the volcanic wall rocks, and consists of stockwork, quartz veinlets, fracture filling stringers and disseminations (Imai, 2005) (Fig. 3.2). The most abundant Cu mineral is chalcopyrite, followed by bornite. Faults and veins carry variable amount of sphalerite, galena, tetrahedrite and stibnite. Enargite is also found in some portions of these veins, accompanying advanced argillic alteration marked by alunite and kaolinite (Imai, 2005). Dizon Mine was operated by Benguet Corporation since 1975 with an open pit for Cu and small quantities of Au and

Ag (Fig. 3.4). The deposit has metal contents averaging 3550 mg/kg of Cu, 746 µg/kg of Au, 2000 µg/kg of Ag, between 6 and 9 mg/kg of Pb and between 52 to 95 mg/kg of Zn (Imai, 2005). The mine was closed in 1997 due to a typhoon-induced landslide that affected the area. Falling metal prices in the world market also affected the mine's ability to recover (Holden and Jacobson, 2012; Holden, 2015).

The Mount Pinatubo volcano is emplaced on top of the Tarlac Formation. The eruptive history of Mount Pinatubo is divided into two parts: (1) Ancestral Mount Pinatubo, an andesite-dacite stratovolcano with K-Ar age of 1.10+/-0.09 Ma (Ebasco Services, Inc., 1977) and 1.09+/-0.10 Ma (Bruinsma, 1983) and (2) modern Mount Pinatubo, an andesitic-dacitic dome complex and stratovolcano, with radiocarbon ages suggesting eruptions from the modern Pinatubo having been clustered in different eruptive periods, from 35,000 to 500 year BP. Mount Pinatubo is surrounded by pyroclastic-flow and lahar deposits. These Miocene-Pliocene volcanic and intrusive rocks originated from the same east-dipping subduction along the Manila trench that continues to the present (Fig. 3.3) (Newhall et al., 1996). The last eruption of the Mount Pinatubo occurred in 1991 and most of the material was deposited on its western slopes, corresponding to this study area (Rodolfo et al., 1996). Lahars occurred in 1991-1992, following the last eruption, dammed the Mapanuepe River, generating the Mapanuepe Lake and representing a natural barrier for the rivers draining the Dizon Mine area (Javellosa, 1984; Newhall et al., 1996; Umbal et al., 1996). In 2002 the Environmental Protection Authority of the Philippines revealed that heavy rains impounded water on the Dizon Mine dams, eroding it, causing the mine wastes to leak into the Mapanuepe Lake, continuing downstream to reach populations of San Marcelino y Castillejos (Orejas, 2002). About 2,000 families live near the mine site, located in an upland area some 30 kilometers east of the San Marcelino town, and the Mapanuepe Lake is a fishing ground and irrigation source (Orejas, 2002) (Figs. 3.1, 3.3, 3.5).

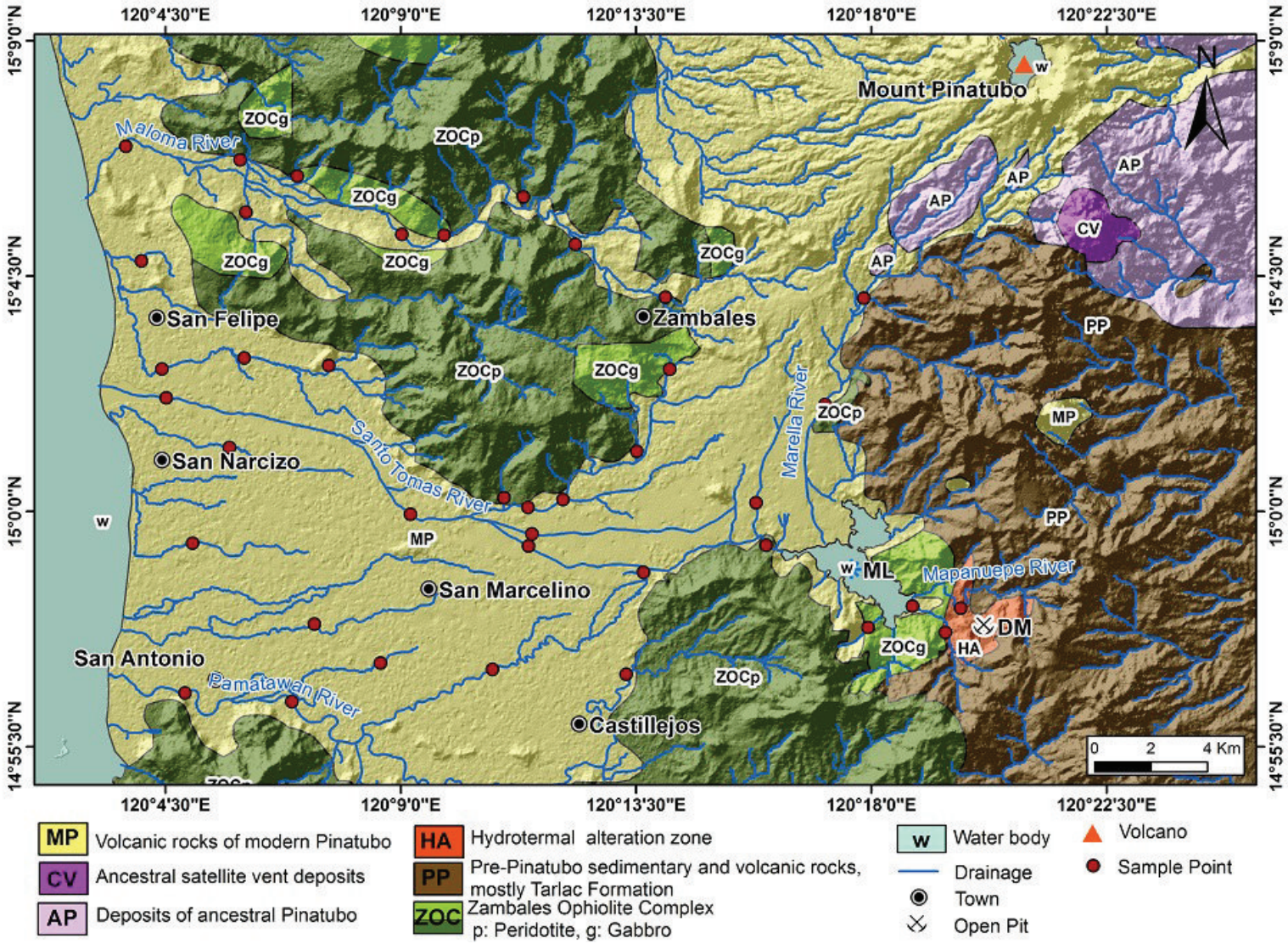

Figure 3.2: Schematic geological map of the study area (modified from Evans et al., 1991 and Imai, 2005).

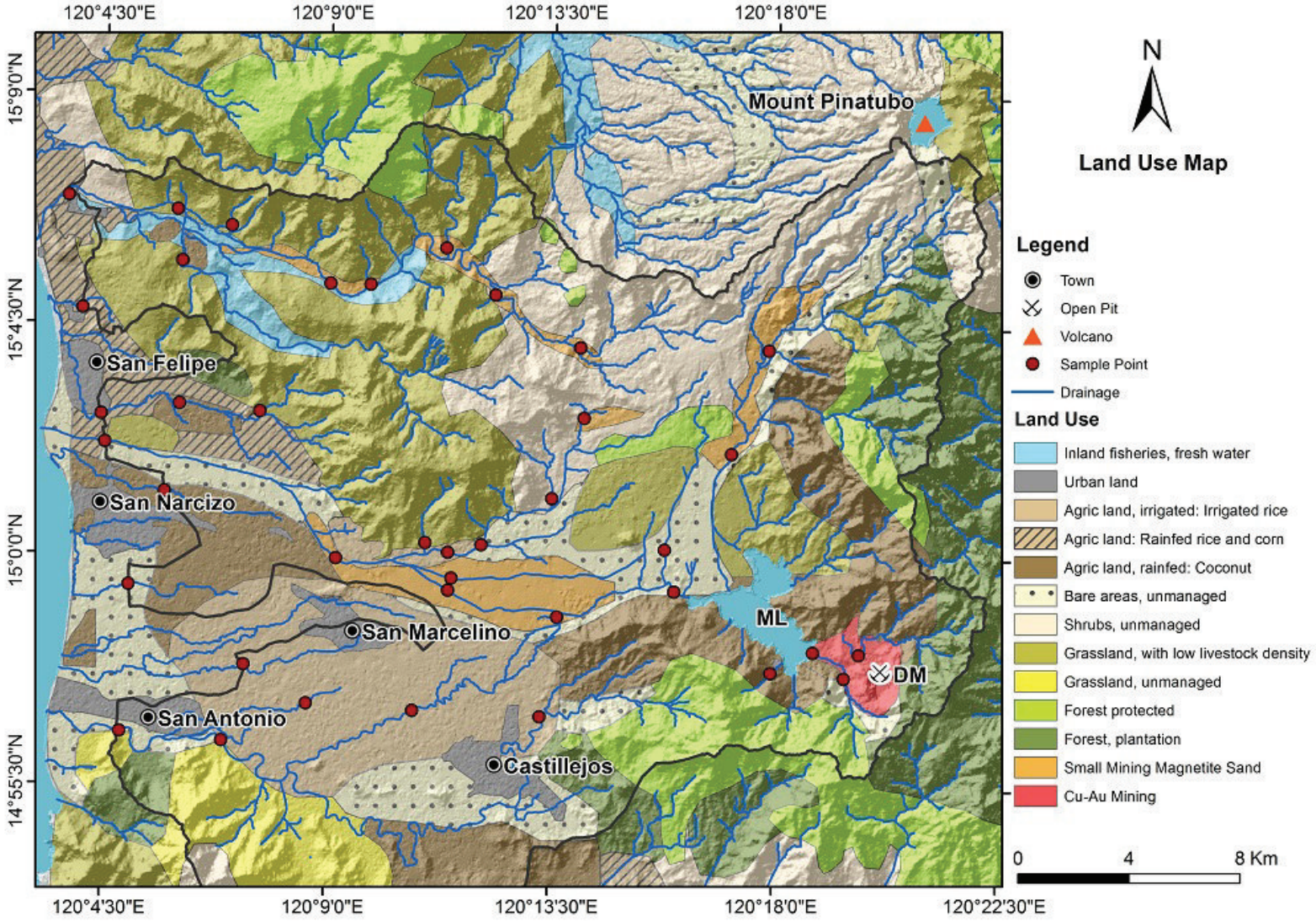

Figure 3.3: Land use map of the study area (modified from De La Torre and Perez, 2013).

3.2.2. Climate, drainage network and land use

The Zambales Mountain Range is characterized by a tropical marine climate, with a mean annual temperature of 26°C, high humidity and abundant rainfalls. The area is fully exposed to the wet southwest monsoon from May to October. The average annual rainfall is 3,800 mm (Moron et al., 2009).

The drainage network in the study area starts from the Mount Pinatubo and Dizon Mine, with flow direction toward the west into an alluvial plain and the South China Sea (Fig. 3.5). In the northeast part of the study area, the Maloma River drains the volcanic materials of Mount Pinatubo and the ZOC ultramafic terrains (Figs. 3.2, 3.5). Southward, the Santo Tomas River represents the most important fluvial channel for the reworking and transportation of the 1991-1992 Mount Pinatubo lahar deposits. The catchment of the Santo Tomas River also includes the Marella River, draining from the southwest slopes of Pinatubo, and the Mapanuepe River, crossing the Tarlac Formation and Dizon Mine area, and draining into the Mapanuepe Lake (Fig. 3.5). The southern edge of the study area is crossed by the Pamatawan River, marking the boundary between the alluvial plain to the north and the ZOC ophiolite sequence to the south (Figs. 3.2, 3.5).

Figure 3.4: Photograph of the Dizon Mine. In the foreground the mine tailings and drainage toward the Mapanuepe Lake.

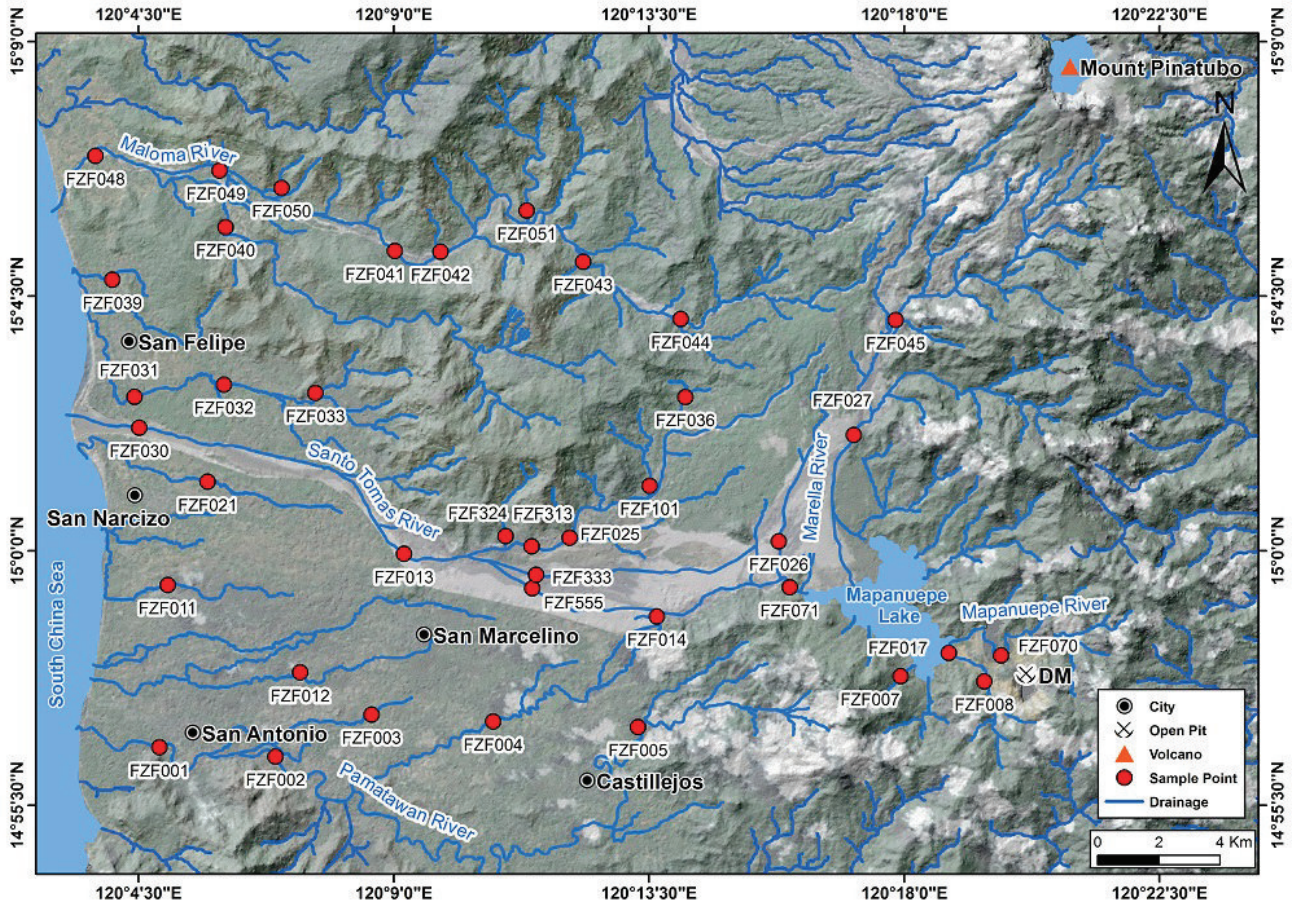

Figure 3.5 Map with the sample sites and drainage network.

The main economic activities in the study area are agriculture (rice, coconut), farming (cattle, duck, chickens and goat) and fishing (Mapanuepe Lake and South China Sea) (Fig. 3.3). In addition, local tourism plays a large and growing role in the economy of the area. Mining is also important, and, after the closure of the Dizon Mine, local mining has been focused on the exploitation of metallic (magnetite sand) and non-metallic (construction material) in the Mount Pinatubo volcanic deposits, along the Maloma, Marella and Santo Tomas Rivers (Fig. 3.3, 3.5). Plans for the future re-opening of the Dizon Mine and exploration of other intrusive-related ore deposits are under development.

The contemporaneous occurrence of different economic activities, tropical climate and volcanism may be responsible for a significant environmental risk in the area. In fact, the large annual rainfalls, and consequent dense drainage dissecting the topography, plays an important role in the downstream diffusion of endogenous geochemical elements, originated in the highlands of the western sector (Mount Pinatubo and Dizon Mine). Also, the past and present mining activities in the Mount Pinatubo slopes and Dizon Mine open pit increase the

remobilization of chemical elements that could enter in the food chain, representing a potential danger to the human health. Toxic elements are transported downstream, by both stream sediments and waters, becoming a potential risk for humans due to economic activities (farming, fishing, agriculture and tourism) active in the area (Figs. 3.2, 3.3, 3.5).

3.3. Sample grid design, sampling and analytical methods

3.3.1. Sample grid design

The study area is characterized by a topographic elevation that varies, from the east to the west, from 1480 m a.s.l. in the Mount Pinatubo/Dizon Mine area to the sea level (Figs. 3.1, 3.5). This topographic configuration, the dense drainage and the high rainfall in the area constitute a main propagation way for the chemical elements, due to the transport of stream sediments, which are a composite product of erosion and weathering of their endogenous sources.

On the premise that the drainage represents a preferential migration route of endogenous chemical elements, from the source areas to the ocean, the sampling grid has been designed in a GIS in order to collect representative information on the catchments in the study area (Fletcher, 1997). For this purpose, stream sediments were collected because they transport elements mobilized by weathering from adjacent slopes into stream beds. Consequently, each stream sediment sample of the Zambales Mountain Range is representative of the composition of the drainage basin and furnishes information on the upstream sources of geochemical anomalies (Fletcher, 1997; Adiotomre, 2014).

The small quantity of samples, imposed by the limited available budget, required great care in the sampling points selection, in order to get the necessary spatial resolution in the areas where possible contamination sources are located (e.g. Dizon Mine, ZOC outcrops), and depict the general distribution of contaminants in the whole study area. To identify the sampling points, the study area of 800 km^2 was subdivided in 4x4 km square cells. For each cell, a sampling point has been located on a stream channel inside it, depending on the stream dimension and point accessibility in the field. As a result, the study area is divided into a set of adjacent watersheds, each belonging to a sampling point, that allows to identify the source areas (watersheds) of the observed geochemical anomalies (Fig. 3.5 and section 3.4.1).

3.3.2. Sampling and sample preparation

In December of 2013 and January of 2014, during the dry season, the 39 stream sediment samples have been collected. Each sample was taken in an accessible section of the selected channel, as indicated by the sampling

grid. Every 15 sampling sites a duplicate sample was collected in the same cell to allow the blind control of the cell sampling variability combined with analytical variability. The sampling points were documented with pictures, notes and spatial information, in order to form a complete GIS database. For sampling, a plastic shovel and gloves have been used. The samples were taken by collecting sediments in 4 points across the channel, later homogenized, quartered and passed by a 2 mm plastic sieve, to remove the coarser fraction, until to get two kilos of sediments. The samples were stored in inert plastic bags and then in a box with ice, to avoid the reaction of the minerals during transport to the laboratory for preparation (Darnley et al., 1995; Salminen et al., 1998).

To prepare the samples for the ICP-MS analysis, they were placed in plastic receptacles and covered with a fabric to avoid contamination from the air. Samples were left to dry thoroughly at room temperature, sieved at <100 mesh fraction (150 µm). The pulps were stored in plastic containers of approximately 30 g, and then sent to Bureau Veritas Laboratories Ltd (Vancouver, Canada) for the chemical analysis by aqua regia digestion followed by ultratrace ICP-MS for the determination of 53 elements: Ag, Al, As, Au, B, Ba, Be, Bi, Ca, Cd, Ce, Co, Cr, Cs, Cu, Fe, Ga, Ge, Hf, Hg, In, K, La, Li, Mg, Mn, Mo, Na, Nb, Ni, P, Pb, Pd, Pt, Rb, Re, S, Sb, Sc, Se, Sn, Sr, Ta, Te, Th, Ti, Tl, U, V, W, Y, Zn and Zr. Accuracy and precision were within acceptable limits. Precision of the analysis was calculated using one in-house replicate, and four blind duplicates submitted by the authors. Accuracy was determined using in-house (ACME) reference materials (STD DS10, STD OXC109) (Table 1). Analytes were not present at detectable levels using method blanks with two samples supplied by the laboratory. Method detection limits for Al, Ca, Fe, K, Mg, Na, P, S and Ti range from 0.001 wt.% (Na, P, Ti) to 0.02 wt.% (S), and from 0.01 mg/kg to 5 mg/kg for all the other elements (Table 3.1).

Analyte	Method	Unit	Detection limit (DL)	Accuracy (%)	Precision (%Relative Percent Difference)
Fe	AQ252	%	0.01	3.72	3.68
Ca	AQ252	%	0.01	4.47	3.76
P	AQ252	%	0.001	8.22	4.11
Mg	AQ252	%	0.01	3.23	2.58
Ti	AQ252	%	0.001	4.04	1.22
Al	AQ252	%	0.01	3.32	1.95
Na	AQ252	%	0.001	1.49	2.99
K	AQ252	%	0.01	0.59	0.00
S	AQ252	%	0.02	3.45	0.00
Mo	AQ252	mg/kg	0.01	5.58	4.90
Cu	AQ252	mg/kg	0.01	7.14	8.70

Pb	AQ252	mg/kg	0.01	7.42	4.94
Zn	AQ252	mg/kg	0.1	7.14	7.32
Ni	AQ252	mg/kg	0.1	3.62	5.36
Co	AQ252	mg/kg	0.1	1.55	3.10
Mn	AQ252	mg/kg	1	1.49	2.97
As	AQ252	mg/kg	0.1	9.84	4.35
U	AQ252	mg/kg	0.05	6.95	6.95
Th	AQ252	mg/kg	0.1	10.67	10.67
Sr	AQ252	mg/kg	0.5	7.30	1.49
Cd	AQ252	mg/kg	0.01	3.61	0.80
Sb	AQ252	mg/kg	0.02	3.52	0.61
Bi	AQ252	mg/kg	0.02	17.60	16.65
V	AQ252	mg/kg	2	0.00	2.33
La	AQ252	mg/kg	0.5	8.00	8.00
Cr	AQ252	mg/kg	0.5	4.03	1.28
Ba	AQ252	mg/kg	0.5	1.06	8.44
B	AQ252	mg/kg	1	0.00	0.00
W	AQ252	mg/kg	0.05	5.72	4.82
Sc	AQ252	mg/kg	0.1	7.14	0.00
Tl	AQ252	mg/kg	0.02	0.59	4.90
Se	AQ252	mg/kg	0.1	8.70	26.09
Te	AQ252	mg/kg	0.02	0.20	0.20
Ga	AQ252	mg/kg	0.1	4.65	4.65
Cs	AQ252	mg/kg	0.02	1.90	3.80
Ge	AQ252	mg/kg	0.1	0.00	0.00
Hf	AQ252	mg/kg	0.02	0.00	16.67
Nb	AQ252	mg/kg	0.02	3.09	1.85
Rb	AQ252	mg/kg	0.1	0.00	3.61
Sn	AQ252	mg/kg	0.1	0.00	6.25
Ta	AQ252	mg/kg	0.05	0.00	0.00
Zr	AQ252	mg/kg	0.1	3.57	7.14
Y	AQ252	mg/kg	0.01	2.96	2.70
Ce	AQ252	mg/kg	0.1	0.00	0.00
In	AQ252	mg/kg	0.02	0.00	8.70
Be	AQ252	mg/kg	0.1	26.98	15.87
Li	AQ252	mg/kg	0.1	5.15	8.76
Ag	AQ252	µg/kg	2	0.89	2.08
Au	AQ252	µg/kg	0.2	1.96	16.97
Hg	AQ252	µg/kg	5	0.67	0.67
Re	AQ252	µg/kg	1	2.00	16.00
Pd	AQ252	µg/kg	10	6.36	5.45
Pt	AQ252	µg/kg	2	5.24	0.52

Table 3.1: Detection limits, accuracy and precision

3.4. Data analysis

Univariate and multivariate statistical analyses of the geochemical data have been performed, and their elemental association using normalized data have been identified by means of factor analysis (FA). For statistical purpose, concentration values below the minimum instrumental detection limit (DL) have been assigned to ½ of the DL (Table 3.1, 3.2).

The statistical distributions of the geochemical data were converted in lognormal to normalize their values showing strong right skewness (Figs. 3.6B, D, F) (Reimann and Filzmoser, 2000; Reimann et al., 2005). The cumulative frequency curves (CFCs) of the analyzed elements show inflections and break-points, reflecting the presence of multiple populations, originated by the geogenic and/or anthropogenic contribution to the concentration values (Reimann et al., 2005) (Figs. 3.6A, C, E). Figures 3.6A, B, C, D, E, F show an example of the histograms and CFCs of As, representing one of the most harmful elements in the area, Cr, which present high concentration in some of the samples related to the ZOC (Fig. 3.2), and Cu, which is the main commodity. Six intervals have been identified on the CFCs using the nearest flexion points, corresponding to the 10, 25, 50, 75 and 98 percentiles. These intervals were used to plot the geochemical maps (Section 3.4.1, Figs. 3.6A, C, E) (De Vivo et al., 2004; Albanese et al., 2007).

The determination of the background ranges is a key point for the definition of the geochemical anomalies, and this study represents the first approach for their calculation for selected chemical elements in the Zambales Mountain Range (Table 3.3) (e.g. Hernández-Crespo and Martín, 2015). The background ranges have been defined by the analysis of the CFCs, at the first and snappish flex of the curve (Reimann et al., 2005, De Vivo et al., 2006) (Figs. 3.6A, C, E) (Table 3.3).

FA is a statistical technique of data reduction used to explain the correlations between observed variables in terms of a smaller number of unobserved variables called factors (e.g. Reimann et al., 2002, Caritat and Grunsky, 2013). FA has been performed using SPSS statistics 20 software (IBM, 2011) on a matrix containing only 27 elements of the 53 analyzed by ICP-MS (Ag, As, Au, Ba, Bi, Ca, Cd, Co, Cr, Cu, Fe, Hg, K, La, Mn, Mo, Na, Ni, P, Pb, Sb, Sr, Th, Ti, U, V and Zn). Excluded from FA were elements with more than 40% of values below the DL (except Hg) and elements with cumulative variances <0.75 (e.g. Sc, Rb, Sn, Li, Mg) (e.g. Reimann et al., 2002; Wang et al., 2015). In addition, also some elements with similar geochemical behavior were not considered (e.g. Cs, Ga, Hf, Nb, Y and Zr). To improve the capability of the data to be associated using FA, they have been normalized with Additive Log Ratio transformation (ALR), as described by Aitchison (1986) and Pawlowsky-Glahn et al. (2011). Then, orthogonal varimax rotation and correlation matrix were used to facilitate the interpretation of results (e.g. Albanese et al., 2007, Wang et al., 2015; Sadeghi et al., 2015). Table 3.4 shows the

resulting three factors model, accounting for the 78.8% of the data variability of the 39 stream sediment samples of the Zambales Mountain Range. Elements with loadings >|0.5| are considered to describe quite effectively the composition of each factor. The three-factor model associations are: F1) La, P, U, Ca, Th, Sr, Ti, V, Ba, K, Na, Zn; F2) Ag, Mo, Bi, Cu, Au, Pb, Sb, Hg, As, Cd, Zn; F3) Cr, Co, Ni, Fe (Tables 3.4 and 3.5).

Element	Unit	Minimum	Maximum	Mean	Median	Std Deviation	Variance	Kurtosis	*MAD
Fe	%	0.62	8.44	1.79	2.29	1.58	2.49	5.27	2.29
Ca	%	0.08	0.66	0.38	0.38	0.14	0.02	0.05	0.38
P	%	0.01	0.23	0.07	0.09	0.05	0.00	0.14	0.09
Mg	%	0.12	7.95	0.31	0.58	1.26	1.59	32.64	0.58
Ti	%	0.01	0.15	0.06	0.06	0.03	0.00	1.15	0.06
Al	%	0.21	2.10	0.53	0.67	0.43	0.19	2.42	0.67
Na	%	0.01	0.23	0.06	0.07	0.05	0.00	0.89	0.07
K	%	0.01	0.15	0.03	0.04	0.02	0.00	12.73	0.04
S	%	0.01	1.22	0.01	0.07	0.22	0.05	22.45	0.07
Mo	mg/kg	0.04	23.84	0.16	1.68	5.29	27.97	11.72	1.68
Cu	mg/kg	9.38	733.17	22.85	62.21	126.66	16041.80	21.44	62.21
Pb	mg/kg	0.70	31.20	1.39	3.82	6.33	40.13	10.74	3.82
Zn	mg/kg	13.50	235.60	33.60	47.25	46.30	2144.07	11.75	47.25
Ni	mg/kg	5.60	1370.50	14.30	109.75	305.83	93531.97	14.50	109.75
Co	mg/kg	2.50	85.20	6.10	12.72	17.18	295.05	9.55	12.72
Mn	mg/kg	98.00	3320.00	272.00	528.21	659.81	435350.27	9.56	528.21
As	mg/kg	0.05	114.80	0.40	7.96	25.13	631.48	13.36	7.96
U	mg/kg	0.03	0.23	0.10	0.11	0.04	0.00	1.17	0.11
Th	mg/kg	0.20	0.90	0.50	0.47	0.15	0.02	0.72	0.47
Sr	mg/kg	9.00	55.30	20.20	23.99	10.15	103.01	0.77	23.99
Cd	mg/kg	0.01	1.27	0.02	0.09	0.24	0.06	17.08	0.09
Sb	mg/kg	0.01	9.93	0.03	0.65	2.20	4.82	12.66	0.65
Bi	mg/kg	0.01	0.94	0.03	0.08	0.18	0.03	16.93	0.08
V	mg/kg	23.00	160.00	58.00	65.21	34.73	1206.11	1.49	65.21
La	mg/kg	1.20	11.20	4.40	5.31	2.57	6.58	-0.32	5.31
Cr	mg/kg	12.40	425.60	32.30	64.85	87.29	7620.39	9.45	64.85
Ba	mg/kg	13.60	75.10	28.00	33.11	15.56	242.13	-0.04	33.11
B	mg/kg	0.50	4.00	1.00	1.18	0.82	0.68	2.27	1.18
W	mg/kg	0.03	23.73	0.03	0.65	3.79	14.38	38.99	0.65
Sc	mg/kg	0.60	12.70	1.70	2.54	2.29	5.26	9.90	2.54
Tl	mg/kg	0.01	0.12	0.01	0.02	0.03	0.00	6.08	0.02
Hg	mg/kg	2.50	1985.00	2.50	93.62	355.88	126649.19	22.99	93.62

Se	mg/kg	0.05	4.50	0.05	0.28	0.89	0.79	17.67	0.28
Te	mg/kg	0.01	3.05	0.01	0.16	0.60	0.36	18.39	0.16
Ga	mg/kg	0.90	4.80	2.60	2.88	1.07	1.14	-0.90	2.88
Cs	mg/kg	0.09	1.84	0.28	0.40	0.38	0.14	6.36	0.40
Ge	mg/kg	0.05	0.10	0.05	0.05	0.01	0.00	16.78	0.05
Hf	mg/kg	0.01	0.12	0.03	0.04	0.03	0.00	-0.46	0.04
Nb	mg/kg	0.01	0.23	0.06	0.08	0.05	0.00	0.71	0.08
Rb	mg/kg	0.50	4.80	1.80	1.92	0.98	0.96	2.81	1.92
Sn	mg/kg	0.10	1.70	0.30	0.40	0.33	0.11	5.46	0.40
Ta	mg/kg	0.03	0.03	0.03	0.03	0.00	0.00	-2.11	0.03
Zr	mg/kg	0.40	5.00	1.30	1.52	0.91	0.83	4.10	1.52
Y	mg/kg	1.20	5.15	3.11	3.06	0.90	0.82	-0.19	3.06
Ce	mg/kg	2.60	27.40	10.30	11.96	5.83	34.03	0.33	11.96
Ln	mg/kg	0.01	0.09	0.01	0.01	0.02	0.00	16.91	0.01
Be	mg/kg	0.05	0.30	0.05	0.10	0.07	0.01	1.61	0.10
Li	mg/kg	0.70	4.60	1.80	1.88	0.90	0.80	1.43	1.88
Ag	µg/kg	7.00	350.00	12.00	36.38	77.92	6071.30	10.97	36.38
Au	µg/kg	0.10	209.80	1.20	11.22	36.99	1368.37	23.08	11.22
Re	µg/kg	0.50	75.00	0.50	4.03	13.46	181.12	21.91	4.03
Pt	µg/kg	1.00	4.00	1.00	1.18	0.60	0.36	14.47	1.18

Table 3.2: Statistical parameters of 39 stream sediment samples (* median absolute deviation)

Element		Statistical Background in the study area	Maximum concentration in the study area	Netherlands Intervention Limits
As (mg/kg)	Arsenic	0.40	**114.80**	55
Cd (mg/kg)	Cadmium	0.02	1.27	12
Cr (mg/kg)	Chromium	39.80	**425.60**	380
Ni (mg/kg)	Niquel	14.30	**1370.50**	210
Cu (mg/kg)	Cooper	23.44	733.17	190
Pb (mg/kg)	Lead	1.39	31.20	530
Hg (µg/kg)	Mercury	25.11	1985	10000
Sb (mg/kg)	Antimonium	0.03	9.93	15
Mo (mg/kg)	Molybdenum	0.16	23.84	200
Zn (mg/kg)	Zinc	33.60	235.60	720

Table 3.3: Background evaluated for selected harmful elements and intervention limits proposed by the Ministry of Housing, Spatial Planning and the Environment of the Netherlands (VROM, 2000).

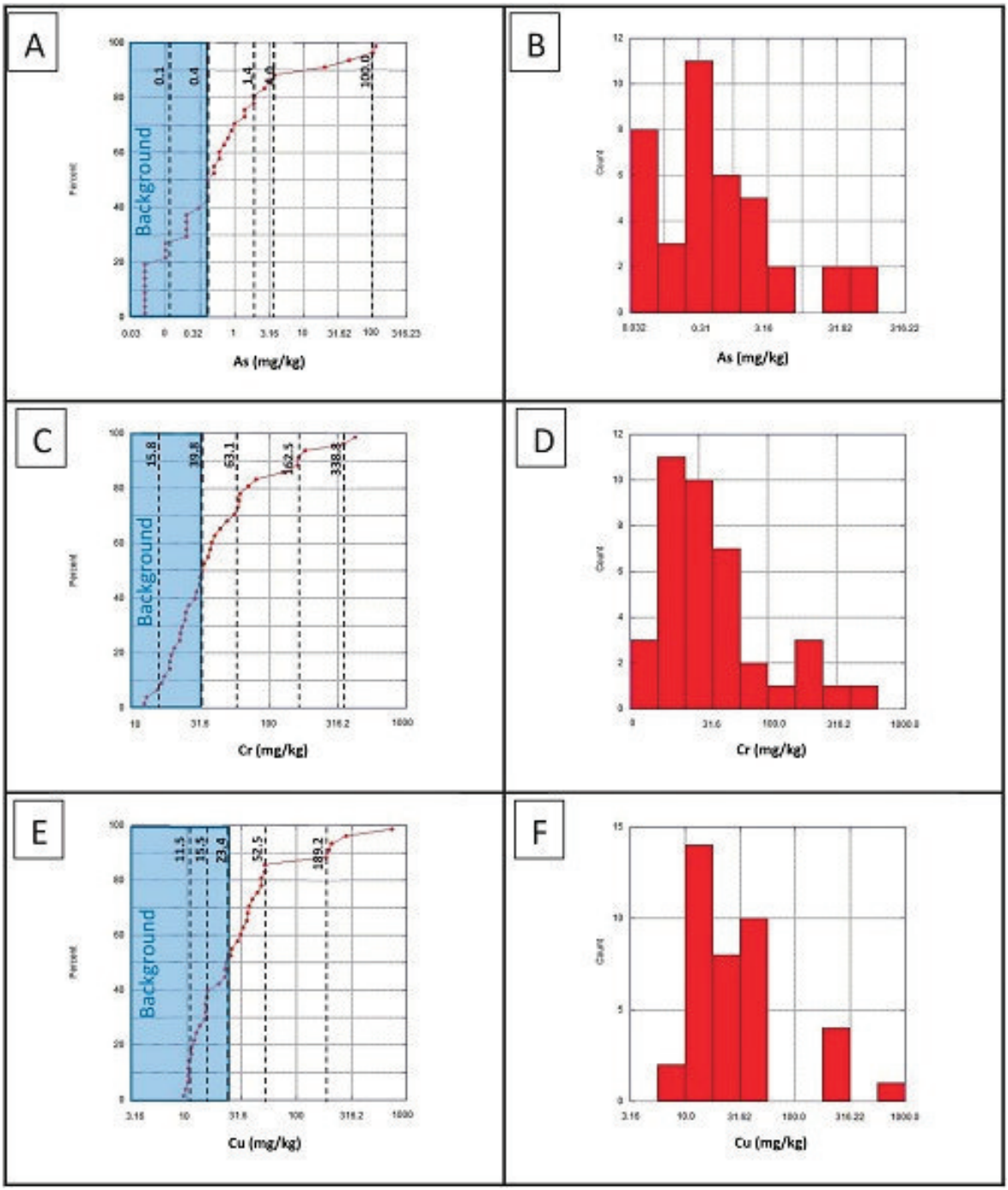

Figure 3.6: Accumulative frequency curves and histograms for As (A and B); Cr (C and D) and Cu (E and F). *MAD median absolute deviation

Elements	F1	F2	F3
Ag	.105	**.926**	-.107
As	-.352	**.717**	-.178
Au	-.052	**.883**	.017
Ba	**.777**	.151	-.109
Bi	.163	**.897**	.092
Ca	**.905**	-.233	.123
Cd	.104	**.711**	.028
Co	-.013	.007	**.859**
Cr	.256	-.228	**.926**
Cu	.091	**.896**	.079
Fe	.449	.439	**.623**
Hg	-.238	**.824**	-.128
K	**.717**	.307	-.476
La	**.935**	.111	.191
Mn	.262	-.041	.247
Mo	.111	**.925**	-.150
Na	**.695**	-.455	-.326
Ni	-.238	-.334	**.771**
P	**.934**	.118	.192
Pb	.100	**.869**	-.126
Sb	-.130	**.852**	-.339
Sr	**.870**	-.280	-.227
Th	**.896**	.199	-.197
Ti	**.836**	-.429	.196
U	**.918**	.159	.088
V	**.813**	.115	.411
Zn	**.591**	**.509**	.273
Eigen Value	8.9	8.6	3.7
Variance %	33.1	32.0	13.6
Cum % of Variance	33.1	65.1	78.8

Table 3.4: Varimax-rotated factor (three-factor model) for 27 selected elements and 39 stream sediment samples. ARL transformed data. In bold loading values > |0.5|. Total variance explained 78.8%

3.4.1. Watershed analysis for geochemical mapping

For several decades, the geochemical analysis of stream sediments has been used as a cost effective tool for mining exploration and environmental studies in areas were stream drainage systems are well developed. This is because the sediments are a composite of the products of weathering and erosion derived from their catchment basins (Fletcher, 1997).

The geochemical mapping from this type of stream sediments composition data can be obtained with geostatistics interpolators based on autocorrelation principles, applying the concept of Euclidian points distance regardless of the topography and complexity of the drainage in the study area, even in natural models where the proximity of sampling points on a map does not often imply that they share correlated variables (e.g. Matheron, 1965; Wakernagel, 1995; Webster and Oliver, 2001; Lima et al., 2003; Zumlot et al., 2009). As an alternative, geochemical maps from stream sediment samples have been produced by drainage analysis and catchment delineation, assigning the value of the element concentration in the sampling location to the upstream watershed (e.g. Spadoni et al., 2005; Spadoni, 2006).

In the present study, considering the number of samples collected in the Zambales Mountain Range in comparison with the density of the drainage network and the extent of the area, geochemical maps have been produced through watersheds delineation. For this result, a new GIS algorithm for geochemical mapping from stream sediment samples has been developed, representing a first approach to identify the areas of geochemical anomalies at the watershed level in the study area (Fig. 3.7).

The first step of the GIS algorithm is to calculate the drainage network (Figs. 3.5, 3.7). For this process, a Shuttle Radar Topographic Mission (SRTM) Digital Elevation Model (DEM) of the study area with resolution of 90 m has been used. The drainage is obtained by the flow direction matrix, which is a hydrologic terrain attribute defining the flow direction from every cell in the DEM (Fig. 3.7). For the gentle lowlands area, where the accuracy of the SRTM DEM is not enough to support the calculation of the flow direction matrix, the drainage was acquired by the digitalization of optical satellite images. The second step uses the same DEM to obtain a slope map, which is then divided into highlands (moderate to high slope areas) and alluvial plains (gentle areas) (Figs. 3.5, 3.7, 3.8A). In the third step of the GIS algorithm, the watersheds map is obtained for the highlands with the analysis of the flow direction matrix and the location of the stream sediment samples. This map shows the catchment upstream of each sampling location in the highlands area (Figs. 3.7, 3.8B). For the alluvial plains area, where the flow direction matrix is not suitable for the precise definition of catchments, a proximity analysis applied to the drainage network identifies the watersheds in the gentle lowlands area upstream of each sampling locations (Figs. 3.7, 3.8C). Catchments in the highlands and in the alluvial plains are then merged

obtaining the final watersheds map (Fig. 8D and Table 3.5). Finally, the results of the geochemical analysis for each stream sediment sample are assigned to the corresponding drainage basin, resulting in the geochemical map for each element at the watershed level (Figs. 3.7, 3.8D). These maps, based on the six intervals defined in section 3.4, delineate the areas (watersheds) where the sources of the geochemical anomalies area located, even if the variation of concentration values inside a single watershed is not calculated (Figs. 3.6A, C, E, 3.8D).

Geochemical maps have been obtained with the GIS algorithm for selected chemical elements considered to be potentially harmful to living beings or associated to the lithology and mineralization/ore occurring in the area (Corby et al., 1951; Villones, 1980; Evans et al., 1991; Newhall et al., 1996; Yumul et al., 1997; Imai, 2005). These elements are: As, Au, Cd, Cr, Cu, Hg, Ni, La, Pb, and V (Figs. 3.8D, 3.9, 3.10).

Also, geochemical maps have been obtained for the factor scores of the three elements associations defined by the FA (F1, F2 and F3, to evaluate their correlations with the geogenic or anthropogenic sources of geochemical anomalies that have been identified in the area (Fig. 3.11) (Table 3.6).

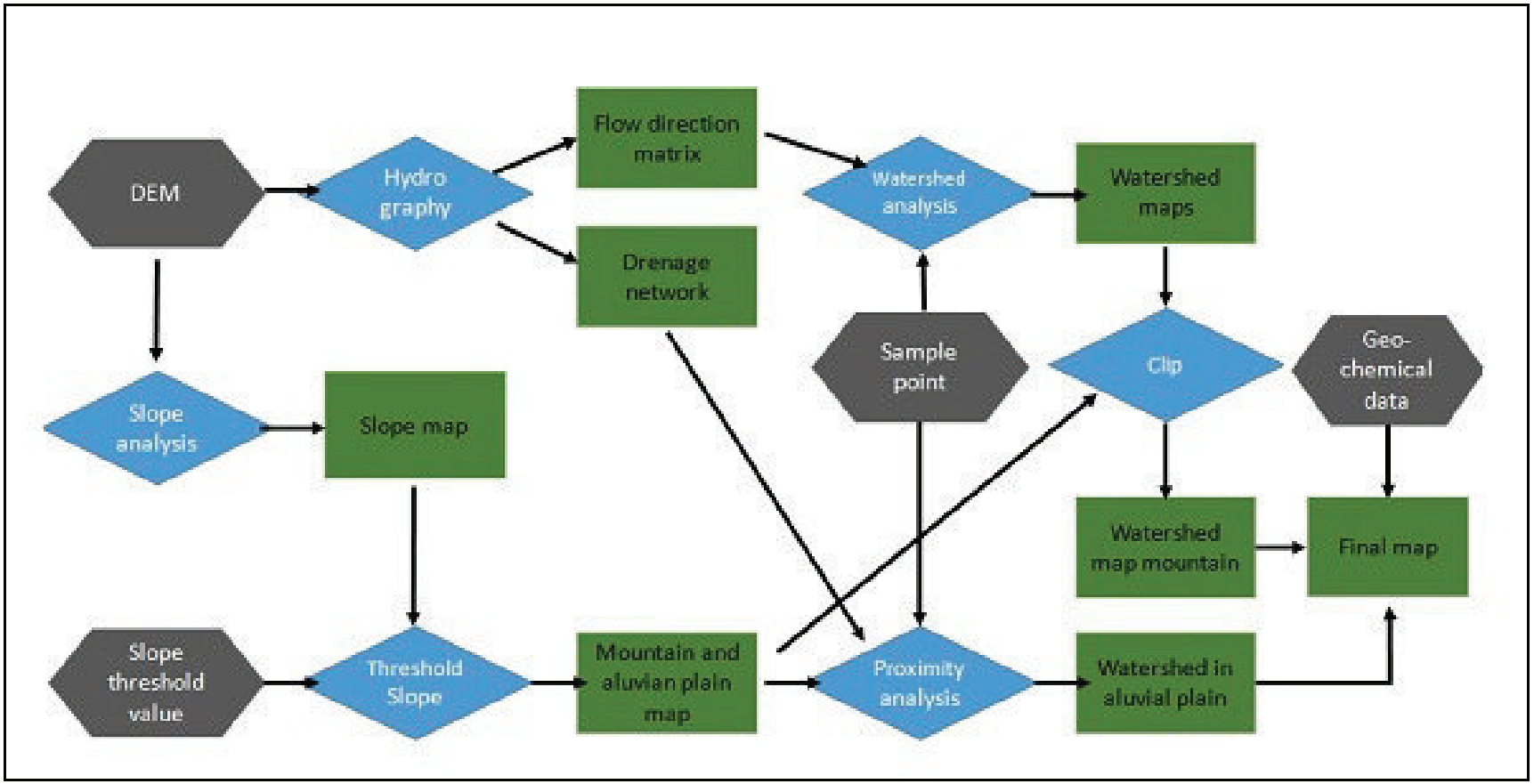

Figure 3.7: Flow diagram of the GIS algorithm for the watersheds mapping.

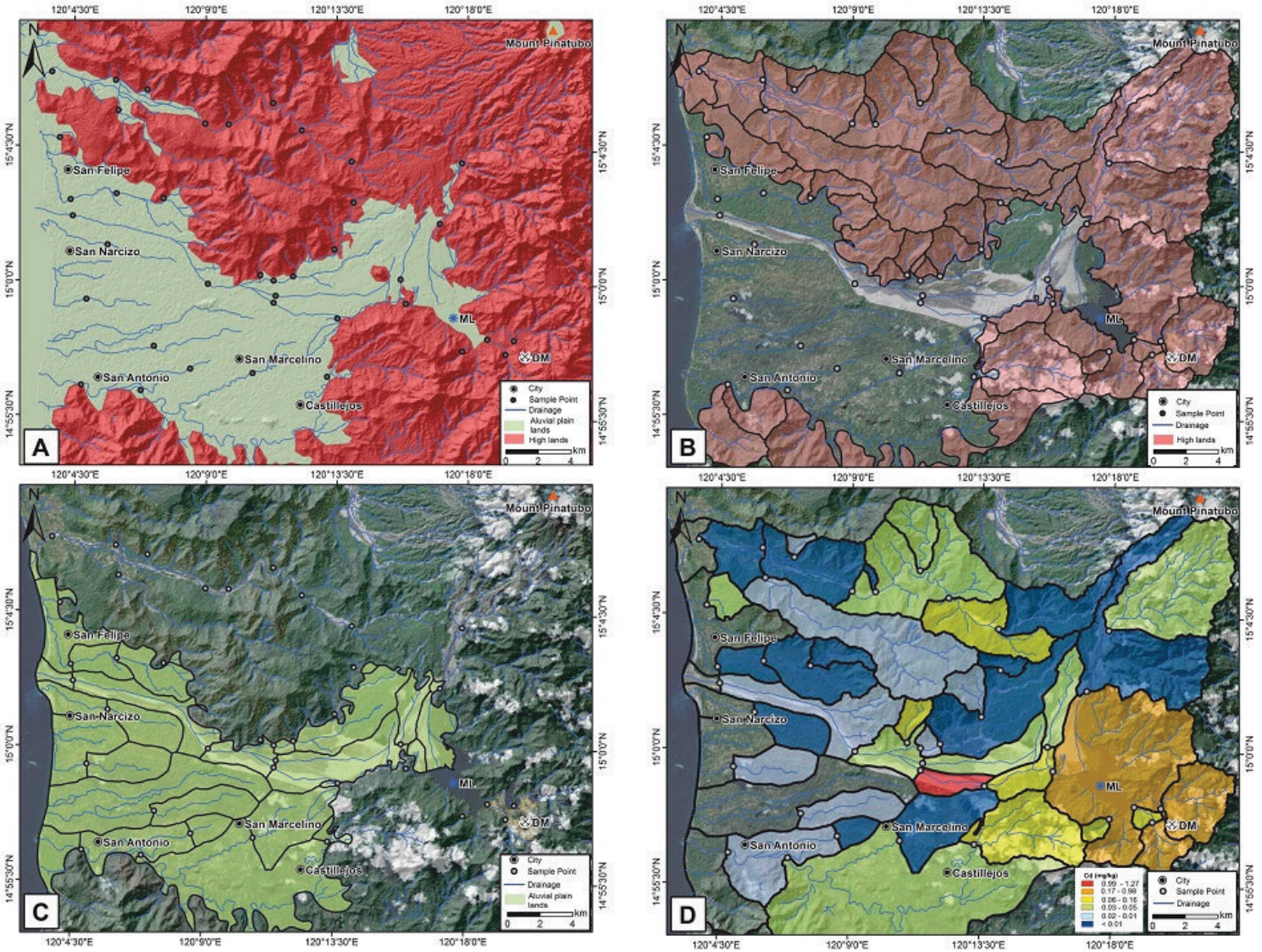

Figure 3.8: Steps for the development of the GIS algorithm. (A) In red the highlands and in green the alluvial plains with slopes under 15%. (B) Sub-basins from the highlands. (C) Sub-basin of the alluvial plains. (D) Geochemical map at the watersheds level using the values of the Cd concentration.

SAMPLE	MEAN SLOPE (%)	MIN HIGHT (masl)	MAX HIGHT (masl)	TOTAL DRAINAGE LENGHT (KM)	CATCHMENT AREA (Km^2)	NUMBER OF STREAM
FZF001	7.5	3.4	717.6	15.7	20.1	6
FZF002	7.0	10.2	1000.0	50.4	84.3	6
FZF003A	1.3	20.4	52.6	1.5	3.8	1
FZF004	1.9	41.7	269.8	15.4	18.1	5
FZF005	11.4	50.3	845.5	19.4	22.9	14
FZF007	20.6	191.3	845.7	1.3	1.9	1
FZF008	16.9	175.2	880.9	6.4	7.4	7
FZF011	1.2	0.0	47.9	4.7	9.9	1
FZF012	1.2	16.4	64.8	6.5	10.5	1
FZF013	4.7	33.3	507.8	8.7	8.8	5
FZF014	8.9	85.1	466.7	6.3	7.0	5
FZF017	12.3	126.4	449.1	1.8	1.7	1
FZF021	1.3	6.7	45.1	5.1	9.2	1
FZF025	5.8	55.5	655.1	27.4	28.8	18
FZF026	2.7	130.3	338.5	2.0	8.4	3
FZF027	15.8	188.7	1317.6	42.6	40.2	33
FZF030	6.6	0.0	660.7	19.5	22.5	11
FZF031	1.2	2.0	27.4	4.9	5.9	3
FZF032	7.8	5.0	698.6	14.7	16.1	9
FZF033	15.3	12.1	697.8	4.9	5.0	3
FZF036	10.3	127.7	516.6	7.4	2.8	3
FZF039	9.0	3.4	328.9	1.9	4.8	1
FZF040	13.3	11.8	772.1	34.1	40.8	34
FZF041	16.1	30.6	925.9	31.5	36.4	30
FZF042	15.9	42.7	502.9	1.6	0.7	1
FZF043	10.4	112.4	773.0	16.3	18.4	12
FZF044	9.1	164.3	662.5	19.1	16.6	20
FZF045	16.4	304.6	1580.0	41.9	37.8	39
FZF048	7.6	0.6	474.5	9.9	11.1	5
FZF049	13.1	7.4	808.5	24.0	19.2	17
FZF050	19.2	32.3	517.1	1.4	1.4	1
FZF051	20.0	93.0	1023.5	9.3	8.4	9
FZF070	16.4	226.1	883.8	13.2	16.1	9
FZF071	11.5	115.7	1073.5	46.6	64.5	49
FZF101	14.1	83.6	599.5	5.0	5.2	4
FZF313	8.3	52.8	427.5	1.3	2.0	1
FZF324	19.2	59.2	652.1	3.5	3.6	3
FZF333	2.0	56.8	291.3	9.0	11.2	3
FZF555	1.3	50.7	108.3	4.3	5.5	2

Table 3.5: Main characteristics of the mapped watersheds, including area, mean slope, maximum and minimum elevation and drainage length.

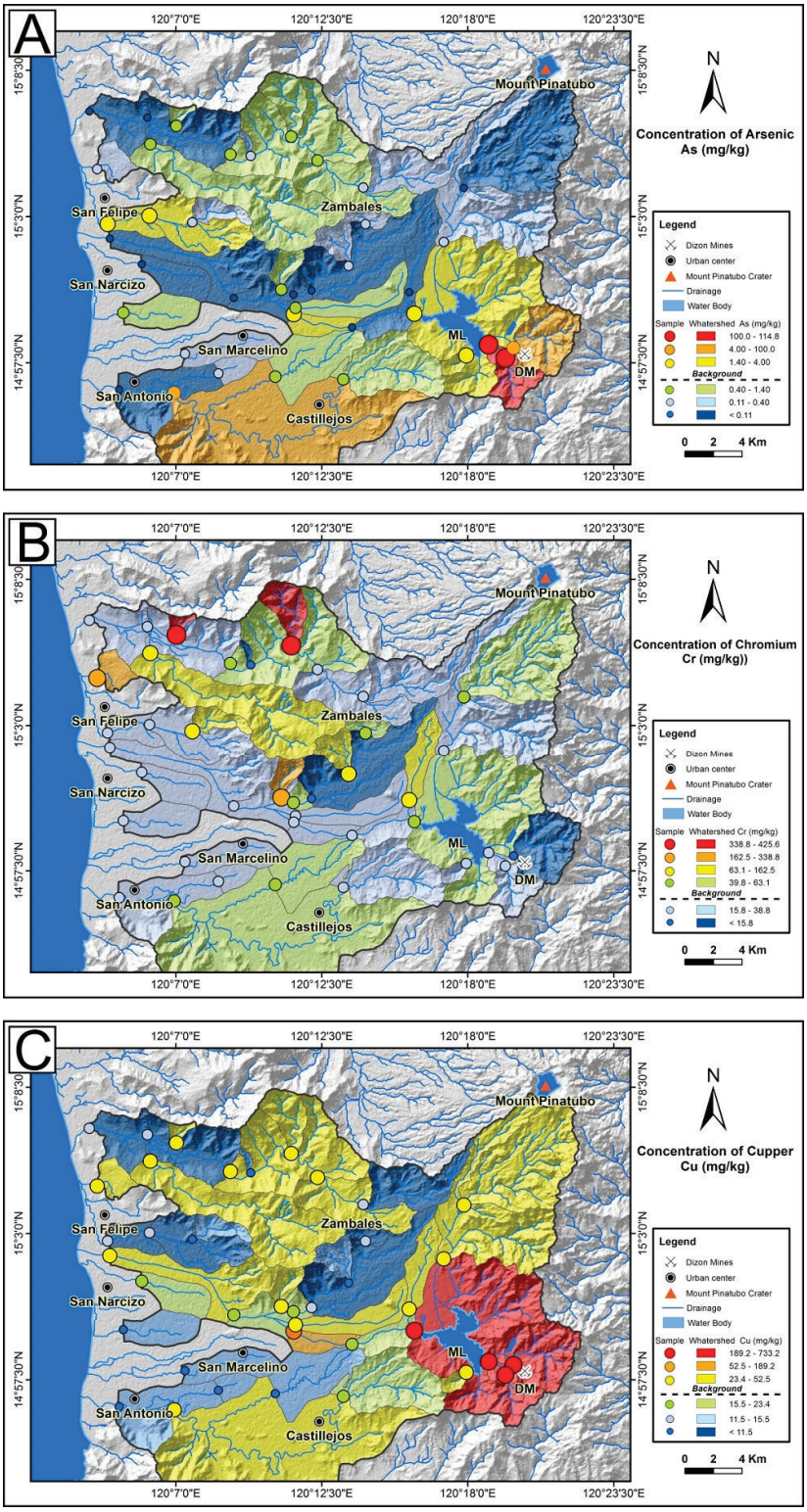

Figure 3.9: Geochemical map of As (A), Cr (B) and Cu (C) based on the watersheds defined by the GIS algorithm. The dotted line in the legend shows the limit of the background values.

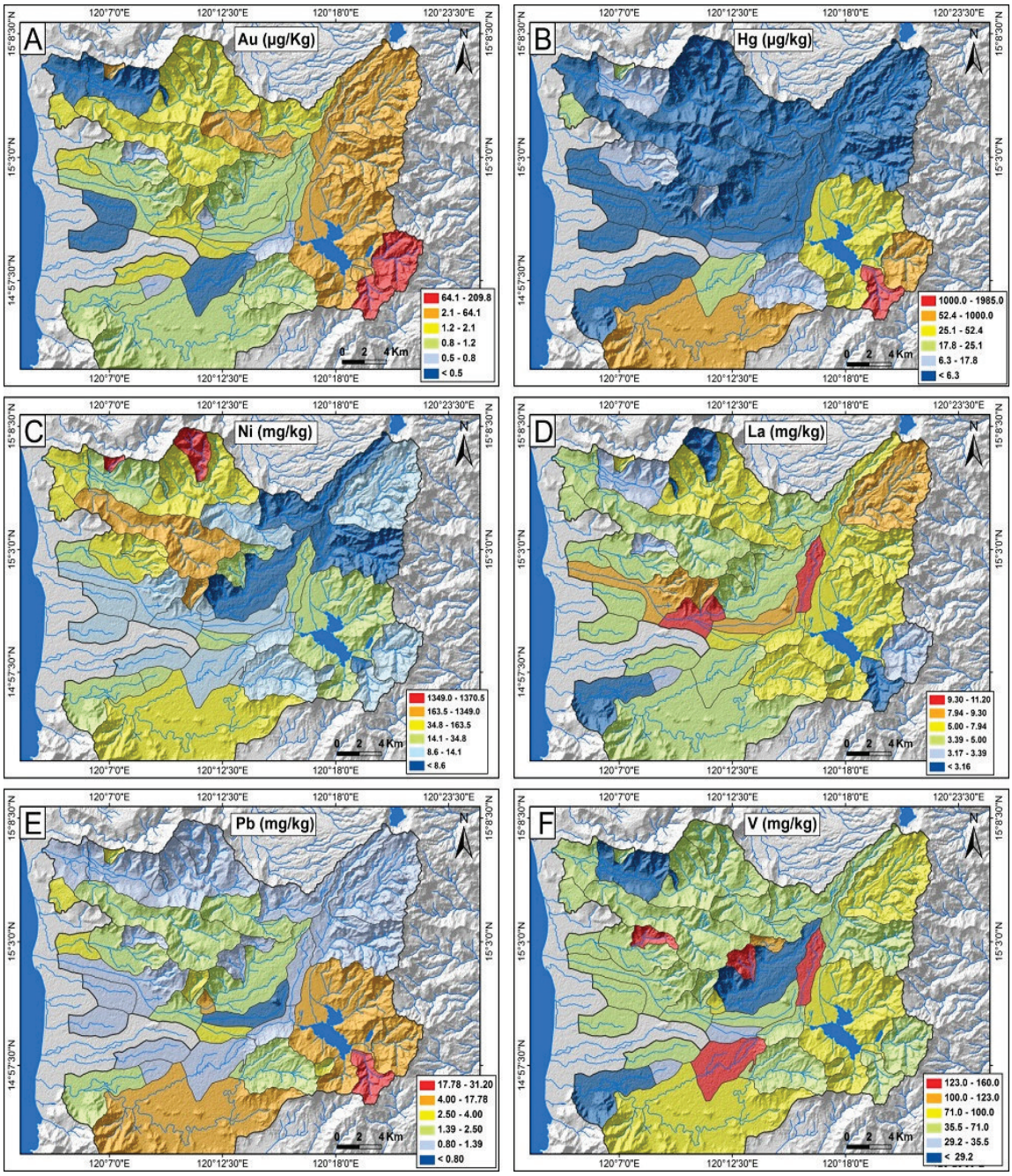

Figure 3.10: Geochemical maps of selected elements representing a risk for the human health or of economic interest. Au (A), Hg (B), Ni (C), La (D), Pb (E) and V (F).

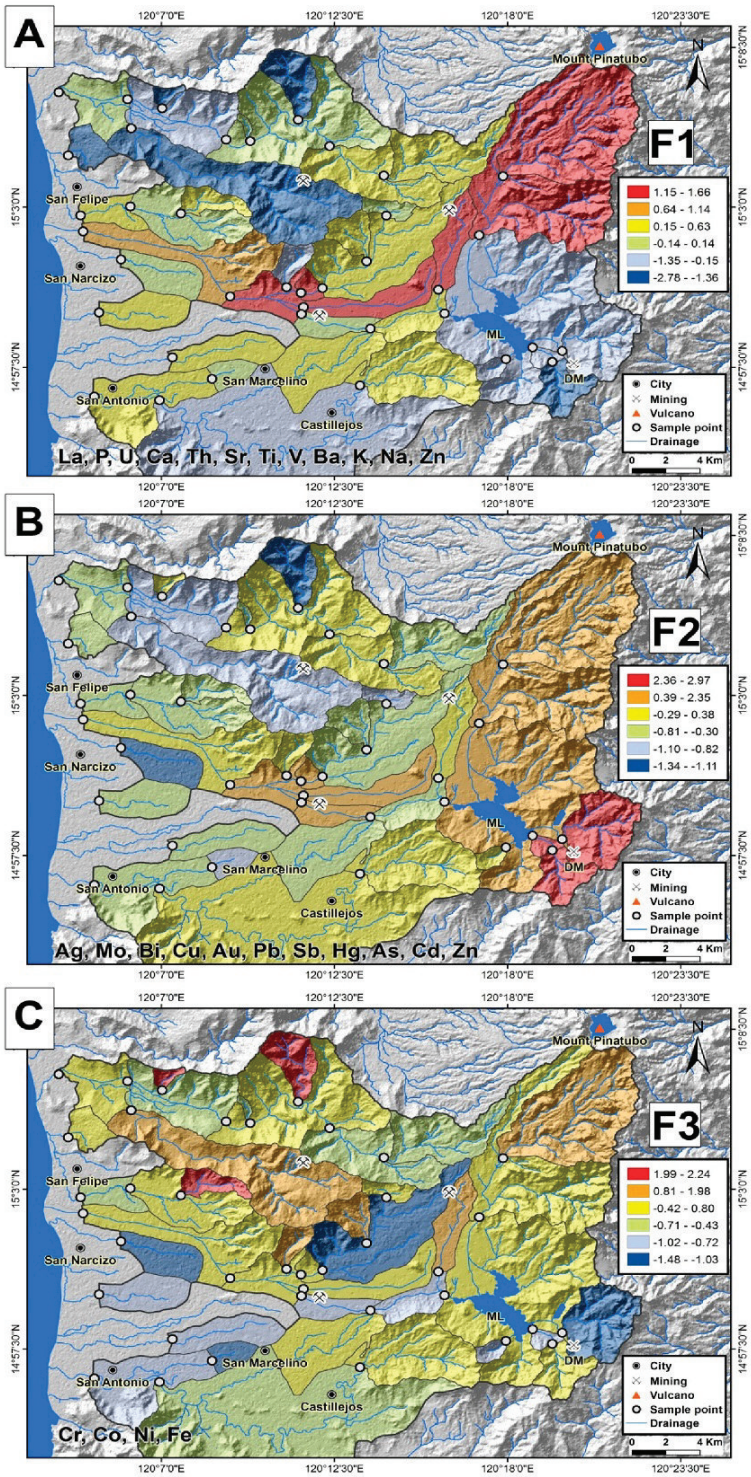

Figure 3.11: Factor score maps for (A) F1 association, (B) F2 association and (C) F3 association. In each map the elements are ordered with decreasing loading.

Factor	% of variance explained	Association	Interpretation
F1	33.1	La, P, U, Ca, Th, Sr, Ti, V, Ba, K, Na, Zn	Andesitic -dacitic volcanic rock and deposits of black sand
F2	32.0	Ag, Mo, Bi, Cu, Au, Pb, Sb, Hg, As, Cd, Zn	Mineralization of porphyry copper
F3	13.6	Cr, Co, Ni, Fe,	Mafic-ultramafic rocks

Table 3.5: Summary and interpretation of the three factor associations. Chemical elements are in decreasing loading order.

3.5. Discussion

3.5.1. Geochemical elements distribution and relationships with the geology and land use

The spatial distribution of the factor scores of FA associations (F1, F2 and F3), along with single chemical element distribution, allow us to locate geochemical anomalies at the watershed level and their relationships with the geology and land use as well. In this section, the spatial distributions of the three FA associations in relationship with the possible geogenic and anthropogenic sources of geochemical anomalies are discussed (Table 3.5 Band Fig. 3.11).

F1 association (La, P, U, Ca, Th, Sr, Ti, V, Ba, K, Na, Zn) accounts for 33.1% of the total data variability. This association shows high and medium-high factor scores corresponding to the Mount Pinatubo volcano area (Table 3.4, 3.5B, Figs. 3.2, 3.11A) (De Hoog et al., 2004). The lahar deposits of this volcano also are the site of placer mining of black sand along the Santo Tomas River, where the F1 association has high to medium-high values (Fig. 3.11A). This area is very important from the economic point of view, because the black sand is rich in Rare Earth Elements and metals that are useful in the industry (Section 3.5.3, Table 3.6, Figs. 3.3, 3.10D, F).

F2 association (Ag, Mo, Bi, Cu, Au, Pb, Sb, Hg, As, Cd, Zn) accounts for 32.0% of the total data variability and appears to be strongly controlled by porphyry copper mineralization. The highest F2 factor scores are accordingly located in the mineralized area of the Dizon Mine (Table 3.4, 3.5B, Fig. 3.11B). In addition, the geochemical maps of some of elements forming F2 association show anomaly in the watersheds upstream of the samples collected in the Dizon Mine area (e.g. Figs. 3.8D, 3.9A ,C, 3.10A, B, E). The F2 factor scores decrease downstream away from the mineralization, showing medium-high values in the watershed embedding the mine wastes around the Mapanuepe Lake (Fig. 3.11B). This suggests that the Dizon Mine is a

source of potentially toxic-metal hazardous elements, for, both, (1) the occurrence of cropping-out and near-surface mineralization that can be eroded and infiltrated by meteoric water, and (2) the mining works that remobilized and exposed a large volume of mineralized rocks in the environment. The spatial distribution of the F2 factor scores suggests that the downstream dispersion of the elements is probably limited by the drainage configuration, with the Mapanuepe lake providing a very low energy environment, allowing the deposition of stream sediments in the lake bed and, thus, a minor toxic-metal carrying capacity of the stream current. F2 also shows medium-high factor scores associated to the Mount Pinatubo deposits along the Santo Tomas and Marella rivers, probably related to the volcanogenic source of the toxic-metal elements (Borisova et al., 2006) (Figs. 3.2, 3.3, 3.8D, 3.9A, C, 3.10A, B ,E, 3.11B, Table 3.4,3.5B).

F3 association (Cr, Co, Ni, Fe) accounts for 13.6% of total data variability and is controlled by mafic-ultramafic rocks. The highest factor scores are located in the catchments in the northwestern sector of the study area (Table 3.4, 3.5B, Fig. 3.11C) where, according to the geological map (Fig. 3.2), mafic-ultramafic rocks of the ZOC ophiolite sequence outcrops. This spatial relationship suggests that the ophiolite rocks weathering and erosion control F3 elements high concentrations (Rossman et al., 1989) (Figs. 3.9B, 3.10C, 3.11C) (Table 3.6).

3.5.2. Geogenic and anthropogenic contamination assessment

The spatial distribution analysis of the geochemical data identified distinct associations of elements related to geological units and economic activities (Table 3.6, Figs. 3.11A, B, C). The high concentration in the environment of dangerous elements and their transport downstream through the drainage network, along with the existence of human settlements and livestock, fishing and agricultural activities, may represent a risk for the human health, due to the possible ingestion of toxic elements through the food chain (Salminen et al., 1998; Järup, 2003).

The Dizon Mine and the associated AMD are potential sources of toxic concentrations of metallic elements like Cu, Pb, Hg and Cd and Zn, among others (Figs. 3.8D, 3.9C, 3.10B, E, 3.11B, D). Also, the extraction of magnetite sand from the Mount Pinatubo lahar deposits represents another potential source of dangerous concentrations of elements like V and U (Figs. 3.10F, 3.11A). Finally, the widespread occurrence of mafic-ultramafic rocks of the ZOC ophiolite sequence, especially in the northern sector of the study area, may constitute a possible source of harmful concentrations of Ni and Cr (Table 3.6, Figs. 3.9B, 3.10C, 3.11C).

Quality guidelines for stream sediments to analyze areas exposed to hazardous concentrations of chemical elements have not been established in the Philippines. Thus, the guidelines proposed by the Ministry of Housing, Spatial Planning and the Environment of The Netherlands (VROM) have been used to identify the

areas where concentration values may represent a risk for the human health (Albanese et al., 2007; VROM, 2000). The VROM (2000) study identifies intervention thresholds for some potentially dangerous metals, above which the functional properties of the soil/sediment for humans, plants and animal life is seriously impaired or threatened (Table 3.3).

The elements that exceed the VROM (2000) thresholds in the study area are As, Cu and Ni (Table 3.3). The concentration of the other metals listed by VROM (2000) is below the intervention thresholds in all the stream sediment samples collected and analyzed in the Zambales Mountain Range (Table 3.3, e.g. Fig. 3.12A). Two watersheds located in the Dizon Mine area, upstream of the Mapanuepe Lake, show As concentration above the reference threshold (Table 3.3, Fig. 3.12C). Also, the Cu concentration is above the intervention value in four watersheds embedding the Dizon Mine and Mapanuepe Lake (Table 3.3, Fig. 3.12D). The high As and Cu content in the stream sediments of the Dizon Mine area could be of geogenic and anthropogenic origin, generated by the porphyry copper mineralization and the mining works, that remobilized a large volume of rocks. Following VROM (2000), a chemical element concentration exceeding the intervention threshold may correspond to a serious case of environmental contamination. In the case of the As and Cu contamination in the Dizon Mine and Mapanuepe Lake area, the occurrence of economic activities, like agriculture and fishing, and towns, like San Marcelino and San Antonio, downstream of the lake poses a significant environmental concern (Figs. 3.3, 3.9A,C, 3.12C,D). For example, the area downstream of the contaminated watersheds hosts wide rice crops, that can efficiently concentrate As and Cd, making it available in the food chain (e.g. Craig 1986; Abernathy et al. 1997; WHO 1999; Patel et al, 2005) (Figs. 3.2, 3.5, 3.11B and 3.12C).

Four watersheds located in the northwestern sector of the study area exceed the intervention value for Ni (Table 3.3, Fig. 3.12B). The occurrence of widespread outcrops of the ZOC ophiolite sequence suggests that the Ni contamination may be of geogenic origin (Figs. 3.2, 3.11B). The watersheds contaminated by Ni and their downstream areas are characterized by the presence of inland freshwater fisheries and livestock grassland, representing a possible threat to the food safety and human health (e.g. Cempel et al., 2006, Cao et al., 2010) (Fig. 3.2).

The As, Cu and Ni contamination and the elevated concentration of other metals, like Pb, Cd, Cr and Hg, have never been reported before in the Zambales Mountain Range (Figs. 3.8D, 3.9A, B, C, 3.10B, E, 3.12A, B, C, D). The potential occurrence of these toxic elements in the food chain, and the consequent health risk for the inhabitants may deserve further in-depth geochemical and environmental studies of water and soils, and, also, the analysis of the elements bioavailability.

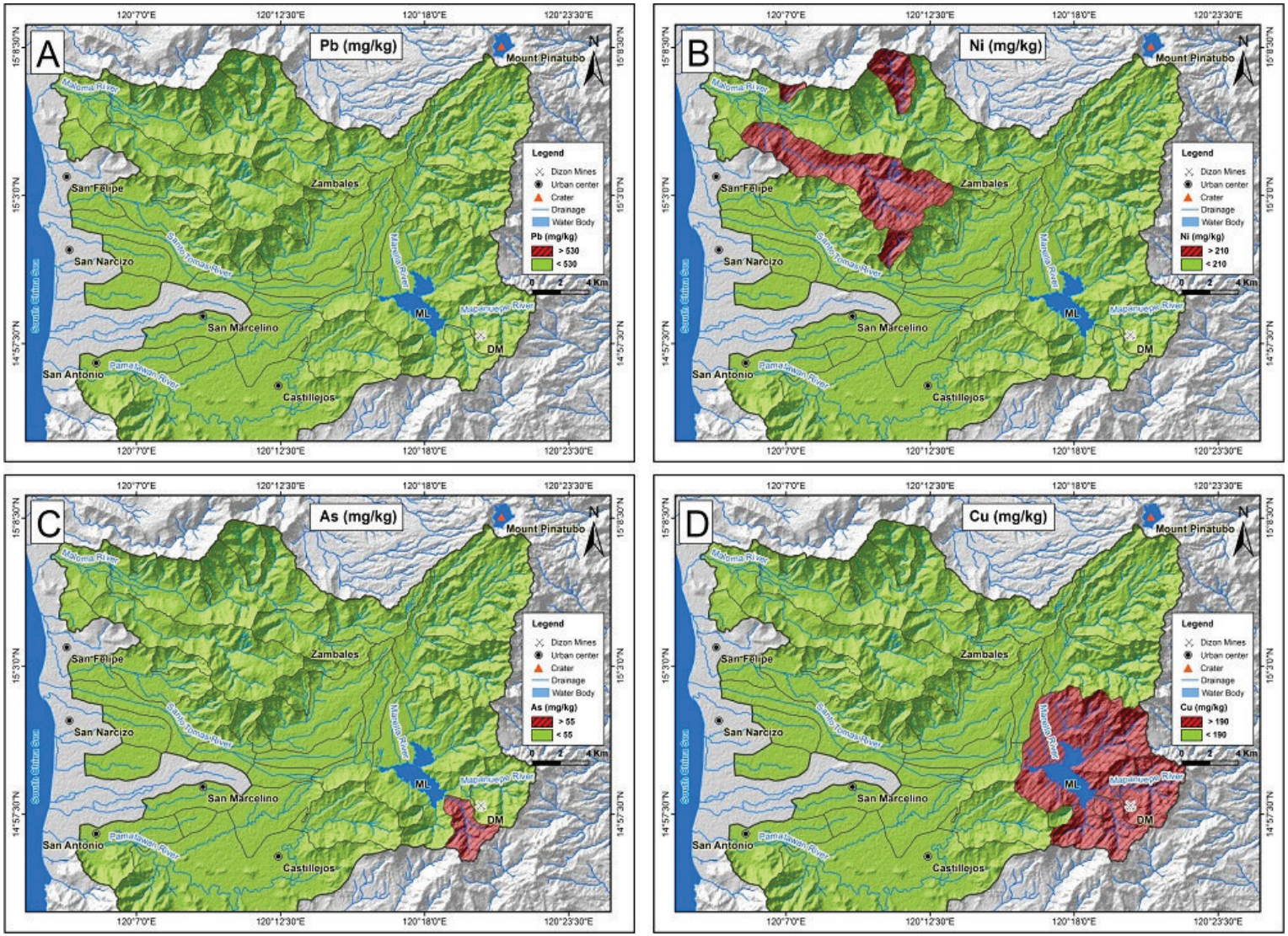

Figure 3.12: Environmental assessment map for Pb (A), Ni (B), As (C), Cu (D) based on the limits defined by VROM (2000). In red the area that exceeds the intervention limit.

3.5.3. Implications for mineral exploration

The study area is characterized by a long mining history, with the exploitation of the Dizon Mine and the extraction of black sand (Fig. 3.2). Both activities are important for the economic development of the area. The geochemical mapping presented in this study, besides the environmental implications discussed in *Section 3.5.2*, may be a useful tool for the exploration of the ore deposits. Anomalous concentration of Cu (189-733 mg/kg), Ag (39.6-350 µg/kg) and Au (2.11-210 µg/kg), associated to a porphyry copper mineralization, has been mapped in the Dizon Mine area (Figs. 3.9C, 3.10A, 3.11B) (Imai, 2005).

Also, the study area is characterized by the occurrence of volcanic black sands along the loose lahar deposits of Mount Pinatubo volcano (1991 eruption), indicating the presence of a placer formation, which may accumulate Rare Earth Elements and metals with economic interest (e.g.: Prater, 1957) (Figs. 3.2, 3.3). The results of the ICP-MS analysis show that the lahar deposits have anomalous values of Rare Earth Elements, like La (11.0 mg/kg), Y (5 mg/kg) and Ce (27.4 mg/kg), and metals, like Ti (0.15 %) and V (160 mg/kg), among others, deserving further studies (Figs. 3.10G,I, 3.11A).

Finally, anomalous concentrations of Cr (152-426 mg/kg) and Ni (163-1370 mg/kg) have been detected in the north and south of the study area, spatially associated to the ophiolite sequence of the ZOC unit (Figs. 3.2, 3.3, 3.9B, 3.10C, 3.11C). These ultramafic rocks, combined with the strong weathering induced by the tropical climate in the area, could be the source of these geochemical anomalies in the stream sediments, representing a potential evidence of Cr and Ni ore deposits (Golightly, 1981).

3.6. Concluding remarks

The definition of the geochemical background and cartography of an area should be regarded as a fundamental tool for the land-use planning and development of economic activities, like mining and agriculture, representing also a first step toward the definition of environmental guidelines.

In this study, the geochemical mapping and the calculation of background values for harmful elements have been accomplished for the first time in a sector of the Zambales Mountain Range by ICP-MS analysis of stream sediment samples and the application of a new GIS algorithm, based on the identification of watersheds. The mapping at the watershed level allowed the identification of anomalous areas with concentration of geochemical elements well above the background values. These geochemical anomalies may represent a potential environmental risk for the economic activities and human settlements in the area, with toxic elements above the concentration limits established by VROM (2000). The study also identified the occurrence

of metals and other elements of economic interest, which may represent an evidence of ore deposits and, thus, a possible contribution to the further economic development of the region.

The data and methods presented in this paper may represent a first knowledge-base for a better management of the natural resources and land use of the Zambales Mountain Range in the Philippines. Indeed, the identified background values and geochemical distribution of potentially harmful elements may be useful in the future for the monitoring of the environmental impact of agriculture, fishing, mining, tourism and other activities in the area.

Acknowledgments

This research was supported by the National Institute of Geological Sciences (NIGS) University of the Philippines Dilliman. The authors are grateful to C.A. Arcilla, A.M. Lagmay, J. de Vera, J.A.M. Galang, S. Salvosa, P.N. Irapta, J. Rafols and Zuzolo, D. for their support to complete this work. Also we want to grateful to Martiya Sadeghi and to the anonymous reviewers for the valuable and the constructive comments.

References

Abernathy C.O., Calderon R.L., Cappell W.R. eds. 1997.Arsenic: Exposure and Health Effects, London: Chapman & Hall.

Adiotomre, E. E. 2014, Enhancing Stream Sediment Geochemical Anomalies Using Spatial Imaging: Case Study from Dagbala and Its Environs. In: of Applied Geology and Geophysics (IOSR-JAGG). V2.Issue 2 .Ver. II. PP 85-96pp.

Aitchison, J., 1986, The statistical analysis of compositional data: Chapman and Hall, London,416 p.

Albanese, S., De Vivo, B., Lima, A., Cicchella, D., 2007. Geochemical background and baseline values of toxic elements in stream sediments of Campania region (Italy). Journal of Geochemical Exploration 93, 21–34.

Aurelio, M.A. 2000. Shear partitioning in the Philippines, Constraints from Philippine Fault and global positioning system data. The Island Arc 9, 584–597.

Borisova, Y.A., Pichavant, M., Polvé, M., Wiedenbeck, M., Freydier, R., Candaudap, F., 2006. Trace element geochemistry of the 1991 Mt. Pinatubo silicic melts, Philippines: Implications for ore-forming potential of adakitic magmatism. Geochimica et Cosmochimica Acta, Elsevier, 70(14), 3702-3716.

Bruinsma, J.W., 1983, Results of potassium-argon age dating on twenty rock samples from the Pinatubo, southeast Tongonan, Bacon-Manito, Southern Negros, and Tongonan, Leyte areas, Philippines: Proprietary report by Robertson Research Ltd. to the Philippine National Oil Company-Energy Development Corporation, 24 p.

Cao, H., Chen, J., Zhang, J., Zhang, H., Qiao, L., Men, Y. 2010. Heavy metals in rice and garden vegetables and their potential health risks to inhabitants in the vicinity of an industrial zone in Jiangsu, China. Journal of Environmental Sciences, 22(11), 1792-1799.

Caritat, P. de, Grunsky, E. 2013. Defining element associations and inferring geological processes from total element concentrations in Australian catchment outlet sediments: Multivariate analysis of continental-scale geochemical data. Applied Geochemistry, 33, 104–126.

Cempel, M., Nikel, G., 2006. Nickel: A Review of Its Sources and Environmental Toxicology. Polish Journal of Environtal Studies, 15(3), 375-382.

Chen Y., Liu Y., Liu Y., Lin .A, Kong X., liu D., Li X., Zhang Y., Gao Y., Wang D., 2012, Mapping of Cu and Pb contamination in soil using combined geochemestry, topography and remote sensing: a case study in the Le'an river floodplain, China. In: International Journal of environmental research and public health. 9, 1874-1886.

Cicchella, D., De Vivo, B., Lima, A., 2005. Background and baseline concentration values of elements harmful to human health in the volcanic soils of the metropolitan and provincial areas of Napoli (Italy). Geochemistry: Exploration-Environment-Analysis 5, 29 -40.

Corby, G. et al., 1951. Geology and oil possibilities of the Philippines. Republic of the Philippines, Department of Agriculture and Natural Resources, Technical Bulletin, 21, 1–363, 57p.

Craig, P.J. 1986. Organometallic Compounds in the Environment,New York: John Wiley & Sons, Inc.

Darnley, A.G., Bjiirklund, A., Belviken, B., Gustavsson, N., Koval, P. C., Plant, J.A., Steenfelt, A., Tauchid, M., Xie Xuejing. 1995. A Global Geochemical Database For Environmental And Resource Management. Recommendation for international geochemical mapping. Final report of IGCP project259. UNESCO publishing.

De Boer, J., Odom, L.A., Ragland, P.C., Snider, F.G., Tilford N.R. 1980. The Bataan orogene: Eastward subduction, tectonic rotations and volcanism in the western Pacific (Philippines), Tectonophysics, 67, 251-282.

Defant, M.J., Maury, R.C., Ripley, E.M., Feigenson, M.D., Jacques, D., 1991. An example of Island-arc petrogenesis: Geochemistry and petrology of the Southern Luzon arc, Philippines. Journal of Petrology. 32(3), 455-500.

De Hoog, J. C. M., Hattori, K. H.,Hoblitt, R.P., 2004. Oxidized sulfur-rich mafic magma at Mount Pinatubo, Philippines. Contrib Mineral Petrol, 146, 750–761.

De La Torre D.M., Perez G.J. 2013. Phenology-Based Classification of Major Crops Areas In Central Luzon, Philippines From 2001-2013. Institute of Environmental Science and Meteorology. University of the Philippines, Diliman, Quezon City PhD Thesis.

De Vivo, B., Lima, A., Albanese, S., Cicchella, D. 2006. Atlante geochimico-ambientale della Regione Campania. Aracne Editrice, Roma. ISBN 88-548-0819-9, 216 p.

De Vivo, B., Lima, A., Siegel., F. 2004. Geochimica Ambientale, Metalli Potenzialmente Tossici. Liguori ed. Napoli, Italia. 448 p.

Ebasco Services, Inc., 1977, Philippine Nuclear Power Plant I: Preliminary Safety Analysis Report, v. 7, section 2.5.H.1, Appendix, A report on geochronological investigations of materials relating to studies for the Philippine Nuclear Power Plant Unit 1.

Evans, C.A., Castaneda, G., Franco, H., 1991. Geochemical complexities preserved in the volcanic rocks of the Zambales Ophiolite, Philippines. J. Geophys. Res. 96, 16251-16262.

Fletcher, W. K., 1997. Stream Sediment Geochemistry in Today's Exploration World. Exploration Geochemistry Paper 2. In "Proceedings of Exploration 97: Fourth Decennial International Conference on Mineral Exploration" edited by A.G. Gubins, 249–260.

Golightly, J.P. 1981. Nickeliferous laterite deposits. Economic Geology, 75th Anniversary Volume, 710-735.

Gupta, S.K., Vollmer, M.K., Krebs, R., 1996. The importance of mobile, mobilizable and pseudo total heavy metal fractions in soil for three-level risk assessment and risk management. Science of the Total Environment, 178(1-3), 11-20.

Hernández-Crespo, C., Martín, M., 2015. The determination of background levels of trace metals in soils and sediments is a key point for the proper assessment of pollution degree. Catena, 133, 206–214.

Holden, W. N. 2015. Mining amid typhoons: Large-scale mining and typhoon vulnerability in the Philippines. The Extractive Industries and Society. 2, 445-461.

Holden, W. N., Jacobson, R. D. 2012. Mining and Natural Hazard Vulnerability in the Philippines: Digging to Development or Digging to Disaster? London: Anthem Press, 277 pp.

Imai, A. 2005 Evolution of Hydrothermal System at the Dizon Porphyry Cu-Au Deposit, Zambales, Philippines. Resource Geology 55 (2), 73-90.

Imai, A. 2002. Metallogenesis of porphyry Cu-Au deposits of the western Luzon arc, Philippines: K-Ar ages, SO3 contents of microphenocrystic apatite and significance of intrusive rocks. Resource Geology 52, 147-161.

Järup, L.2003. Hazards of heavy metal contamination. British Medical Bulletin. 68: 167-82.

Javellosa, R.S. 1984, Morphogenesis and neotectonism of the Santo Tomas Plain, southwestern Zambales, Luzon, Philippines: unpublished M.Sc. thesis, International Institute for Aerospace Survey and Earth Sciences (ITC), Enschede, The Netherlands, 103 pp.

Kampa, M., Castanas, E. 2008. Human health effects of air pollution. Environmental Pollution. 151 (2), 362-367.

Karig, D.E. 1983. Accreted terrenes in the northern part of The Philippines Archipielago. Tectonics 2(2), 211-236.

Lima A., De Vivo,B., Cicchella, D., Cortini, M., Albanese, S. 2003. Multifractal IDW interpolation and fractal filtering method in environmental studies: an application on regional stream sediments of (Italy), Campania region. Applied Geochemistry. 18, 1853-1865.

Malihan, T. D. 1982. Geology of the Dizon porphyry copper gold ore body. In: Proceedings of Seminar on developing New Open Pit Mines in the Philippines, First University of the Philippines Geology Lectures, Manila, 27-49.

Matheron, 1965. Les Variables régionalisées et leur estimarion. Ed. Masson, Paris 306 pp.

Moron, V., Lucero, A., Hilario, F., Lyon, B., Robertson, A.W. and DeWitt, D., 2009: Spatio-temporal variability and predictability of summer monsoon onset over the Philippines. Climate Dynamics, 33, 1159–1177.

Newhall and Punongbayan (Eds.), 1997. Fire and Mud: Eruptions and Lahars of Mount Pinatubo, Philippines. Univ. of Washington, 1126 pp.

Newhall, C., Daag, A., Delfin, FD Jr., Hoblitt, R. ,McGeehin, J. Pallister, J., Regalado, M., Rubin, M., Tubianosa, B Jr., Tamayo,R Jr., Umbal, J. 1996. Eruptive History of Mount Pinatubo In: Newhall, C., Punongbayan, R. (eds). Fire and Mud: Eruptions and Lahars of Mount Pinatubo, Philippines, Institute of Volcanology and Seismology, Quezon City, and University of Washington Press, Seattle, 195-196.

Orejas, T. 2002. Mining firm allays fear of disaster. Philippine daily inquirer across the nation. Sept 4. A14p.

Prater, L.S. 1957. Black sands. Idaho bureau of mines and geology. Moscow, Idaho, 16 pp.

Patel, K.S.,Shrivas,K., Brandt, R., Jakubowski, N., Corns, W., Hoffmann, P., 2005. Arsenic contamination in water, soil, sediment and rice of central India. Environmental Geochemistry and Health. 27(2),pp 131–145

Pawlowsky-Glahn, V. and Buccianti, A., 2011. Compositional Data Analysis: Theory and Applications, John Wiley & Sons, Ltd, 378 pp.

Philippines Statistics Authority, 2010. Statistical Tables on Sample Variables from the results of 2010 Census of Population and Housing - Zambales. https://psa.gov.ph/

Prater, L.S. 1957. Black sands. Idaho bureau of mines and geology. Moscow, Idaho, 16 pp.

Reimann, C., Filzmoser, P., Garrett, R.G. 2005. Background and threshold: critical comparison of methods of determination. Science of the Total Environment, 346, 1-16.

Reimann, C., Filzmoser, P., Garrett, R.G. 2002. Factor analysis applied to regional geochemical data: problems and possibilities. Applied Geochemistry 17, 185-206.

Reimann, C., Filzmoser, P., 2000. Normal and lognormal data distribution in geochemistry: death of a myth. Consequences for the statistical treatment of geochemical and environmental data. Environmental Geology 9, 1001-1014.

Rodolfo, K., Umbal, J., Alonso, R., Remotigue, M., Paladio, M., Salvador, J.,Evangelista, D., Miller, Y. 1996. Two years of lahars on the western flank of Mount Pinatubo, Philippines: initiation, flow processes, deposits, and attendant geomorphic and hydraulic changes. In: Newhall C, Punongbayan R (eds) Fire and mud: eruptions and lahars of Mount Pinatubo. Philippine Institute of Volcanology and Seismology, Quezon City, and University of Washington Press, Seattle, 989–1013.

Roque, V.P., Jr., Reyes, B.P., Gonzales, B.A. 1972, Report on the comparative stratigraphy of the east and west of the mid-Luzon Central Valley, Philippines: Mineral Engineering Magazine, Philippine Society of Mining, Metallurgical, and Geological Engineers, 24, 11-62.

Rossman, D.L., Castaneda, G.c., Bacuta, G.c., 1989. Geology of the Zambales ophiolite, Luzon, Philippines. Tectonophysics, 168, 1-23.

Sadeghi, M., Billay, A., Carranza, E., 2015. Analysis and mapping of soil geochemical anomalies: Implications for bedrock mapping and gold exploration in Giyani area, South Africa. Journal of Geochemical exploration. 154, 180-193.

Salminen, R., Tarvainen, T., Demetriades, A., Duris M., Fordyce F.M., Gregorauskiene V., Kahelin H., Kivisilla J., Klaver G., Klein H., Larson J. O., Lis J., Locutura J., Marsina K., Mjartanova H., Mouvet C., O'Connor P., Odor L., Ottonello G., Paukola T., Plant J.A., Reimann C., Schermann O., Siewers U., Steenfelt A., Van der Sluys J., De Vivo B. and Williams L. 1998. FOREGS Geochemical Mapping Field Manual, Geological Survey of Finland, Espoo, 42 pp.

Spadoni, M., 2006. Geochemical mapping using a geomorphologic approach based on catchments. Journal of Geochemical Exploration, 90, 183-196.

Spadoni, M., Voltaggio, M., Cavarretta, G. 2005. Recognition of areas of anomalous concentration of potentially hazardous elements by means of a subcatchment-based discriminant analysis of stream sediments. Journal of Geochemical Exploration 87, 83-91.

Umbal, J.V., Rodolfo, K., 1996. The 1991 Lahars of Southwestern Mount Pinatubo and evolution of the Lahar-Dammed Mapanuepe Lake. In: Newhall C, Punongbayan R (eds) Fire and mud: eruptions and lahars of Mount Pinatubo. Philippine Institute of Volcanology and Seismology, Quezon City, and University of WashingtonPress, Seattle, 951–971.

Villones, R., 1980. The Aksitero Formation: Its implications and relationship with respect to the Zambales ophiolite: Philippine Bureau of Mines and Geosciences, Technical Information Series, 16-80, 21 pp.

VROM (Ministry of Housing, Spatial Planning and the Environment, The Netherlands), 2000. Circular on target and intervention values for soil remediation. Netherlands Government Gazette of the 24th February 2000, no. 39.

Wakernagel, H. 1995. Multivariate Geostatistics. An Introduction with Applications. Springer-Verlag, Berlin, Heidelberg, New York, 235 pp.

Wang, M., Albanese, S., Lima, A., Cannatelli, C., Cosenza, A. Lu, W., Sacchi, M., Doherty, A., De Vivo, B. 2015. Compositional analysis and pollution impact assessment: A case study in the Gulfs of Naples and Salerno. Estuarine, Coastal and Shelf Science, 160, 22–32.

Webster, R., Oliver, M.A. 2001. Geostatistics for Environmental Scientists 271 pp.

WHO. 1999 Arsenic in Drinking Water, Geneva, 210.

Wolfe, J.A., Self, S., 1983. Structural lineaments and Neogene volcanism in Southwestern Luzon. In: Hayes D E eds. The Tectonic and Geological Evolution of Southeast Asian Seas and Islands (Part 2), Geophysics Monograph (Series 27), Washington, AGU, 157-172.

Yumul, G.P.J., Dimalanta, C.B. 1997. Geology of the Southern Zambales Ophiolite Complex, (Philippines): juxtaposed terranes of diverse origin. Journal of Asian Earth Sciences, 15(4), 413-421.

Zumlot, T., Goodell, P., Howari, F., 2009. Geochemical mapping of New Mexico, USA, using stream sediment data. Environ. Geol. 58, 1479–1497.

Chapter 4 – Other publications about geologic hazard, environmental geochemistry and GIS

4.1. Marine sediments in the Bagnoli area

This chapter is part of the "*Geochemical Atlas of Napoli and Salerno Gulfs sea sediments", in progress, to be published by Aracne Editrice, Roma.*

Authors: Minolfi G., Zuluaga M.C., Wang M., Sacchi M., Albanese, S., Lima, A., De Vivo B.

4.1.1. Introduction

Bagnoli is located in the western part or the city of Naples, along the Tyrrhenian Sea, in the Gulf of Pozzuoli (Italy) (Fig. 4.1.1). The area belong to an active volcanic field (Campi Flegrei), characterized by a strong thermal activity. Bagnoli has been subjected to an intensive industrial activity for around one century, until 1991. As expected for this type of anthropogenic activities, a significant impact altered the natural configuration of the whole area, especially in the 70s and 80s, when there were no environmental standards. The result was a heavy pollution in the air, water, soil and sediments, eventually harming residents and workers at the site. The industrial activities in the area determined a potential high concentration of toxic metals (e.g. As, Cd, Cu, Hg), Polycyclic Aromatic Hydrocarbons (PAHs) and Polychlorobiphenyls (PCB) (e.g. Albanese et al., 2010). Also, geogenic contributions from volcanism and hydrothermal fluids may have increased the content of toxic metals in the environment (Damiani et al., 1987; Sharp e Nardi, 1987; De Vivo et al., 1995). Decommissioning of the Bagnoli industrial site had a strong social and economic impact for Naples. After the end of the industrial activities, Bagnoli has been reconverted into a tourist and recreational site, which implies the need for an evaluation and recovery study of the area.

The data used for this study were already used by Albanese et al (2010); to such data base have been added some new data from sea sediments of the Napoli and Salerno Gulfs to produce new maps for metals, PAH and PCB only for the Bagnoli Bay.

As a part of the PhD program, an evaluation of the environmental risk has been done for a 14 km^2 marine area located in front of the Bagnoli site and used for touristic activities and fishery. 123 surface marine sediment samples (depth 0-10 cm) collected between November 2004 and March 2005, following the directives of the national program for assessment of marine pollution of highly contaminated Italian coastal areas, then prepared and analyzed for inorganic elements with Inductively Coupled Plasma-Optical Emission Spectrometry (ICP-OES) and Atomic Absorption spectrometry (AAS) for (Al, As, Be, Cd, Co, Cr, Cu, Fe, Hg, Mn, Ni, Pb, Sn, V, Zn) and PAH and PCB by the ICRAM laboratories. The metal distribution has been processed in a GIS for the

calculation of geochemical maps and the environmental hazard assessment for toxic metals pollution (Wang, 2014). Later, for the Napoli and Salerno Gulfs 103 samples of sea sediments have been analyzed for PAHs (Acenaphthylene, Anthracene, Benza$_a$nthracene, Benzoapyrene, Benzo$_b$fluoranthene, Benzoghiperylene, Benzokfluoranthene, Chrysene, Dibenzoahnthracene, Fluoranthene, Fluorene, Indeno$_{123}$dpyrene, Naphthalence, Phenanthrene, Pyrene) and and 109 samples for Organochlorine Pesiticides (OCPs) (a-HCH, HCB, b-HCH, r-HCH, d-HCH, Heptachlor, Aldrin, Heptachlor-exo, Trans-Chlordan, o,p'-DDE, a-Endoslfan, cis-Chlordane, trans-Nonachlor,p,p'-DDE, Dieldrin, o,p'-DDD, Endrin, b-Endosulfan, p,p'-DDD, o,p'DDT, cis-Nonachlor, Endrin aldehyde, endosulfan-sal, p,p'-DDT, Endrin ketone, methoxychlor) by Gas Chromatography-Mass Spectometry (GC-MS) in Key Laboratory of Biogeology and Environmental Geology of the Ministry of Education (Wuhan, P.R.C) (Wang, 2014). The complete set of maps compiled for metals, PAHs and OCPs will be included and discussed in the "Geochemical Atlas of Napoli-Salerno Gulfs sea sediments" in progress.

The resulting geochemical maps and environmental hazard assessment, depicting the areas where toxic metals, PAHs and OCPs area above the limits established by the Italian law, show that the marine area considered in the study has a significant environmental risk, that may harm the touristic activities and fishery. These new maps and environmental risk analysis will be published, within 2017, in the "*Geochemical Atlas of Napoli-Salerno Gulfs sea sediments*" (in progress).

4.1.2. Study area

Bagnoli is located in the Campi Flegrei collapse caldera, which is part of the K-series of the Roman co-magmatic province (Peccerillo, 1985; Washington, 1906). The composition of the volcanic products varies from trachybasalts to phonolitic and peralkaline trachytes (Di Girolamo, 1978; Armienti et al., 1983). The coastal area in front of the Bagnoli brownfield industrial site is part of a shelf facing the shoreline of the Gulf of Pozzuoli (Fig. 4.1.1). The shelf extends from the coastline toward the 50 m bathymetry and borders a central recently collapsed area (12–10 kyr bp) (De Pippo et al., 1988). Volcanic banks (Nisida, Pentapalummo and Miseno) bordered by an external Würmian shelf are present on the southern side of the collapsed area (De Pippo et al., 1988). The presence of submarine hydrothermal springs located along a NW–SE axis, in the eastern sector of the Gulf of Pozzuoli, is clearly related to the secondary volcanic activity of the Campi Flegrei area (Sharp and Nardi, 1987). On the seabed, surface sediment grain size is mostly sandy, becoming silty in correspondence with some sheltered areas along the coastline that are characterized by low energy for sediment transport (Cocco et al., 1988). In the Bagnoli–Fuorigrotta area, the water table is found slightly above sea level and can be intercepted at shallow depths, especially on the south side of the local railroad. The

groundwater of the Bagnoli plain, resupplied directly by rainfall, is part of a wider groundwater body which spans the whole Campi Flegrei area and discharges directly to the sea (Celico and Habetswallner, 1999a,b).

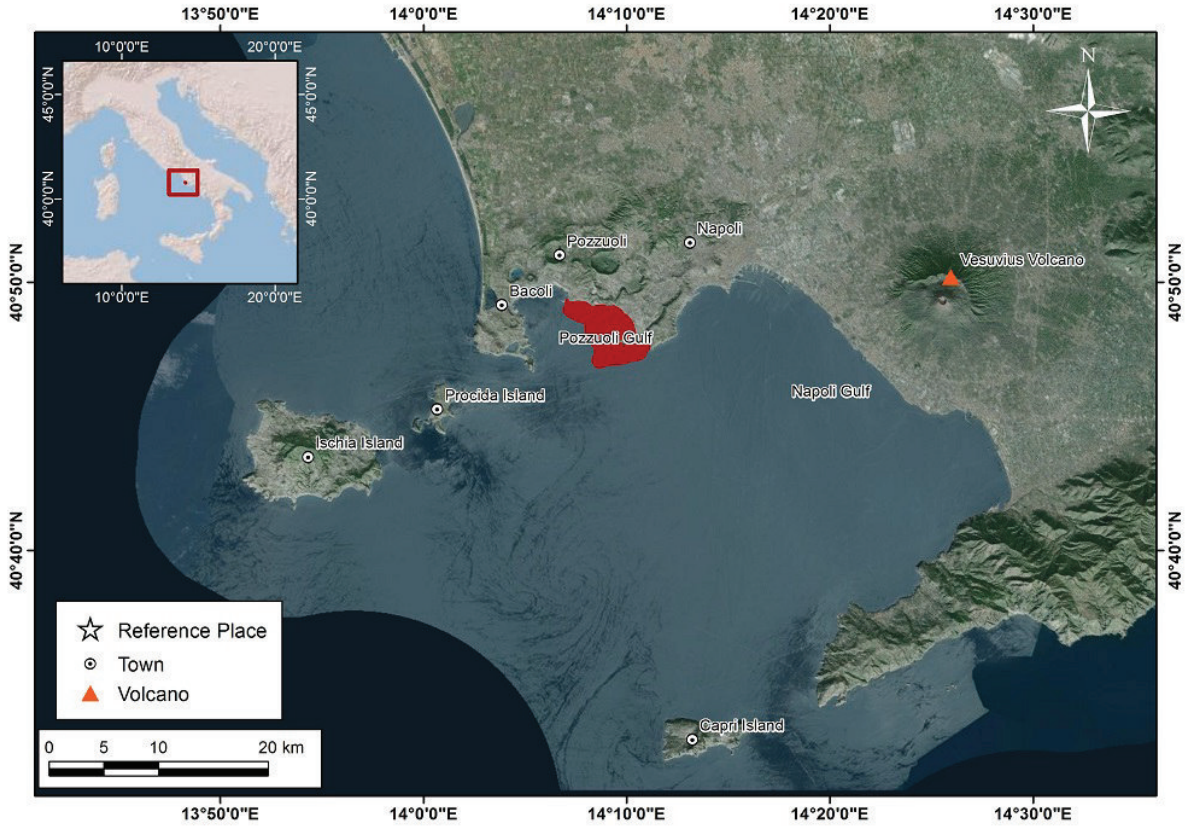

Figure 4.1.1: Map with the localization of the study area in red.

4.1.3. Methodology

The analytical results of the ICP-OES and AAS for selected chemical elements (Al, As, Be, Cd, Co, Cr, Cu, Fe, Hg, Mn, Ni, Pb, Sn, V, Zn) and the GC-MS for PCB and PAHs published by Albanese et al. (2010) and Wang (2014) have been imported in a GIS database. Univariate analysis of the inorganic elements, and PAHs concentrations in the marine sediment samples has been performed. For statistical computation, data below the instrumental detection limit (DL) have been assigned to ½ of the DL. The cumulative frequency curves (CFCs) of the elements analyzed in the topsoil show inflections and break-points, reflecting the presence of multiple populations, originated by the geogenic and/or anthropogenic contribution to the concentration values (e.g., Fig. 4.1.2) (Reimann et al., 2005). Eight intervals have been identified on these CFCs using flexion points of the curve near

the 10, 25, 50, 75, 90, 95 and 98 percentiles (e.g., De Vivo et al., 2016; Zuluaga et al., 2017). These intervals were used to plot the marine sediments geochemical maps (De Vivo et al., 2004; Albanese et al., 2007). The final marine sediments geochemical maps for the selected organic elements and PAHs have been calculated from the scattered samples using the Inverse Distance Weighted (IDW) interpolation method.

The calculated geochemical maps have been compared to the update Italian environmental law N°56 of 2009, establishing the intervention limits for inorganic elements, PCB and PAHs in marine sediments. The resulting intervention maps identify the areas with potentially harmful concentration values that should be remediated.

4.1.4. Results and discussion

The new geochemical and intervention maps that have been calculated for the Bagnoli area constitute a significant advancement in the knowledge of the environmental quality of this contaminated site. With respect to previous published works, these maps consider a larger number of inorganic elements and organic compounds and uses the most updated intervention limits established by the Italian law (e.g. Albanese et al., 2010). Large geochemical anomalies have been depicted by the new geochemical maps in the marine area in front of the Bagnoli site (e.g. Fig. 4.1.3). Also, wide sectors of this area are well above the intervention limits established by the updated Italian law of 2009, as shown by the intervention maps (e.g. Fig. 4.1.4).

The marine area that has been studied is under a significant environmental risk related to the high concentration of potentially harmful inorganic elements and organic compounds. After the publication of the new maps in the "*Geochemical Atlas of Napoli and Salerno Gulfs sea sediments*", further studies will be required to establish the best procedures to reduce the risk and remediate the marine environment, considering that touristic activities and fishery commonly occurs where these maps identify dangerous geochemical anomalies.

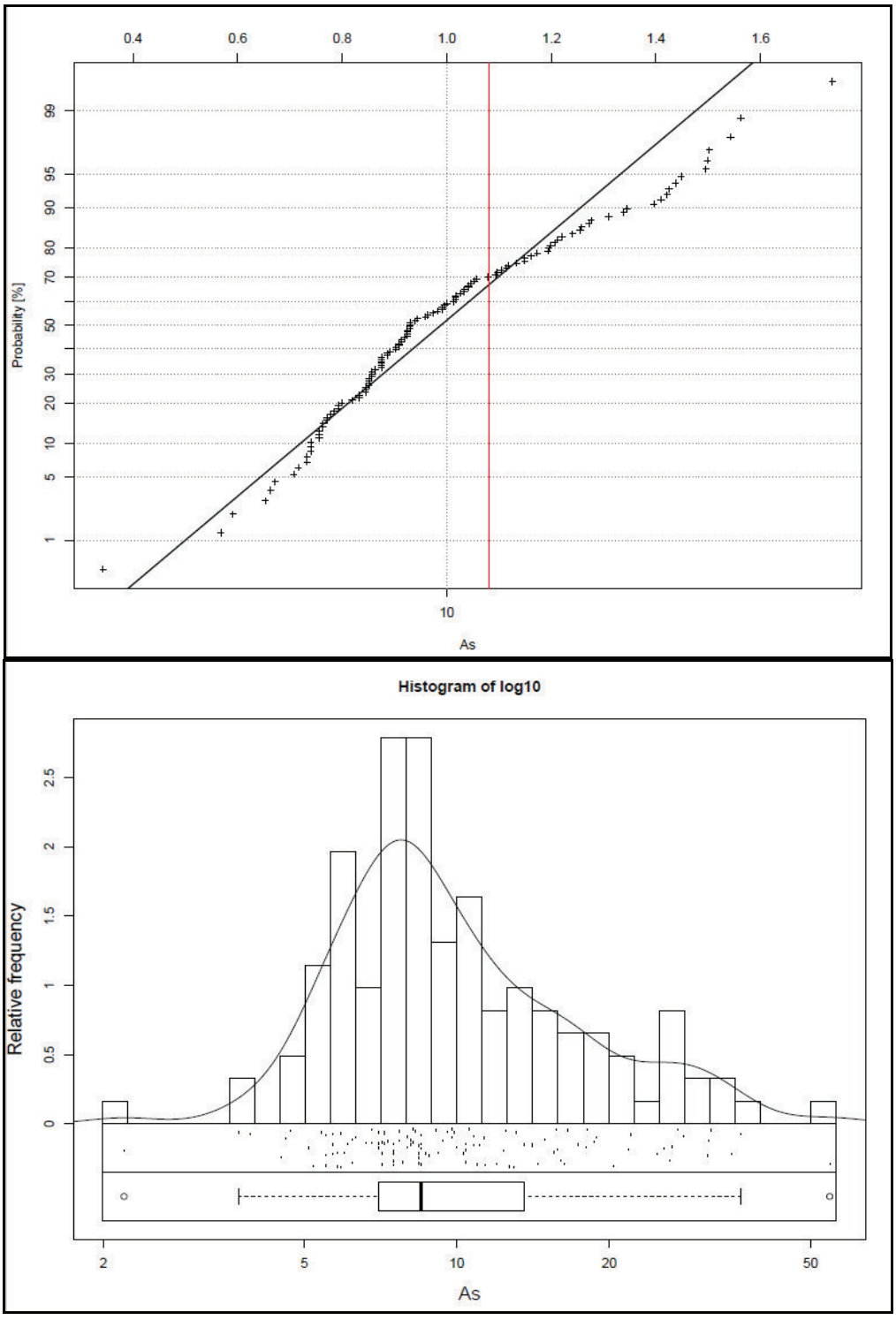

Figure 4.1.2: Accumulative frequency curves and histograms for As.

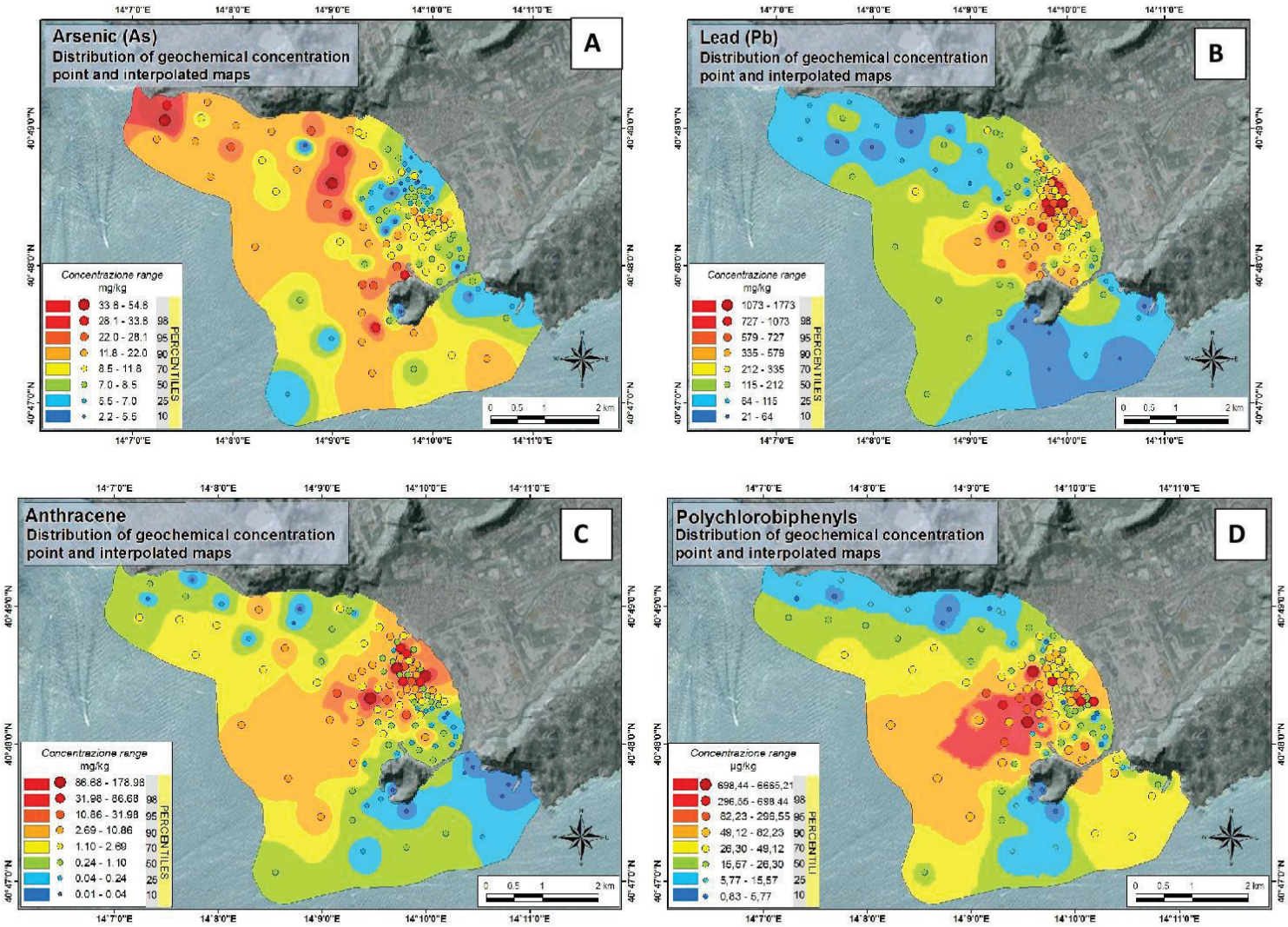

Figure 4.1.3: Geochemical distribution of (A) As (mg/kg), (B) Pb (mg/kg), (C) Anthracene (mg/kg) and (D) PCB (µg/kg),concentration in the area of Bagnoli using IDW algorithm.

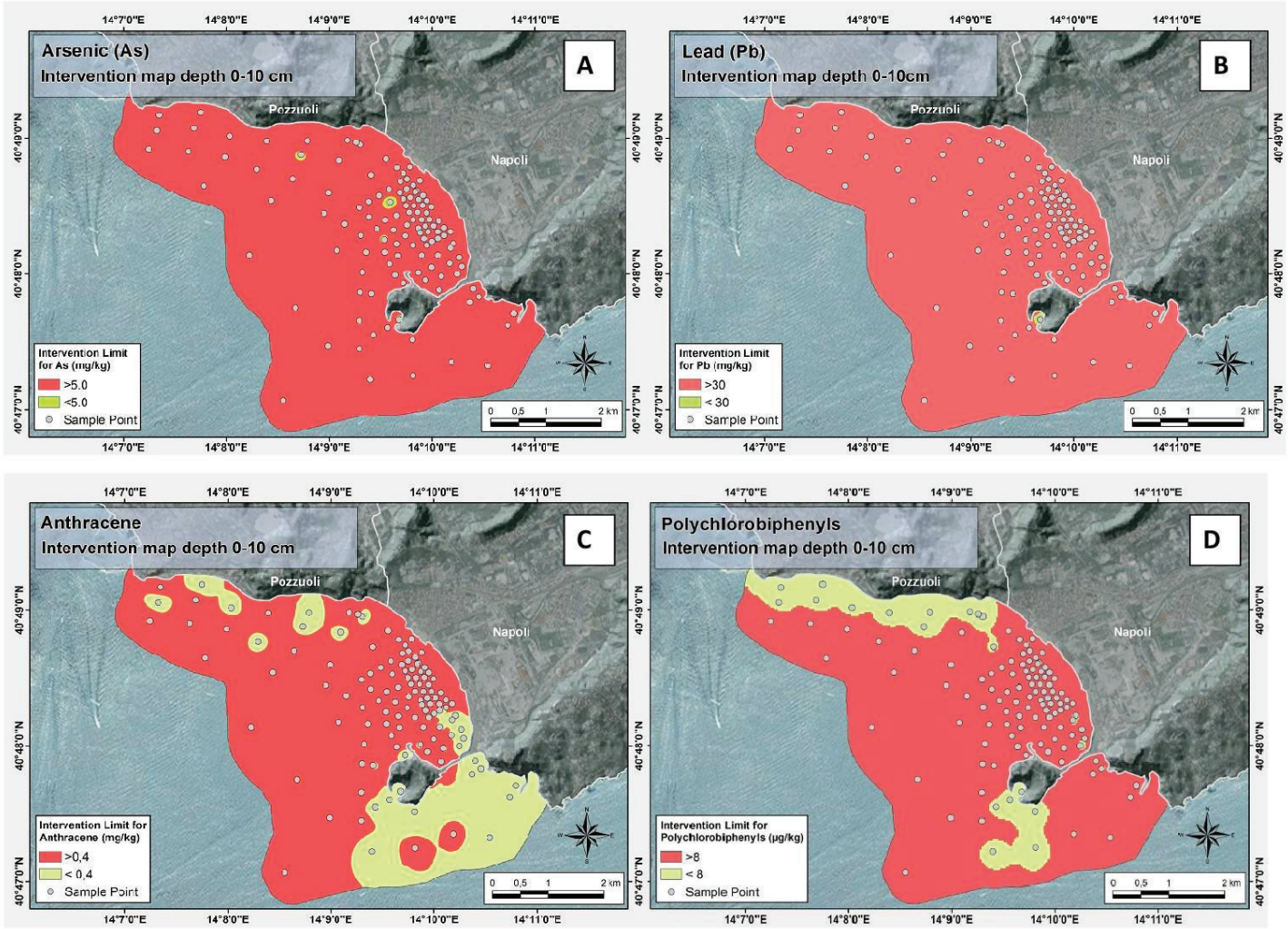

Figure 4.1.4: Environmental assessment map for (A) As (mg/kg), (B) Pb (mg/kg), (C) Anthracene (mg/kg),) and (D) PCB (µg/kg), based on the limits defined by the Italian legislation for marine sediments 2009. In red the area that exceeds the intervention limit.

References

Albanese, S., De Vivo, B., Lima, A., Cicchella, D., Civitillo, D., Cosenza, A., 2010. Geochemical baselines and risk assessment of the Bagnoli brownfield site coastal sea sediments (Naples, Italy) Journal of Geochemical Exploration 105: 19–33.

Armienti, P., Barberi, F., Bizouard H., Clocchiatti, R., Innocenti, F., Metrich, N., Rossi M., Sbrana, A., 1983. The Phlegraean Fields: magma evolution within a shallow magma chamber. J. Volcanol. Geotherm. Res., 17, 289 – 311.

Celico, P., Habetswallner, F., 1999a. Prime considerazioni idrogeologiche sull'area dell'ex Ilva di Bagnoli. Società Bagnoli S.p.A., Napoli.

Celico, P., Habetswallner, F., 1999b. Considerazioni idrogeologiche sull'area dell'ex Ilva di Bagnoli. Società Bagnoli S.p.A., Napoli.

Cocco, E., De Magistris, M.A., De Pippo, T., 1988. Distribuzione e dispersione dei sedimenti nella piattaforma costiera del golfo di Pozzuoli. Mem. Soc. Geol. It. 41, 983–993.

Damiani V., Baudo R., De Rosa S., De Simone R., Ferretti O., Izzo G. e Serena F., 1987. A case study: Bay of Pozzuoli (Gulf of Naples, Italy). Hydrobiologia, 149, 201-211.

De Pippo, T., Pescatore, T., Vecchione, C., 1988. Caratteri granulometrici dei sedimenti dei terrazzi del golfo di Pozzuoli. Mem. Soc. Geol. It. 41, 1005–1014

De Vivo B., Török K., Ayuso R. A., Lima A. e Lirer L., 1995. Fluid inclusion evidence for magmatic silicate/saline/CO2 immicibility and geochemistry of alkaline xenoliths from Ventotene island (Italy). Geochim. Cosmochim. Acta, 59, 2941-2953.

De Vivo, B., Lima, A., Albanese S., Cicchella, D., Rezza, C., Civitillo D., Minolfi, G., Zuzolo, D., 2016. Atlante geochimico–ambientale dei suoli della Campania. Aracne Editrice, Roma. 330 pp.

Di Girolamo P., 1978. Geotectonic setting of Miocene-Quaternary volcanism in and around the eastern Thyrrenian sea border (Italy) as deduced from major element geochemistry, Bull. Volcanol. 41, 229-250.

Peccerillo A., 1985. Roman comagmatic province (Central Italy): evidence for subduction-related magma genesis. Geology, 13, 103-106.

Reimann, C., Filzmoser, P., Garrett, R.G. 2005. Background and threshold: critical comparison of methods of determination. Science of the Total Environment, 346, 1-16.

Sharp W. E. and Nardi G., 1987. A study of the heavy metal pollution in the bottom sediments at Porto di Bagnoli (Naples) Italy. J. Geoch. Expl., 29, 49-73

Washington H. S., 1906. The Roman Comagmatic Region. Carnegie Inst. of Washington, 57, 199 pp.

Zuluaga, M.C., Norini, G., Lima, A., Albanese S., David, C.P., De Vivo, B. 2017.Stream sediment geochemical mapping of the Mount Pinatubo-Dizon Mine area, the Philippines: Implications for mineral exploration and environmental risk Journal of Geochemical Exploration. 175: 18–35.

4.2. Alluvial fan mapping

This article is published in Geomorphology, 2016, 273, 134–149. ISSN 0169-555X.

Delineation of alluvial fans from Digital Elevation Models with a GIS algorithm for the geomorphological mapping of the Earth and Mars

Gianluca Norini[a,*], Maria Clara Zuluaga[b], Iris Jill Ortiz[c,d], Dakila T. Aquino[c], Alfredo Mahar F. Lagmay[c,d]

[a]Istituto per la Dinamica dei Processi Ambientali - Sezione di Milano, Consiglio Nazionale delle Ricerche, Milano, Italy

[b]Dipartimento di Scienze della Terra, dell'Ambiente e delle Risorse, Università degli Studi di Napoli Federico II, Napoli, Italy

[c]Nationwide Operational Assessment of Hazards, Department of Science and Technology, Philippines

[d]National Institute of Geological Sciences, University of the Philippines, Diliman, Quezon City, Philippines

* Corresponding author: G. Norini, tel. +390266173334, fax +390228311442, gianluca.norini@cnr.it

Abstract

Alluvial fans are prominent depositional geomorphic features present in nearly all global climates on Earth, and also found on Mars. In this study, we present a Geographic Information System (GIS) algorithm designed for the semi-automated detection of alluvial fans that are connected to their contributing upstream drainage network, from the analysis of Digital Elevation Models (DEMs). Through a combination of spatial analysis procedures, the GIS algorithm generates maps of alluvial fans and their upstream source drainage and watersheds. Tests of the algorithm in areas with well-known alluvial fans indicate that this new GIS procedure is capable of high-accuracy mapping of the fan apexes and correct delineation of fan deposits, in both arid and humid climates. Possible future applications of the GIS algorithm presented in this study include the systematic survey of alluvial fans at the local, regional and planetary scales, important for geologic hazard assessment, studies on the evolution of climate, analysis of continental sedimentary environments, understanding of the interplay between the endogenous dynamics and exogenous processes, and the evaluation of natural resources.

4.3. Basement-volcano interplay in the Colima Volcanic Complex

This article is accepted for publication in: Volcán de Colima - Managing the Threat, Varley N., Komorowski J.C. (Eds.), 2017, Springer-Verlag, Berlin, Heidelberg, Hardcover. ISBN 978-3-642-25910-4.

Basement-volcano interplay in the Colima Volcanic Complex: origin and behavior of active faults systems in the edifice interior

Gianluca Norini[1], Federico Agliardi[2], Giovanni Crosta[2], Gianluca Groppelli[1], Maria Clara Zuluaga[3]

[1]Istituto per la Dinamica dei Processi Ambientali, Consiglio Nazionale delle Ricerche, Italy
[2]Department of Earth and Environmental Sciences, University of Milano-Bicocca, Italy
[3]Dipartimento di Scienze della Terra, dell'Ambiente e delle Risorse, Università degli Studi di Napoli Federico II, Italy

Abstract

The Colima Volcanic Complex (CVC) is one of the most prominent volcanic edifices within the Tran-Mexican Volcanic Belt (TMVB). Its evolution has been characterized by complex interactions among regional tectonics, basement geometry and rheology, and different volcanic edifices formed in several stages.

In the first part of this review paper, the state-of-the-art in the CVC structural and geological knowledge is summarized and discussed. Such knowledge is based on published structural, geological, geophysical, geodetic and petrological data and models, which allow identifying three main fault systems and defining the general geometrical properties of the volcano feeding system. The significance and supporting evidence for the Colima Rift faults, Tamazula Fault and volcano spreading structures, as well as their interactions with the CVC, are presented.

In the second part of the paper, numerical models are performed to integrate previous knowledge and test the effects of different structural scenarios and different mechanical assumptions on the onset of gravitational spreading of the volcanic complex. Also, the state of activity of the three fault systems and their control on the feeding of the volcanic activity and flank instability are discussed.

Finally, the main findings on the CVC structural arrangement are resumed, and the most important future needs to improve the knowledge on the interaction between regional tectonics, volcanic edifices and basement rheology are indicated, for an area where eruptions and sector failures represent a potential high risk for more than 500,000 people.

4.4. GIS analysis of the seismic susceptibility in the Mantova-Cremona area

Some of the GIS mapping tools used during the PhD have also been applied for the acquisition of geological, geotechnical and geophysical data for the seismic characterization of the territory after the earthquakes occurring in northern Italy in 2012.

The product is a technical report with maps written in Italian and officially published in 2015 in the Regione Lombardia website, Italy:

http://www.territorio.regione.lombardia.it/cs/Satellite?c=Redazionale_P&childpagename=DG_Territorio%2FDetail&cid=1213281110167&pagename=DG_TERRWrapper

RAPPORTO TECNICO

Acquisizione ed elaborazione di dati geologici, geotecnici e geofisici per la caratterizzazione sismica di parte del territorio lombardo ricadente nell'Area Pilota del Progetto GeoMol – Programma Europeo "Spazio Alpino"

A cura di:

Coordinamento:	Gianluca Norini[1]
Cartografia geomorfologica, tessiturale, altimetrica e GIS:	Doriano Castaldini[2], Mauro Marchetti[2], Fulvio Baraldi[2], Cinzia Lanfredi Sofia[2], Gianluca Norini[1] e Maria Clara Zuluaga[1,3]
Sondaggi stratigrafici:	Fulvia Aghib[1], Fulvio Baraldi[2], Doriano Castaldini[2], Andrea Di Capua[1,5], Giulia Furlanetto[1], Gianluca Groppelli[1], Cinzia Lanfredi Sofia[2], Mauro Marchetti[2], Gianluca Norini[1], Roberta Pini[1], Cesare Ravazzi[1]
Scenario sismico:	Alberto Marcellini[1], Alberto Tento[1], Rosastella Daminelli[1], Daniele Gerosa[6]
Indagini geofisiche:	Graziano Boniolo[1], Grazia Caielli[1], Adelmo Corsi[1], Roberto de Franco[1], Andrea Di Capua[1,5]
Geotecnica:	Johann Facciorusso[4]
Idrogeologia:	Angelo Cavallin[5]

[1]*Istituto per la Dinamica dei Processi Ambientali del Consiglio Nazionale delle Ricerche*
[2]*Dipartimento di Scienze Chimiche e Geologiche dell'Università degli Studi di Modena e Reggio Emilia*
[3]*Dipartimento di Scienze della Terra, dell'Ambiente e delle Risorse, Università di Napoli Federico II*
[4]*Dipartimento di Ingegneria Civile ed Ambientale dell'Università degli Studi di Firenze*
[5]*Dipartmento di Scienze dell'Ambiente e del Territorio e di Scienze della Terra dell'Università degli Studi di Milano-Bicocca*
[6]*SIGNA srl, Boltiere (Bg)*

Milano, 30 settembre 2015

5. Concluding remarks

The principal achievements of the thesis can be summarized as follows:

- A new GIS algorithm, based on the identification of watersheds, was designed for the geochemical mapping of the Zambales Province in The Philippines. It is a powerful tool for the cartography of stream sediments, especially in areas with intense rainfalls and abrupt topography.
- A geochemical mapping and the calculation of background values for harmful elements have been accomplished for the first time in a sector of the Zambales Province in the Philippines.
- The use of factor analysis as a powerful tool to recognize multielemental associations, allowing the identification of sources and processes that produce the observed distribution of geochemical elements.
- Lead isotopic analysis is used to identify the geogenic and/or anthropogenic origin of contamination. In the Huelva Province in the SW of Spain, the analysis performed in soil and human hair samples demonstrates well defined signatures related to the sources of contamination.
- The occurrence of metals in soils is frequently closely linked to the local geology and historical patterns of land use. The geochemical, geological and land use maps that were produced for the Huelva Province, shows clear spatial relationship among geochemical anomalies, geological units and anthropogenic activities.
- The environmental assessment that has been carried out in this study allows us to identify sectors where multi-element concentration of metals may represent a risk for human health.
- The definition of the geochemical background and cartography of an area should be regarded as a fundamental tool for the land-use planning and development of economic activities, like mining, industrial and agriculture, representing also a first step toward the definition of environmental guidelines.

References

Andalucia Region-CMAJA (Consejería de Medio Ambiente de la Junta de Andalucía), 1999. Los criterios y estándares para declarar un suelo contaminado en Andalucía y la metodología y técnicas de toma de muestra y análisis para su investigación. http://www.juntadeandalucia.es

Goldschmidt,V. M. 1954, Geochemistry: London, Oxford University Press,730 p.

Lima A., De Vivo,B., Cicchella, D., Cortini, M., Albanese, S. 2003. Multifractal IDW interpolation and fractal filtering method in environmental studies: an application on regional stream sediments of (Italy), Campania region. Applied Geochemistry. 18, 1853-1865.

Matheron, 1965. Les Variables régionalisées et leur estimarion. Ed. Masson, Paris 306 pp.

Spadoni, M., Voltaggio, M., Cavarretta, G. 2005. Recognition of areas of anomalous concentration of potentially hazardous elements by means of a subcatchment-based discriminant analysis of stream sediments. Journal of Geochemical Exploration 87, 83-91.

Spadoni, M., 2006. Geochemical mapping using a geomorphologic approach based on catchments. Journal of Geochemical Exploration, 90, 183-196.

Wakernagel, H. 1995. Multivariate Geostatistics. An Introduction with Applications. Springer-Verlag, Berlin, Heidelberg, New York, 235 pp.

Webster, R., Oliver, M.A. 2001. Geostatistics for Environmental Scientists 271 pp.

Zuluaga, M.C., Norini, G., Lima, A., Albanese S., David, C.P., De Vivo, B. 2017.Stream sediment geochemical mapping of the Mount Pinatubo-Dizon Mine area, the Philippines: Implications for mineral exploration and environmental risk Journal of Geochemical Exploration. 175: 18–35.

Zumlot, T., Goodell, P., Howari, F., 2009. Geochemical mapping of New Mexico, USA, using stream sediment data. Environ. Geol. 58, 1479–1497